# Mechanisms of the pro-lipolytic and anti-obesity effects of the VGF-derived peptide TLQP-21

A DISSERTATION SUBMITTED TO THE FACULTY OF
THE UNIVERSITY OF MINNESOTA BY

**Cheryl Cero**

IN PARTIAL FULFILLMENT OF THE REQUIREMENTS
FOR THE DEGREE OF

DOCTOR OF PHILOSOPHY

Advisor: Alessandro Bartolomucci, PhD

Minneapolis, MN
October 29, 2015

# ACKNOWLEDGEMENTS

After finishing my Master Degree I knew I wanted to go to graduate school, but I certainly had no idea I would have ended up in the US, in the Midwest, in Minneapolis, Minnesota to pursue my dream. I had an outstanding luck to have met Dr. Zofia Zukowska that suggested applying to the Integrative Biology and Physiology Graduate Program, and for this I am extremely grateful. Your enthusiasm for science and life has left lasting effects. Thank you for encouraging me to start this great journey.

During my rotation in Dr. Alessandro Bartolomucci's laboratory, I knew I found *my* project and decided to join your lab. Your vision, creativity and motivation have guided me throughout this project, from the thesis proposal up to this thesis manuscript. Without your help, patience and assistance none of this work would have happened. Thank you for giving me endless support and encouragement, this thesis proves it. I could not have imagined for a better mentor! Thank you for having faith in me.

I am extremely grateful for the guidance provided by my Thesis Committee, Dr. John Osborn, Dr. David Bernlohr and Dr. Douglas Mashek who have been a constant source of reference providing constructive comments and advise during my thesis research. Your valuable input is what has helped me improve my critical thinking and understanding the importance of details. Special thanks to Dr. Osborn for having your door always open and creating the ideal environment for me as a graduate student.

I am also deeply grateful for the advice, valuable suggestions and help received from Dr. Scott O'Grady, for your encyclopedic knowledge on all things, molecular and general, that helped me pursuing key experiments for my research, and Dr. Gianluigi Veglia for allowing me to do a direct research study in your lab learning more about the chemical synthesis of peptides. Also, thank you both for opening your laboratories and giving me access to your equipment.

Without the continuous support and help from current and past lab members this work wouldn't have been possible. I am especially thankful for the help and advise that Maria provided throughout the *in vivo* experiments; to Allison for the expertise

and help with the *in vitro* studies and to Rana who came in early morning and stayed late night helping me with the cell culture studies.

To all the IBP graduate students, peer support was absolutely key in my journey as a gradate student, thank you. In particular, Dalay and Evelyne my classmates, who were there for me from day 1, for the study sessions, for the great advice helping overcome moments of struggle, and for the yummy food. To Nathan and Tim, for helping me discover Minnesota, for the camping, the backpacking experience on the Superior Hiking Trail, the parties, the beer pong nights and many stimulating scientific and not so scientific conversations.

A very special thank you to all my friends, the far and the close ones, thank you for helping me keep the right balance of life outside the lab.

# DEDICATION

I would like dedicating this thesis to my family, to my mother Gabriella and father Floriano, who have shaped my character and made me the person I am today. Even though you have not been literally besides me during these years, your moral support has helped got me here. I am extremely grateful for all your sacrifices in providing me the best education and future. Thank you for allowing me to follow my dreams and ambitions throughout my life.

To my siblings, nieces and nephews, I have missed so many birthdays and Christmases, but thank you for understanding and supporting me.

To Fabio, for your unconditional love, support, motivation and encouragement. Your patience and understanding have helped me get where I am. Thank you for convincing me to undertake this challenge and following me across seas and continents to achieve my goals. I am the luckiest person on earth to have you by my side. Looking forward for more adventures together.

# CONTRIBUTIONS

Me, Cheryl Cero wrote entirely Chapter 1, Chapter 3, Chapter 4 and Chapter 5. I contributed to writing Chapter 2. I performed all experiments included in the thesis except for what detailed below.

- Mrs. A. Gurney, who works in the laboratory of Dr. Alessandro Bartolomucci helped at the realization of *in vitro* studies presented in Chapter 2 and 3.
- Dr. M. Razzoli, who works in the laboratory of Dr. Alessandro Bartolomucci helped at the realization of in vivo studies presented in Chapter 4.
- Rana Mohamed, an undergraduate who worked in the laboratory of Dr. Alessandro Bartolomucci helped at the realization of *in vitro* studies presented in Chapter 2 and 3.

Chapter 2:

- Dr. R. Verardi, Dr V.V. Vostrikov, Dr T. Gopinath and Dr. G. Veglia synthesized TLQP-21 and R21A mutant peptides and performed all the NMR spectrometry studies.
- Dr. P.D. Braun and Dr. L. Vulchanova performed the receptor crosslinking studies.
- Dr. C. Severini and Dr R. Possenti performed the gastric contraction assay.
- Dr. F. Sassano and Dr. B. Roth that performed the GPCR β-arrestin recruitment assay.

Chapter 3:

- Mr. N. Zaidman and Dr. S. O'Grady, contributed greatly with the design and execution of FURA-2AM experiments.

Chapter 4:

- Dr. P. Poggi and Dr. L.J. Baier, performed the C3aR1 gene expression analysis.
- Dr. Z. Guo and Dr. J.M. Miles, performed the in vivo lipolysis study in rats.
- Dr. G. Veglia helped with the Metabolomic analysis performed at the Minnesota NMR Center.

# ABSTRACT

Obesity is a major public health problem; in the U.S. nearly one third of the population is obese. The adipose tissue is innervated by the sympathetic nervous system (SNS), which regulates fat mass by playing a key role in initiating lipolysis and regulating lipid mobilization. **TLQP-21**, a 21 amino acid peptide encoded by the pre-pro-peptide VGF (non acronymic) expressed in the brain and sympathetic neurons innervating the adipose organ. Complement 3a receptor 1, C3aR1, is the target receptor for TLQP-21. Based on previous finding where peripheral TLQP-21 decreases adipocyte diameter and enhance β-adrenergic receptors (β-ARs) lipolysis in adipocytes the hypothesis tested in my thesis is that C3aR1 and β-ARs are required for TLQP-21 anti-obesity effects and the pro-lipolytic effects are mediated by increased mobilization of $[Ca^{2+}]_i$.

Departing from the first experimental structural analysis of TLQP-21 in solution and receptor-bound state, we tested our hypothesis using a combined *in vitro* and *in vivo* approach. Using 3T3L1 cells and pre-adipocytes as our *in vitro* model, we determined that TLQP-21 enhances lipolysis via increased intracellular $Ca^{2+}$ concentration $[Ca^{2+}]_i$, and activation of the MAPK/ERK pathway. The physiological effects of TLQP-21 were investigated *in vivo* using wild type, β-less ($\beta_1$, $\beta_2$, $\beta_3$-AR KO) and C3aR1 KO mice. Chronic TLQP-21 treatment in obese wild type mice significantly decreased body weight and fat mass promoting an overall healthier metabolic phenotype. Conversely β-less and C3aR1 KO resulted fully resistant to the anti-obesity effects.

Herein we identified the mechanism of TLQP-21 pro-lipolytic and anti-obesity effect and could thus be regarded as a novel target for pharmacotherapies of obesity.

# TABLE OF CONTENTS

# LIST OF TABLES

# LIST OF FIGURES

**CHAPTER FOUR**

**CHAPTER FIVE**

# Chapter One

# INTRODUCTION

## 1.1 SIGNIFICANCE OF THESIS

Obesity is globally increasing and is becoming a significant public health problem; in the U.S. more than one third of the population is obese [Ogden et al., 2014]. Visceral obesity is the main risk factor for type 2 diabetes, cardiovascular disease, liver dysfunction and metabolic syndrome [Després and Lemieux, 2006].

The adipose tissue is innervated by the sympathetic nervous terminals (SNS), that release norepinephrine (NE) whose main function is to regulate fat mass by initiating lipolysis and regulating lipid mobilization via the beta-adrenergic receptor (β-ARs) activation [Bartness and Bamshad, 1998]. However, obese patients often have impaired catecholamine-induced lipolysis [Arner, 1999].

A helpful treatment of obesity cold be a drug molecule that specifically increases lipolysis, however sympathomimetic drugs cause many unwanted side effects. A pharmacotherapy that directly targets fat stores without over activating the sympathetic nervous system would be ideal for the treatment of obesity and its comorbidities.

In this thesis we describe how the VGF derived peptide, TLQP-21 can limit obesity by specifically increasing lipolysis through the MAPK pathway without causing ectopic fat deposition or adverse effects, instead it promotes an overall healthier phenotype in obese mice.

# 1.2 STRUCTURE, DISTRIBUTION and FUNCTION of VGF and its DERIVED PEPTIDES

## 1.2.1 Structure of VGF, a neurotrophin inducible gene

VGF (not acronymic) neurosecretory protein was identified for its rapid and ruboust transcriptional regulation by nerve growth factor (NGF) and other neurotrophins including BDNF and NT3 in rat pheochromocytoma PC12 cells [Levi et al., 1985; Cho et al., 1989; Salton et al., 1991; Bonni et al., 1995]. The *vgf* is a single copy gene composed of three exons and two small introns that interrupt the 5' untranslated encoding sequence; while exon 3 encodes for the entire protein coding sequence of VGF (**Figure 1.1**) [Hahm et al., 1999]. cAMP response element (CRE) and CCAAT box are essential for NGF induction of *vgf*, and is it mediated through the Ras-dependent signaling pathway [D'Arcangelo et al., 1996]. The primary VGF gene product is evolutionary conserved among species with an 85% identity [Ferri et al., 2011]. The *vgf* gene encodes a 617-amino acid polypeptide in humans, and a 615- amino acid protein in rats [Levi et al., 1985], present on chromosome 7q22 in humans [Canu et al., 1997] and on chromosome 5 in mice [Hahm et al., 1999].

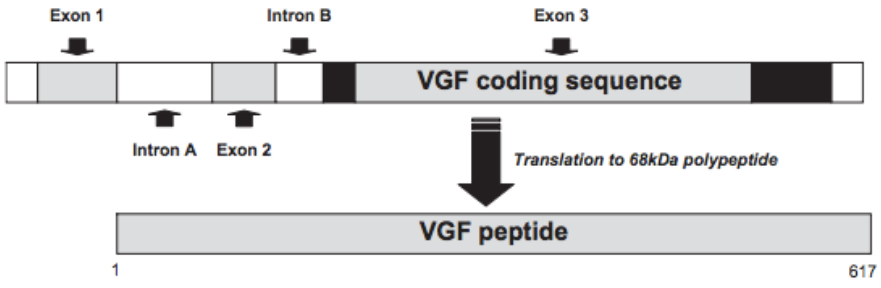


**Figure 1.1. Schematic diagram of the *vgf* gene** (adapted from Jethwa and Ebling, 2008). The entire VGF protein sequence is encoded by exon 3.

The VGF protein has a typical secretory leader sequence of 22 amino acid (single peptide) at the N-terminal, which promotes translocation into the endoplasmic reticulum [Levi et al.,1985]. Following cleavage between amino acid 23 and 24, a highly acidic 68kDa VGF precursor polypeptide is generated rich in proline and

glycine [Salton et al., 1991]. However, in western blot analysis, the VGF protein is detected as a doublet of an 80-90kDa protein due to no post-translational modification after protein biosynthesis takes place and the very high proline content that reduces electrophoretic mobility of the protein [Levi et al., 1985].

### 1.2.2 Processing of VGF derived peptides

Within the VGF polypeptide, ten potential cleavage sites with basic amino acid residues for prohormone convertases 1/3 and 2 (PCs), members of the family of subtilisin/kexin-like serine proteinases [Seidah and Chrétien, 1999; Steiner, 1998] have been identified (**Figure 1.2**). These ten cleavage sites are also highly conserved across species. However, since some N-terminal human VGF peptides do not present the classic motifs for PC cleavage, it is possible that other endoproteases, yet to be identified, are also involved in processing of VGF [Levi et al., 2004]. Thus, the number of VGF peptide might be greater than currently known.

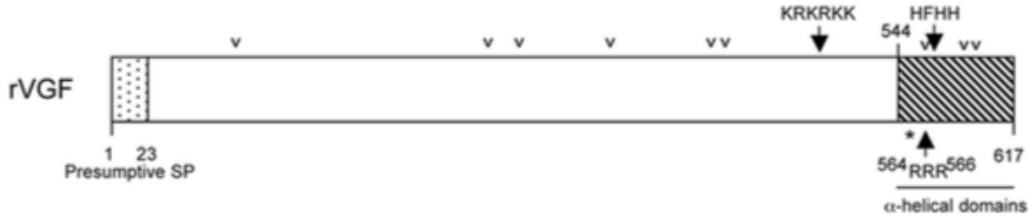


**Figure 1.2. Schematic diagram of potential cleavage sites for prohormone convertases in the VGF structure** (adapted from Bartolomucci et al., 2011). The arrowheads represent paired or multiple basic residues that are potential PC cleavage sites, the asterisk represents a noncanonical cleavage site 553RPR555 that is cleaved to generate a number of peptides.

Upon cleavage, proVGF yields a number of smaller peptides that together with proVGF are stored in large dense core secretory granules in neuronal and neuroendocrine cells, and released in response to membrane depolarization stimuli through regulated secretory pathways [Trani et al., 2002; Possenti et al., 1989]. Garcia et al., [2005] showed that along with an N-terminal signal peptide-containing domain, the C-terminal 73-amino acid fragment of VGF, containing two predicted α-helical loops and four potential prohormone convertase (PC) cleavage sites (**Figure 1.2**), is necessary and sufficient to sort into large dense core vesicle and the

regulated secretion from PC12 and INS-1 cells. Because of the processing, packaging, storing and regulated release of VGF and its fragments, VGF is considered part of the granin family of peptides [Bartolomucci et al., 2011].

VGF is a multifunctional peptide precursor. Through western blot analyses and mass spectrometry several VGF peptides have been identified and some have been shown to be biologically active. In western blots analysis, besides the 80-90kDa protein, using a panel of antibodies against the C-terminal nonapeptide of rat VGF protein, two species with apparent molecular weights of 20 kDa (VGF20 or NAPP129) and 10 kDa (VGF10 or TLQP-62) are detected in rat brain homogenates, in extracts of primary cultures of cerebellar granule cells and in neuronal, endocrine, and pancreatic β-cell lines. The cleavage sites used for NAPP129 is $KRKRKK_{488}$ motif targeted by both PC1/3 or PC2, while the Arg-Pro-$Arg_{555}$ ($RPR_{555}$) sequence (rat VGF) preferentially cleaved by PC1/3 gives raise to peptides containing the N-terminal TLQP motif (**Figure 1.2**) [Trani et al., 2002]. Others peptides of 18 kDa and 6 kDa (VGF18 and VGF6 or HFHH41) are also often detected in western blots [Trani et al.,1995; 2002; Possenti et al., 1999]. The first VGF peptide identified was a C-terminal AQEE 30 or Peptide V in bovine posterior pituitary [Liu et al., 1994]. Presently known N-terminal and C-terminal VGF derived peptides in mouse are depicted in **Figure 1.3**.

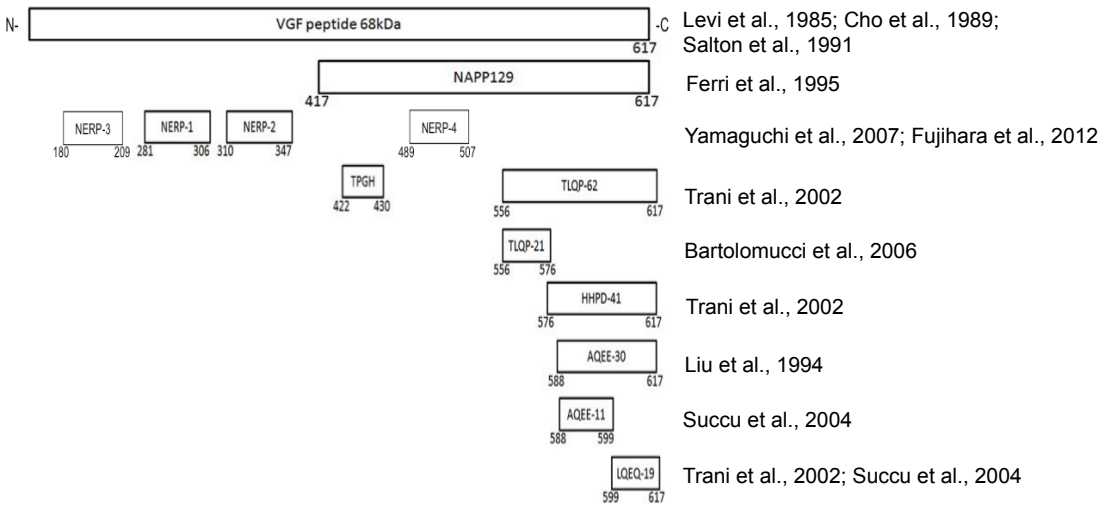


**Figure 1.3. VGF derived peptides in rat** [modified from Lewis et al., 2015]. The proVGF polypeptide and derived peptides along with the first study where the specific peptide was first described.

In human cerebrospinal fluid three N-terminal fragments (amino acids 23–62 APPG40, 26–62 APPG37, and 23–59 GRPE37) have been identified [Stark et al., 2001]. By convention the VGF derived peptides are designated by the four N-terminal amino acids and the total length [Levi et al., 2004], for example VGF10 is called TLQP-62. Several biologically active VGF peptides have been identified in rodents and possess multiple biological activities, including regulation of energy balance, pain, depression, stress, gut contraction, sex behavior and reproduction. See **Table 1.1**.

| Peptide name and Amino acid position in the VGF (rat) sequence | Biological function | References |
|---|---|---|
| NERP-1 (285-309) | suppress vasopressin secretion, penile erection | Toshinai et al. 2009; Melis et al., 2012 |
| NERP-2 (313-350) | suppress vasopressin secretion, orexigenic effects, locomotor activity, body temperature, oxygen consumption, penile erection, enhances glucose stimulated insulin secretion (GSIS) | Toshinai et al., 2010; Melis et al., 2012; Moin et al., 2012 |
| NERP-3 (180-209) | induces vasopressin secretion | Fujihara et al., 2012 |
| TLQP-62 (556-617) | enhances GSIS, memory, orexigenic effects, induces behavioral mechanical and cold hypersensitivity, increases neuronal excitability | Petrocchi et al., 2015; Lin et al., 2015; Brancia et al., 2010; Moss et al., 2008, Bartolomucci et al., 2007 |
| HHPD-41 (577-617) | orexigenic effects | Bartolomucci et al., 2007 |
| TLQP-21 (556-576) | increases energy expenditure, increases lipolysis, feeding behavior, anti-hypertensive, enhances GSIS, modulates inflammatory pain, regulates apoptosis, modulates stress response and gastric contractility | Bartolomucci et al., 2006; Jethwa et al., 2007; Possenti et al., 2012; Fargali et al., 2014; Fairbanks et al., 2014; Severini et al., 2008; 2009; Zhang et al., 2013; Stephens et al., 2012; Petrella et al. 2012: Razzoli et al., 2012: Sibilia et al., 2012; |
| AQEE-30 (588-617) | facilitates penile erection, induces thermal hyperalgesia | Succu et al., 2004; 2005; Riedl et al., 2009 |
| LQEQ-19 (599-617) | facilitates penile erection, induces thermal hyperalgesia | Succu et al., 2004; 2005; Riedl et al., 2009 |

**Table 1.1. VGF derived biologically active peptides.** The VGF derived peptides known to exert a biological function along with the study where the specific functions were first described.

### 1.2.3 Tissue distribution of VGF and its derived peptides

VGF is widely expressed in several neurons throughout the brain with the highest expression being in the hypothalamus, especially in the preoptic, periventricular, paraventricular (PVN), supraoptic (SON), suprachiasmatic (SCN), and arcuate nuclei

(ARC) [van den Pol et al., 1989; Salton et al., 1991; Snyder and Salton, 1998; Wisor et al., 1997; Razzoli et al., 2012].

During embryogenesis VGF mRNA is restricted to specific neurotrophin targets in the central and peripheral nervous system. More specifically, VGF expression in the peripheral nervous system (PNS) is found in the dorsal root ganglion and sympathetic ganglia, neural crest cells migrating to enteric ganglia, in primordia of the vagal (X) complex, in the α- and γ-motor neurons of the ventral horn and in the dorsal horn neurons of the spinal cord, cranial nuclei, basal forebrain, adrenal and pituitary [Snyder and Salton, 1998; Snyder et al., 1998; Ferri et al., 1992]. In later embryogenesis VGF expression is also detected in the esophagus, stomach and pancreas [Levi et al., 2004]. At birth VGF mRNA expression is found in neurons throughout the brain and additionally found in a subset of peripheral neuroendocrine tissues, including the anterior and posterior pituitary lobes, adrenal medulla, β-cells of the pancreas, and gastrointestinal tract [Salton et al., 1991; Snyder and Salton, 1998; Ferri at al., 1992; Brancia et al., 2010].

VGF C-terminal peptides and NERP peptides have been found in several hypothalamic locations and endocrine organs [Yamaguchi et al., 2007; Mishiro-Sato et al., 2010; Cocco et al., 2007]. In pancreatic islets, VGF C-terminus peptides are detected in glucagon and in pancreatic polypeptide cells, while TLQP-11 (rat $VGF_{556–567}$) and TLQP-21 (rat $VGF_{556–576}$) peptides are restricted to somatostatin containing D-cells. NERP-1 is found in most islet cells, including alpha and beta cells [Cocco et al., 2007]. In the adrenal gland, TLQP peptides are restricted to only to the adrenalin cells [D'Amato et al., 2008]. In the gut, VGF derived peptides are found in the ghrelin, somatostatin, enterochromaffin, enterochromaffin-like, and principal cells. The C-terminal peptides are found in the gastric innervation [Ferri et al., 2011].

### 1.2.4 Physiological functions of VGF and derived peptides

The tissue specific expression and distribution of VGF and its derived peptides suggest different physiological roles in these different tissues [Bartolomucci et al., 2011].

#### *Energy balance*

The regulation of eating behavior and energy metabolism is regulated by many nuclei of the CNS, particularly the hypothalamus, which modulates the action of the central

and peripheral mediators activating catabolic or anabolic pathways [Horvath, 2005; Williams et al., 2000; Schwartz et al., 2000]. The ARC expresses receptors for leptin, insulin and ghrelin, and responds to peripheral metabolic changes by finely regulating feeding and energy expenditure [Horvath, 2005]. These two processes occur through distinct neural pathways [Cone, 2001], with the activation of the different sub-population of the ARC. Activation of cells neuropeptide (NP) Y / agouti-related peptide (AGRP) located in the medial ARC determines the activation of the anabolic pathway where food intake is stimulated and energy expenditure is reduced; while activation of the proopiomelanocortin/cocaine- and amphetamine-regulated transcript (POMC/CART) neurons located in the lateral ARC produces catabolic effects, decreased food intake and increased energy expenditure [Schwartz et al., 2000]. More specifically, activation of the POMC/CART neurons by leptin triggers the release of $\alpha$-melanocyte–stimulating hormone ($\alpha$ -MSH) from POMC axon terminals, which in turn activates melanocortin receptor 4 (MC4R), leading to suppressed food intake and increased energy expenditure [Horvath, 2005]. Overexpression of the agouti protein ($A^y/a$) or its receptors, while ablation of MC4R ($MC4R^{-/-}$) or $\alpha$-MSH, all cause decrease in satiety signal induces the onset of obesity associated with hyperphagia, hyperinsulinemia, and hyperglycemia [Barsh et al. 1999]. These genetic models show how the central melanocortin system regulates energy balance as well as glucose homeostasis [Barsh et al. 1999].

The NPY/AGRP and POMC/CART neurons project to other regions of the hypothalamus including the paraventricular nucleus (PVN), zona incerta, perifornical area (PFA) and lateral hypothalamus (LHA), known as the second order neurons [Schwartz et al., 2000]. NPY release in LHA/PFA regions that express thyrotropin-releasing hormone (TRH), corticotropin-releasing hormone (CRH) oxytocin (OXY) causes orexigenic effects; whereas $\alpha$-MSH from the POMC neurons in the PVN stimulates anorexic effects [Schwartz et al., 2000]. Integration of peripheral signals with central signaling regulates feeding behavior, energy expenditure, and energy storage.

### *Vgf and energy balance*

The high expression of VGF in the hypothalamus [van den Pol et al., 1989] first suggested that VGF and its derived peptides could be play a role in energy balance since this brain region plays an important role in the regulation of energy

homeostasis [Cone et al., 2001]. VGF is expressed in POMC and NPY neurons in ARC and its expression is modulated by the nutritional status [Hahm et al., 1999; 2002]. Fasting induced the expression of *vgf* in the NPY neurons, while feeding switches the expression to POMC neurons [Hahm et al., 1999]. Moreover, similar to NPY, in fasting conditions leptin administration inhibits the fasting induced increase in VGF mRNA suggesting that leptin regulates VGF expression [Hahm et al., 2002]. Additionally, VGF expression in the ARC of leptin-deficient *ob/ob* and leptin receptor-mutant *db/db* mice resembled the expression of fasted wild-type mice [Hahm et al., 2002]. These data implied VGF in the central regulation of energy homeostasis.

In addition to the expression of VGF in the ARC, the best evidence of VGF regulating energy homeostasis is from the VGF knock out mice [Hahm et al., 1999]. The VGF $^{-/-}$ mice at birth are identical to heterozygous and wild type mice. A few days after birth a VGF $^{-/-}$ are substantially smaller in size and weight compared to wild-type littermates, with 50-70% less weight at weaning and during adulthood [Hahm et al., 1999]. Lower body weight was paralleled by approximately 50% less body fat compared to wild-type littermates confirming decreased adiposity. As expected, consistent with decreased peripheral adiposity, leptin levels were decreased as well as serum glucose and insulin levels, while serum corticosterone level was increase, a metabolic profile similar to fasting. However, food intake was comparable to wild type mice or increased per grams of body weight. VGF $^{-/-}$ mice fed ab libitum displayed a 600 to 800% increase in hypothalamic AgRP and NPY gene expression and 75% decrease of POMC mRNA, resembling the phenotype of mice fasting 48h [Hahm et al., 1999; Mizuno et al., 1998]. Additionally, compared to the wild type mice, VGF $^{-/-}$ mice are hyperactive [Hahm et al., 1999] and hypermetabolic with a 50% increase in $O_2$ consumption along with an increase expression of uncoupling protein in BAT and significantly smaller white adipose depots and adipocyte diameter [Watson et al., 2009], due to increased sympathetic innervation and lipolysis [Fargali et al., 2012]. Moreover, VGF$^{-/-}$ mice presented reproductive abnormalities similar to leptin deficient mice suggesting that the reduced circulating leptin was insufficient to activate the hypothalamic-pituitary-gonadal axis (HPG) [Hahm et al., 1999].

Further studies demonstrated that VGF deletion prevents obesity and reduces weight gain in obese mouse models, even under high fat conditions and gold thioglucose [Hahm et al., 2002] blocking the development of hyperglycemia and hyperinsulinemia pinpointing the requirement of VGF in the development of obesity [Watson et al., 2005]. Ablation of the *vgf* gene in $A^y$/a suppresses the obese phenotype, however,

ablation of the *vgf* gene in ob/ob mice blocked hyperphagia given by the lack of leptin signaling on the melanocortin system, but did not prevent the development of increased adiposity or reduced body temperature. These results lead to the hypothesis that VGF might be acting downstream of AgRP-melanocortin circuits [Hahm et al., 2002].

### *Vgf-derived peptides and energy homeostasis*

The lean, hypermetabolic and resistant to obesity phenotype attributes an anabolic role to VGF, however ablating the vgf gene does not elucidate which of its derived peptides are driving the anabolic effects.

Administration of TLQP-21, identified in rat brain by of immunoprecipitation, microcapillary liquid chromatography–tandem mass spectrometry and database searching algorithms [Bartolomucci et al., 2006] in mice and Siberian hamsters induced catabolic effects [Bartolomucci et al., 2006; Jethwa et al., 2007]. In Bartolomucci et al., [2006], 14 days of itracerebroventricular (i.c.v.) TLQP-21 treatment in chow fed mice induced an increase in resting energy expenditure and rectal temperature associated by an increase in catabolic markers in peripheral organs without affecting body weight and food intake. Specifically, elevated epinephrine content, up-regulation of β2-ARs were found in the brown adipose tissue; while uncoupling protein 1 (UCP-1) peroxisome proliferator-activated receptor δ (PPAR δ) and β3-AR were increased in epididymal white adipose tissue [Bartolomucci et al., 2006]. Chronic i.c.v. TLQP-21 treatment in high fat diet fed mice prevented the onset of the obese phenotype limiting weight and fat gain, normalizing gherin levels, lowering serum leptin and triglycerides (TG) levels, while free fatty acids (FFA) and glucose level were unaffected [Bartolomucci et al., 2006]. Moreover, hypothalamic expressions of agouti-related protein (AgRP), NPY, α-melanocyte-stimulating hormone (α-MSH), POMC, and corticotrophin-releasing hormone (CRH) were normalized by TLQP-21 treatment in high fat diet mice [Bartolomucci et al., 2007]. These data show that i.c.v. administration of TLQP-21 limits the early phase of diet-induced obesity by enhancing energy expenditure and catabolic pathways in the adipose organ [Bartolomucci et al., 2006].

Similar catabolic effects are reported in Jethwa et al., [2007] using Siberian hamsters, normally used as a seasonal model of energy balance to understand the hypothalamic mechanisms regulating energy balance [Jethwa et al., 2007]. During

winter Siberian hamsters become hypophagic and catabolize abdominal fat reserves as an energy source losing up to 40% of their total body weight [Bartness et al., 1989; Klingenspor et al., 1996] paralleled with a significant increase in VGF mRNA in the arcuate nucleus during winter when catabolic compared to the summer when anabolic [Barrett et al., 2004]. Acute i.c.v. administration of TLQP-21 to Siberian hamsters decreased food intake and body weight in a dose dependent manner without affecting energy expenditure. Chronic treatment caused a sustained reduction in food intake and a decrease in body weight and abdominal fat pad content, again with no effects on oxygen consumption suggesting that the weight loss was given by a reduced caloric intake rather than increases in metabolic rate [Jethwa et al., 2007]. Together these data are in contrast with the anabolic drive observed in the VGF $^{-/-}$ mice suggesting that the VGF derived peptides exerts catabolic effects [Hahm et al., 1999].

Bartolomucci et al., [2007] report preliminary evidences suggesting that i.c.v. injections of TLQP-62 and its cleaved product HHPD-41 increase feeding behavior in overnight fasted mice exerting opposite effects compared to TLQP-21 [Bartolomucci et al., 2007]. Another prevalently anabolic VGF derived peptides is NERP-2, an N-terminal peptides [Toshinai et al., 2010; Melis et al., 2012]. i.c.v. administration of NERP-2 in rats increases food intake through the orexin pathway [Toshinai et al., 2010]. Moreover NERP-2 injections acutely increased body temperature, oxygen consumption and locomotor activity via the orexin system [Toshinai et al., 2010].

From these studies it has emerged that some of the VGF derived peptide have opposing physiological effects, some exert catabolic effects (TLQP-21), while others oppose these effects by driving anabolic functions (TLQP-62; HHPD-41; NERP-2) suggesting that the germline VGF $^{-/-}$ model could be obscuring the specific actions of its peptides.

# 1.3 THE ADIPOSE ORGAN

## 1.3.1 Adipocytes

Adipocytes are classically divided into white and brown, while a third putative cell type named beige/brite have recently been proposed [Giralt et al., 2013]. White adipocytes are the primary long-term storage of chemical energy under the form of triacylglycerol; brown adipocytes express UCP1 and play an important role in energy expenditure by heat production [Rothwell and Stock, 1987]. These cell types have specific morphological and physiological differences, their own vascular and nerve supply and distributed in distinct locations of the body [Cinti, 2001]. Conventionally white adipocytes are considered leptin positive and UCP1 negative cells, while brown adipocytes are UCP1 positive and leptin negative cells [Cinti et al., 1997]. Brown adipocytes are normally present within several subcutaneous and visceral white adipose depots (WAT) and are not exclusive to interscapular fat [Cinti, 2012]. Brown adipocytes are the primary cells in brown adipose tissue. The adipose organ is innervated and vascularized [Bartness and Bamshad, 1998], with the brown adipose tissue (BAT) being five-six times more innervated and vascularized than white adipocytes [Cinti, 2012]. However, certain stimuli such as cold and catecholaminergic stimulation can induce increased vascularization and innervation in WAT with an increase in the number of brown adipocytes within WAT [Murano et al., 2009]. The process is known as “browing” of the adipose tissue where white adipocytes morphologically and functionally resemble a brown adipocyte [Cinti, 2002]. These beige/brite (brown in white) cells, also called “brown like” cells have characteristics of white and brown adipocytes, they are leptin and UCP1 postive cells found within the white adipose depots and considered protective against diet induced obesity [Wu et al., 2012; Walden 2012; Himms-Hagen et al., 2000]. It has been suggested that the brown like cells are a result of the conversion or transdiffrentiation of the white fat cells to brown adipocytes [Cinti, 2002] or are generated by specific beige precursor cells [Wu et al., 2013].

## 1.3.2 Morphology, distribution and function of white adipocytes

WAT serves several functions: it is a thermal insulator, provides mechanical support for organs, has a role in the inflammation process through pre-adipocytes acting as

macrophage like cells [Cousin et al., 1999], it is an endocrine organ [Kershaw and Flier, 2004], and most importantly it is the storage site of lipids under the form of triacylglycerols (TAG) that provide a long term fuel reserve [Cinti, 2001].

The major component of adipose tissue are the parenchymal cells called adipocytes, but also stromal vascular cells, blood vessels, nerves and lymph nodes build up the tissue. One big large lipid droplet and few and small mitochondria with randomly oriented cristae characterizes the unilocular white adipocytes (**Figure 1.4**) [Cinti, 2001]. 90% of the cell volume is occupied by the single cytoplasmic triacylglycerol-(TAG) containing lipid droplet that displaces the cell nucleus and organelles against the plasma membrane, giving the cell a ring shape [Cinti, 2001].

White adipose depots (WAT) are not as richly vascularized as brown depots, however an extensive capillary network surrounds each adipocyte [Crandall and DiGirolamo, 1990], that plays an important role in increasing substrate delivery for triglyceride clearance after feeding and transporting the lipolyitic products (non-esterified free fatty acids and glycerol) during fasting or during exercise [Rosell and Belfrage, 1979; Pénicaud et al., 2000], as well as many other secreted protein factors (leptin, resistin, adiponectin, cytokines) to other organs [Yildiz et al., 2004; Steppan et al., 2001].

White depots are primarily located in three major anatomical areas: visceral or intraperitoneal fat pads that surround the inner organs and are divided into perigonadal, perirenal, retroperitoneal, mediastinic, and mesenteric; subcutaneous adipose depot divided into interscapular, subscapular, axillary, cervical and inguinal; and dermal adipose, a relatively continuous sheath of lipid [Cinti, 1999; Kissebah and Krakower, 1994]. Even though the exact mechanisms are still unknown, it has been shown that visceral/intraabdominal fat; mostly perigonadal and mesenteric fat are the greatest risk factor for insulin resistance and metabolic abnormalities [Bergman et al., 2006]. This is likely due to anatomical position of the visceral fat (portal circulation into the liver) and the molecular characteristics such as increased lipolytic ability [Bergman et al., 2006; Després et al., 2008]. Abdominal obesity is a major risk factor for chronic diseases including, type 2 diabetes, cardiovascular disease, cancer and metabolic syndrome [Kahn et al., 2006; Després et al., 2008] that leads to premature death.

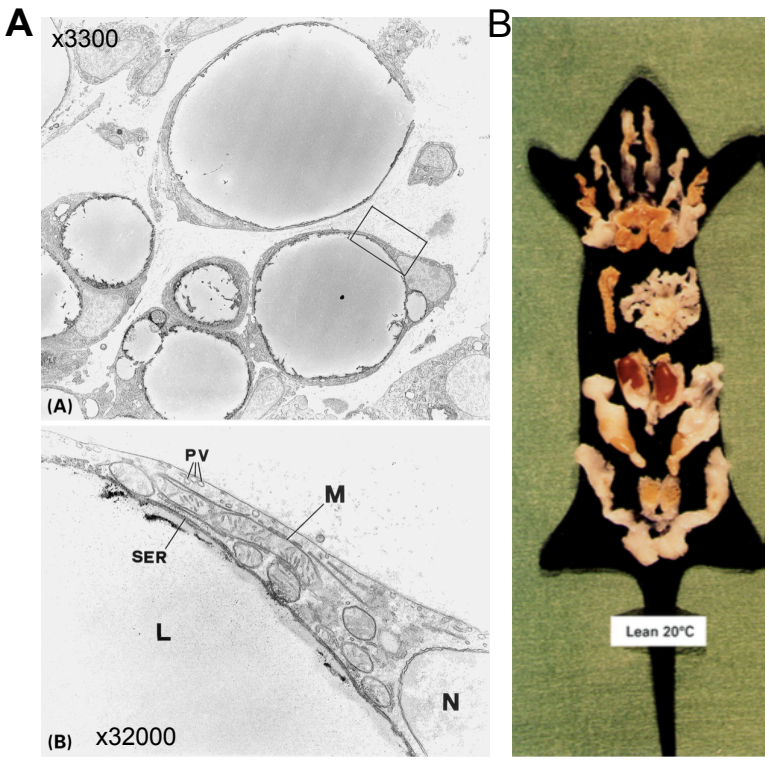


**Figure 1.4. Morphology and distribution of white adipose tissue.** (**A**) Transmission electron microscopy of epididymal white adipose tissue and enlargement of the framed area in A, showing the cytoplasm of a white adipocyte containing few and small mitochondria (M) with randomly-oriented cristae. PV, pinocytosis vesicles; SER, smooth endoplasmic reticulum; L, lipid droplet. N, nucleus. (**B**) Gross anatomy of the adipose organs of adult mice kept at 20°C and at 4°C. (From Cinti. The adipose organ: morphological perspectives of adipose tissues. Proc Nutr Soc. 2001 Aug; 60(3):319-28.)

### 1.3.3 Innervation of white adipose depots

Sympathetic innervation of white adipose tissue (WAT) was shown over 100 years ago [Dogiel, 1898]. In situ immunohistochemistry was first used to identify direct sympathetic innervation in WAT. TH-positive, substance P and CGRP positive nerves within the white depots were indicative of SNS and sensory innervation [Bartness and Bamshad, 1998; Bartness et al., 2009, Bamshad et al., 1998; Giordano et al., 1996]. Sympathetic innervation differs in the different white adipose depots; perirenal and retroperitoneal visceral fat and subcutaneous scapular fat have the highest simpato-sensory innervation [Slavin and Ballard, 1978; Youngstrom and

Bartness, 1995]. Parenchymal fibers that express tyrosine hydroxylase (TH), an enzyme that is widely considered to be a marker of sympathetic/noradrenergic fibers [Giordano et al., 2008] have been shown to have at least three physiological functions in WAT: 1) regulation of cell proliferation and fat mass, the higher the innervation the lower the proliferation [Hausman et al. 2001; Foster and Bartness, 2006], 2) control some of the proteins secreted by the adipocytes [Trayhurn et al., 1995] and most importantly lipid mobilization or lipolysis [Bartness and Bamshad, 1998; Bartness et al., 2002].

The role of SNS innervation for lipid mobilization in WAT was assessed with electrophysiology recording [Niijima, 1989], chemical or surgical denervation, and electrical stimulation [Bartness and Bamshad, 1998]. Surgical sympathectomy reduces lipolysis in the denervated depots, while electrical stimulation of sympathetic nerve endings stimulates lipolysis and the release of free fatty acids (FFA) [Bartness and Bamshad, 1998]. However, surgical denervation is not fully selective for the SNS nerves since it affects sensory innervation too, therefore the reduction in lipolysis cannot be not purely attributed to the direct effect of SNS on adipocytes.

Pseudorabies virus (PRV) as a trans-synaptic retrograde neural tracer has been used to identify the CNS–SNS–WAT circuitry, identifying the SNS nuclei that project their efferent neurons to white fat [Bamshad et al., 1998]. This method, besides providing neuroatomical evidence of SNS within WAT also allowed elucidating the different grade of SNS innervation in the white fat depots [Bartness, 1995; Bamshad et al., 1998]. The different degree of innervations accounts for the difference in lipid mobilization among the fat pads [Youngstrom and Bartness, 1995]. After inoculation in epididymal (eWAT) and subcutaneous inguinal WAT (iWAT), PRV-infected sympathetic preganglionic cells were present in the *spinal cord* (intermediolateral cell group, central autonomic nucleus), the *brainstem* (nucleus of the solitary tract, lateral and rostroventrolateral reticular nuclei, and the C1/rostroventrolateral, rostroventromedial and caudal raphe nuclei/areas, ventral and alpha portions of the gigantocellular reticular nucleus and the raphe magnus nucleus), the *midbrain* (periaqueductal gray) and *forebrain* (hypothalamic regions: arcuate nucleus, dorsal, lateral, paraventricular, suprachiasmatic, nuclei and medial preoptic area; non-hypothalamic regions: zona incerta, medial amygdala, septum and bed nucleus of the stria terminalis) (**Figure 1.5**) [Bamshad et al., 1998]. Within the hypothalamic region, labeled neurons were detected in nuclei involved in food intake and body weight and most importantly lipid mobilization in WAT [Bartness, 1995; Zaia et al.,

1997]. Moreover, PRV inoculations have also allowed the identification of the ganglion innervating iWAT, T13 caudally, and eWAT, cells in ganglia T13 and L1-L2 [Youngstrom and Bartness, 1995].

Many tissues are innervated by both the SNS and the parasympathetic nervous system (PSNS) where they exert opposing effects. Controversial evidence is shown for parasympathetic innervation in WAT. Krejer et al. [2007] after chemically denervating the SNS innervation in WAT using the catecholaminergic neurotoxin 6-hydroxy-dopamine (6OHDA) to selectively destroy the SNS innervation sparing the parasympathetic nerves in white fat, and subsequent PVR inoculation, show bilateral and dense labeling in the dorsal motor nucleus of the vagal nerve (DMV) of the brain stem. Moreover, a selective and specifically surgically vagotomy in WAT (parasympathectomized) reduced insulin-mediated glucose and free fatty acid uptake and increase in HSL activity suggest that the physiological role of this parasympathetic input has anabolic effects on white adipocytes' metabolism opposing the catabolic action of SNS in WAT [Kreier and Buijs, 2007]. On the other hand, Giordano et al. [2006] show no histochemical evidence for three proven immunohistochemical markers of PSNS innervation, vesicular acetylcholine transporter (VAChT), markers for parasympathetic nerves; vasoactive intestinal peptide (VIP) and neuronal nitric oxide synthase (nNOS) the only two known neurotransmitters of parasympathetic noncholinergic nerves in visceral and subcutaneous fat pads of lean (C57) and obese mice (ob/ob) as well as in rats [Giordano et al., 2006]. Moreover, using the same sympathectomy approach followed by injection of PRV into the SNS denervated tissue to label the proposed PSNS outflow from brain to WAT, no labeling in the sympathetic chain, spinal cord or brain was detected compared to the vehicle-injected WAT inoculated with PRV suggesting a complete lack of significant WAT PSNS innervation and the presence of only WAT SNS innervation.

Aside from the immunohistochemical evidence of sensory innervation in white fat depots [Bartness et al., 1998; Foster and Bartness, 2006], also neuroatomical evidence has been provided by application of the anterograde tract tracer true blue into inguinal and dorsal subcutaneous WAT that labels pseudounipolar neurons in the dorsal root ganglia [Fishman and Dark, 1987]. Sensory neurons in the dorsal root ganglia reach white depots [Fishman and Dark, 1987] and are thought to participate in the neural negative feedback control of the SNS innervation, reducing the SNS

drive to WAT therefore regulating the lipolytic rate and body fat accumulation in WAT [Song et al, 2009; Bartness et al., 2010].

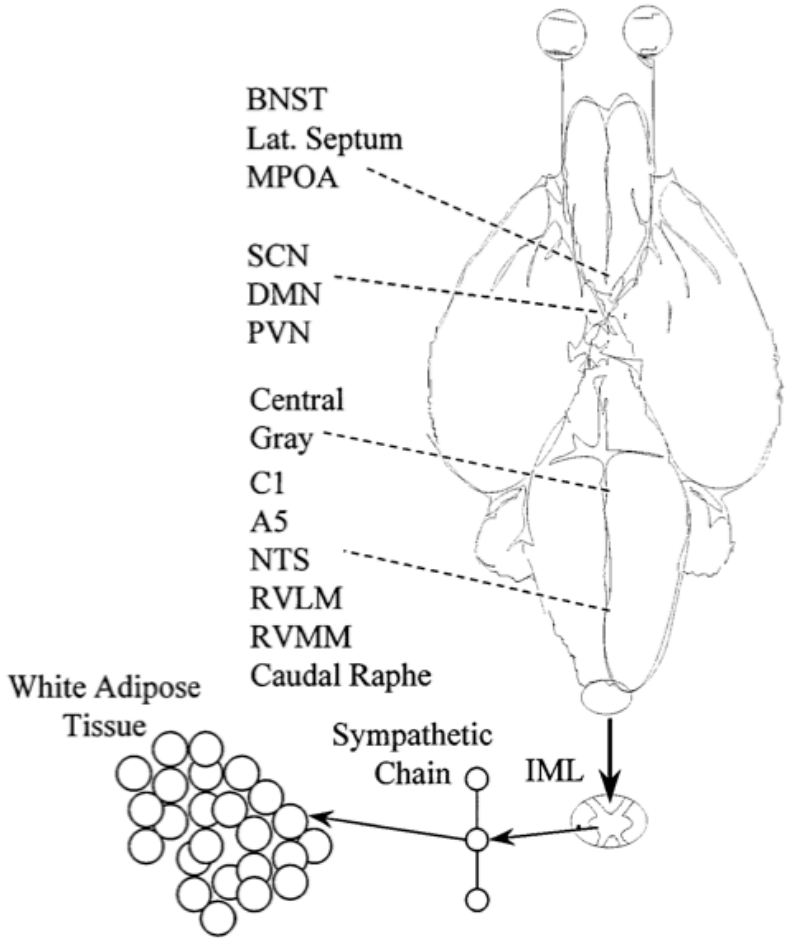


**Figure 1.5. Schematic diagram of the sympathetic nervous system outflow from the central nervous system to white adipose** (From Bartness and Bamshad, 1998). Pseudorabies virus (PRV) was injected into the inguinal subcutaneous and epididymal white adipose tissue pads. PRV only travels through circuits retrogradely and only in synaptically connected neurons. This yields a hierarchical chain of functionally connected neurons labeling circuits from their end to their beginnings in a backward manner.

BNST, bed nucleus of the stria terminalis; Lat Septum, lateral septum; MPOA, medial preoptic area: SCN, suprachiasmatic nucleus; DMN, dorsal medial nucleus; PVN, paraventricular nucleus of the hypothalamus; C1, C1 epinephrinergic cell group; A5, A5 noradrenergic cell group; NTS, nucleus of the solitary tract; RVLM, rostral ventrolateral medulla; RVMM, rostral ventromedial medulla; Caudal Raphe, caudal raphe nuclear group; IML, intermediolateral cell column of the spinal cord.

### 1.3.4 Lipolysis in white adipose depots

Lipolysis is a tightly regulated catalytic pathway where TAG, the main energy source of the body, are hydrolyzed to generate fatty acids and glycerol. Upon increased energy demand, TAG stores are mobilized by their hydrolytic cleavage into non-esterified fatty acids (NEFAs), delivered via circulation to peripheral organs for β-oxidation and ATP production. Impaired lipolysis is often associated with obesity where basal lipolysis is increased releasing higher amounts of NEFA's in circulation that may contribute to the development of insulin resistance and decreased responsiveness to stimulated lipolysis [Large et al., 1999; Arner, 1999].

Many enzymes and regulatory proteins are involved in the regulated process of lipolysis, but the three most important and crucial lipases involved are adipose triglyceride lipase (ATGL) that performs the first step hydrolyzing TAGs to generate diacylglycerols (DAGs) and NEFA's, hormone-sensitive lipase (HSL) hydrolyses DAGs generating monoacylglycerols (MAGs) and NEFA's and finally monoglyceride lipase (MGL) that cleaves MAGs into NEFAs and glycerol [Zimmermann et al., 2004; Villena et al., 2004; Holm, 2003]. HSL is able to hydrolyze TAG, DAG and MAG, with the relative maximal hydrolysis rates for TAG:DAG:MAG being 1:10:1 [Lass et al., 2011], showing that HSL is the rate limiting enzyme for DAG hydrolysis. ATGL is the rate limiting enzyme for TAGs hydrolysis, in fact ATGL deficiency is associated with limited lipolysis and significant fat accumulation [Haemmerle et al., 2006]; while HSL deficient mice do not show increased fat deposition and are not overweight or obese [Haemmerle et al., 2002]. Moreover, in the absence of ATGL, NEFA and glycerol mobilization in response to β-adrenergic stimulation is only around 30%, suggesting that ATGL is essential for the full sympathetic induced lipolysis in adipocytes [Schweiger et al., 2006].

Lipolysis has a central role in lipid and energy homeostasis. Catecholamines are the primary activators of lipolysis, however other hormones, including glucagon and natriuretic peptides are important stimulating agents of lipolysis [Slavin et al., 1994; Sengenès et al., 2000]. Catecholamines, mainly neurotransmitter norepinephrine (NE), released from the postganglionic sympathetic nerve terminals innervating white depots [Arner, 2005; Bartness et al., 2009] bind and activate the β-adrenoreceptors (β-ARs) [Bartness and Bamshad, 1998; Bartness et al., 2009] present on the plasmatic membrane of the adipocytes. There are three type of β-ARs ($\beta_1$, $\beta_2$ and $\beta_3$), $\beta_3$-ARs being the most abundant in mature adipocytes [Collins and Surwit, 2001].

The activation of β-ARs triggers intracellular signalling that initiate lipolysis and regulate lipid mobilization.

Briefly, when NE binds to $G_s$-coupled β-AR it activates adenylyl cyclase (AC), which increases intracellular cyclic AMP (cAMP) resulting in the activating of cAMP dependent protein kinase A (PKA) [Jaworski et al., 2007]. PKA phosphorylates HSL in three serine residues (563, 659, and 660) that causes activation and consequent translocation from the cytosol to the lipid droplet where it can exert its mechanism of action [Holm, 2003]. PKA also phosphorylates perilipin [Clifford et al., 2000], the lipid droplet associated protein, moving it from the lipid droplet so that a larger surface of the lipid droplet is exposed to the lipases [Holm, 2003]. PKA also promotes the dissociation CGI-58 from the lipid droplet surface allowing for the interaction and activation of ATGL [Lass et al., 2006]. ATGL's enzymatic activity is co-activated by the protein comparative gene identification-58 (CGI-58) [Lass et al., 2006], this activation is induced during fasting and by glucocorticoids [Zimmermann et al., 2004]; while protein G0S2 specifically inhibits ATGL [Yang X et al., 2011]. Together the hydrolase activity of ATGL and HSL are responsible for more than 95% of lipolysis in murine WAT is given by the hydrolase activity of ATGL and HSL [Schweiger et al., 2006]. Besides PKA, HSL has phosphorylation sites for other protein kinase such extracellular signal-regulated kinase (ERK1/2) [Greenberg et al., 2001; Rapold et al., 2013; Drira et al., 2014]; glycogen synthase kinase-4 [Olsson et al., 1986]; $Ca^{2+}$/calmodulin-dependent kinase II, and AMP-activated kinase (AMPK) that can regulate the enzymes' activity [Garton et al., 1989]. To this date no effective regulators have been found for MGL and it is thought to be constitutively active [Lass et al., 2011].

Insulin exerts the most potent anti-lipoytic activity in adipocytes through the PI3K/Akt pathway and activation of protein kinase B (PKB) to induce phosphorylation of phosphodiesterase 3B (PDE3B). Activation of PDE3B results in the decrease of cAMP and thus PKA activity, reducing the phosphorylation of HSL and perilipin causing decrease in lipolysis [Langin, 2006]. NE, released by the postganglionic catecholaminergic neurons can also bind the $\alpha$-ARs ($\alpha_1$ or $\alpha_2$). Activation of $\alpha_2$-AR by NE switches on the counteracting mechanism of $\beta$-ARs since $\alpha_2$ AR is coupled to G inhibitory ($G_i$) protein receptors that inhibit AC lowering cAMP levels, thus limiting lipolysis [Lafontan et al., 1997]. On the other hand, $\alpha_1$ AR subtype has not been linked to lipolysis regulation so far, while it is involved in the control of glycogenolysis and lactate production [Lafontan et al., 1997].

### 1.3.4 TLQP-21 and lipolysis in white adipose depots

Other hormones and products of the sympathetic neurons beside NE regulate lipolysis including TLQP-21 [Possenti et al., 2012] and NPY [Turtzo et al., 2001]. NPY acting through its Y2 receptors (Y2R) on the adipocyte membrane promotes adipogenesi and down-regulates lipolysis [Valet et al., 1990; Turtzo et al., 2001; Kuo et al., 2007].

Our laboratory identified TLQP-21 as a neuropeptide regulator of NE-induced lipolysis [Possenti et al., 2012]. We showed that TLQP-21 is present in a subpopulation of sympathetic nerve fibers innervating WAT but not in adipocytes. Moreover, we showed for the first time that TLQP-21 does bind in a specific manner to the membrane of adipocytes from various fat pads and this binding was saturable. The binding was further increased in white depots of obese mice. Peripheral chronic TLQP-21 treatment in mice decreases adipocyte diameter, and increases tyrosine hydroxylase (TH) enzymatic activity and NE content in WAT. Contrarily to the increase in energy expenditure shown after i.c.v. treatment of the TLQP-21 peptide [Bartolomucci et al., 2006], peripheral treatment did not increase plasma epinephrine or temperature suggesting that peripheral TLQP-21 treatment does not activate central pathways [Possenti et al., 2012]. Peripheral TLQP-21 treatement increases sympathetic nerve sprouting in WAT [Possenti et al., 2012]. Incubation of primary mouse adipocytes with TLQP-21 and isoproterenol (ISO) led to the observation that TLQP-21 acts as a neuromodulator on adipocytes by increasing ISO-induced lipolysis [Possenti et al., 2012]. In 3T3L1 adipocytes TLQP-21 also potentiates ISO-induced phosphorylation of AMPK and HSL, but not PKA and PKC [Possenti et al., 2012]. These *in vivo* and *in vitro* findings indicate TLQP-21 as a novel pro-lipolytic agent that potentiates NE/β-AR-induced lipolysis. Moreover, TLQP-21 has been shown to increase intracellular $Ca^{2+}$ levels ($[Ca^{2+}]_i$) in several cell lines including cerebellar granules [Severini et al., 2008], GH3 [Petrocchi et al., 2013], brain and spinal cord-derived primary microglia [Chen et al., 2013], and insulinoma cell lines [Petrocchi et al., 2015]. Based on these evidences we hypothesized that TLQP-21 would bind to a seven transmembrane domain receptor on adipocytes membrane; perhaps a $G_q$ coupled receptor that activates phospholipase C beta (PLCβ) [Possenti et al., 2012]. In 2013 Hanneduche et al., using CHO-K1 cell line and rat ovary cell line O-342 identified the GPCR, C3aR1 (Complement 3a Receptor 1) as the target receptor for TLQP-21 [Hanneduche et al., 2013]. The C3aR1 receptor is expressed

on adipocytes and its expression is increased in obesity [Mamane et al., 2009], a finding in agreement with our receptor binding data [Possenti et al., 2012]. Furthermore, TLQP-21 modulation of pain [Rizzi et al., 2008; Fairbanks et al., 2014] can be mediated by the multiligand-binding protein gC1qR expressed in macrophages and microglia [Chen et al., 2013].

## 1.4 AIM OF this THESIS

TLQP-21 has been shown to enhance adrenergic-induced lipolysis in adipocytes and to target the C3aR1. However the structure of TLQP-21, the mechanism of C3aR1 activation, as well as the molecular mechanisms of TLQP-21 mediated lipolysis have yet to be elucidated. Therefore, the primary goal of this thesis is to determine TLQP-21 structure and function and to identify its pro-lipolytic and anti-obesity effect using a combined *in vitro* and *in vivo* approach.

# Chapter Two

# The TLQP-21 Peptide Activates the G-protein-coupled receptor C3aR1 via a *Folding-upon-Binding* Mechanism

Cheryl Cero[1#], Vitaly V. Vostrikov[2#], Raffaello Verardi[2#], Cinzia Severini[3], Tata Gopinath[2], Patrick D. Braun[4], Maria F. Sassano[5], Allison Gurney[1], Bryan L. Roth[5], Lucy Vulchanova[7], Roberta Possenti[3,6], Gianluigi Veglia[2*], Alessandro Bartolomucci[1*]

[1] Department of Integrative Biology and Physiology, University of Minnesota, Minneapolis, MN 55455

[2] Department of Biochemistry, Molecular Biology and Biophysics, University of Minnesota, Minneapolis, MN 55455

[3] Institute of Cell Biology and Neurobiology, National Research Council, Rome, Italy 00143

[4] Department of Pharmaceutics, University of Minnesota, Minneapolis, MN 55455

[5] Department of Pharmacology and National Institute of Mental Health Psychoactive Drug Screening Program School of Medicine, University of North Carolina, Chapel Hill, NC 27599.

[6] Department of Medicine of System, University of Rome 'Tor Vergata', Rome, Italy 00133.

[7] Department of Veterinary and Biomedical Sciences, University of Minnesota, Saint Paul, MN 55108.

[#] denotes equal contribution.

This chapter contains an original research article previously published:

**Structure. 2014 Dec 2;22(12):1744-53.**

## 2.1 SUMMARY

TLQP-21, a VGF-encoded peptide is emerging as a novel target for obesity-associated disorders. TLQP-21 is found in the sympathetic nerve terminals in the adipose tissue and targets the G-protein-coupled-receptor (GPCR) Complement-3a-Receptor1 (C3aR1). So far, the mechanisms of TLQP-21-induced receptor activation remained unexplored. Here, we report that TLQP-21 is intrinsically disordered and undergoes a *disorder-to-order* transition, adopting a α-helical conformation, upon targeting cells expressing the C3aR1. We determined that the hot spots for TLQP-21 are located at the C-terminus, with mutations in the last four amino acids progressively reducing the bioactivity and, a single site mutation (R21A) or C-terminal amidation abolishing its function completely. Interestingly, the human TLQP-21 sequence carrying a S20A substitution activates the human C3aR1 receptor with lower potency compared to the rodent sequence. These studies reveal the mechanism of action of TLQP-21 and provide molecular templates for designing agonists and antagonists to modulate C3aR1 functions.

**Graphical Abstract**

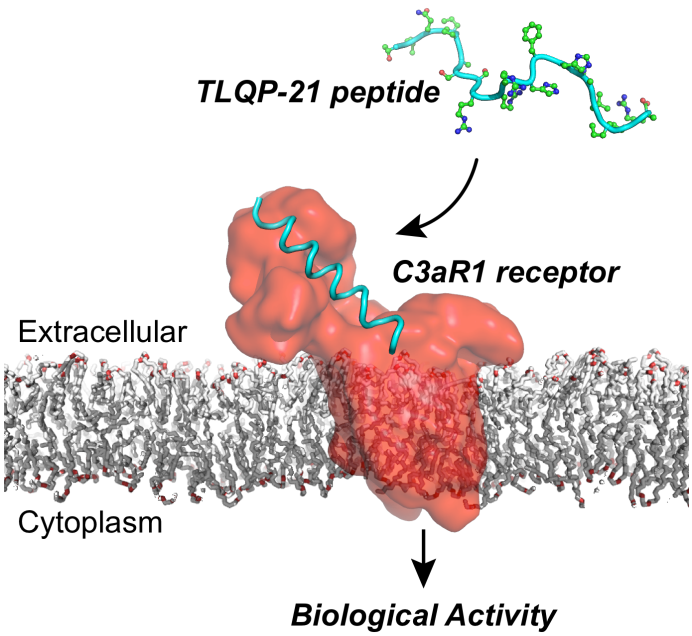

## 2.2 INTRODUCTION

The *Vgf* gene is a member of the extended granin family of peptide-precursor proteins that encodes a 615 amino acid pro-peptide (617 in rodents) [Bartolomucci et al., 2001]. This pro-peptide is processed to yield several bioactive fragments, with at least eight possessing non-redundant biological functions [Bartolomucci et al., 2011; Hahm et al., 1999]. Due to their involvement in the pathophysiology of human diseases such as psychiatric, neurological and metabolic disorders as well as several tumors, VGF peptide fragments are also being investigated as possible disease biomarkers [Bartolomucci et al., 2011]. The best studied fragment is the C-terminal internal peptide designated TLQP-21, whose sequence and function we have identified and extensively characterized [Bartolomucci et al., 2006]. TLQP-21 is a multifunctional peptide that regulates energy balance [Bartolomucci et al., 2006, Jethwa et al., 2007, Possenti et al., 2012], glucose metabolism [Stephens et al., 2012], gastric function [Severini et al., 2009], nociception [Rizzi et al., 2007, Chen et al., 2013, Fairbanks et al., 2014], blood pressure regulation [Fargali et al., 2014], reproduction [Aguilar et al., 2013] and stress [Razzoli et al., 2012]. Importantly, it was found that a central infusion of TLQP-21 increases energy expenditure and prevents obesity in rodents [Bartolomucci et al., 2006, Jethwa et al., 2007]. Additionally, chronic peripheral infusions of TLQP-21 in obese rodents led to decreased adipocyte diameter [Possenti et al., 2012] improved hypertension [Fargali et al., 2014] and diabetes [Stephens et al., 2012], making it an important target to counteract obesity-associated disorders. However, the molecular mechanisms of TLQP-21 function are still largely unknown. The recent discovery that TLQP-21 directly targets the Complement 3a receptor 1 (C3aR1) has reinvigorated both physiological and pharmacological interest for this peptide as a potential drug target [Hannedouche et al., 2013]. C3aR1 is a member of the GPCR superfamily, characterized by seven transmembrane domains and a large second extracellular loop [Klos et al., 2013, Roglic et al., 1996]. While its role in the innate immune response is well established, C3aR1 is now emerging with a much broader pattern of expressions in different tissues and functions involving cell metabolism [e.g. Mamane et al., 2009; Lo et al., 2014]. In obesity, a significant increase of adipose-tissue specific C3aR1 expression has been found [Mamane et al., 2009], with concomitant increase of TLQP-21 binding affinity [Possenti et al., 2012]. Additionally, knockout studies targeting C3,

C3aR1 and VGF suggest direct involvement of the C3aR1 receptor in both adiposity and energy balance [Mamane et al., 2009, Hahm et al., 1999, 2001, Roy et al., 2008, Fargali et al., 2012, Watson et al., 2005]. Here, we used solid-state NMR spectroscopy in combination with photoaffinity labeling, biological assays as well as alanine-scanning mutagenesis to elucidate the structural determinants of TLQP-21 binding to C3aR1. We studied the binding of TLQP-21 to cells expressing the receptor as well as receptor knockout cells. We found that the TLQP-21 peptide is intrinsically disordered but adopts an ordered helical conformation upon interacting with cells expressing the C3aR1 receptor. Furthermore, we determined that the C-terminal domain of the peptide comprises the hot-spots for its biological function, with the R21A mutation able to abrogate TLQP-21 activity completely. Finally, we found that the human sequence of TLQP-21 carrying a S20A substitution activates human C3aR1 receptor with lower potency than the rodent sequence. Overall, these studies reveal a folding-upon-binding mechanism for the activation of the C3aR1 receptor by the TLQP-21 peptide, and identify the hot-spots to tune its biological function.

## 2.3 EXPERIMENTAL PROCEDURES

**Peptide Synthesis and NMR spectroscopy.**

*General.* All solvents used were HPLC grade. DIEA and TFA (peptide synthesis grade) were purchased from Fisher. Fmoc-protected amino acids, HBTU and HOBt, were purchased from AnaSpec. Preloaded Fmoc-AA-PEG-PS resins were purchased from Applied Biosystems. N-Fmoc isotopically labeled amino acids were purchased from Cambridge Isotope Laboratory. All other reagents were obtained from Sigma-Aldrich.

*Synthesis of TLQP22.1* Starting with Fmoc-ARG−PEG-PS resin (initial loading 0.18 mmol/g), the 21 residue peptide TLQP21 was synthesized using Fmoc solid-phase synthesis on a CEM microwave peptide synthesizer. Side-chain protecting groups were 2,2,4,6,7-pentamethyldihydrobenzofuran-5-sulfonyl (Pbf) for Arg, triphenylmethyl (Trt) for Gln and His; and tert-butyl ethers (tBu) for Ser and Thr. Fmoc removal was achieved using a solution of 20% piperidine in DMF for 5 min. HBTU/HOBt/DIEA couplings required 7 min preactivation time following reaction times of 60 min. Upon reaction completion, the peptide-resin was deprotected and cleaved from the resin in batches of 200 mg with 2 mL of reagent B: 85% TFA, 5% phenol, 5% water, 5% TIPS for 4 h at 25 °C under mechanical stirring. The cleavage mixture was then filtered and the resin was washed with 2 mL reagent B. The cleaved peptide fractions were pooled together and precipitated by addition of 200 mL of cold diethyl ether and incubated for 24 h at 4 ºC. The precipitated peptide was collected by centrifugation and washed three times with 200 mL of cold diethyl ether. The crude peptide pellet was dried under $N_2$ gas flow and dissolved in 50 mL of HPLC grade water. The crude peptide was filtered using a 0.2 μm polycarbonate filter and purified by reversed-phase HPLC on a C18 preparative column (Vydac, 218TP15 C18; 15 μm particles, 22 × 250 mm). The crude peptide solution was pre-equilibrated with 90% HPLC buffer A (99.9% water, 0.1% trifluoroacetic acid) with a flow rate of 10 mL/min. Peptide purification protocol consisted of: 1) linear gradient from 10% to 20% of buffer B (acetonitrile and 0.1% TFA) in 30 min and 2) subsequent isocratic elution. Fractions containing peptides were determined by analytical HPLC and pooled together before lyophilization. The molecular weight of the purified peptide was determined using ESI-MS (Agilent MSD SL Ion Trap). To remove TFA ions from the peptide, a simple exchange method was followed. Briefly,

ion exchange resin (AG1-X8, Biorad) was prepared by washing with 10 vol of acetic acid (2.16M), followed by 10 vol of acetic acid (0.16M) and finally 5 vol of water. Purified peptide was dissolved in water at a concentration of approximately 4mg/mL and loaded onto the equilibrated resin. After one hour of incubation with shaking, the peptide was eluted from the resin by gravity and the resin was washed with water. Pooled peptide was aliquoted and the volume accurately measured. Samples from several aliquots were taken and submitted for amino acid analysis. Amino acid analysis was performed by the Protein Chemistry Laboratory (Texas A&M University). Ion-exchanged peptides were lyophilized and stored at -20 ºC until use.

*NMR spectroscopy* (Veglia et al., 2012). For solution NMR experiments, the TLQP-21 peptide powder was dissolved in 120mM NaCl, 20mM NaHPO4, pH 7.0, 5% $D_2O$ and transferred into a Shigemi tube. Heteronuclear single quantum (HSQC) and multiple quantum (HMQC) correlation experiments were run to verify the labeling pattern in the isotopically labeled peptides. Magic angle spinning (MAS) samples were prepared by dissolving 0.5 to 1 mg of TLQP21 in 20 µL of 20 mM phosphate buffer, 120mM NaCl at pH 7.0. The suspension was vortexed and briefly sonicated. The mixture was transferred to a 3.2 mm thin wall rotor MAS rotor. 3T3L1, N38 or splenocytes were centrifuged in 2.15 mL microfuge tubes for 2 min at 13300 rpm. Twenty microliters of wet cell pellet were pipetted into a clean 0.5 mL microfuge tube and (where applicable) incubated with the selective C3aR1 antagonist SB 290157 for 3 hr at 4 ºC. The cell pellet was added to 2.10 mg of lyophilized TLQP-21 powder, briefly vortexed and incubated at 37 ºC overnight. The mixture was transferred to a 3.2 mm thin wall rotor MAS rotor. All of the NMR experiments were performed on a VNMRS spectrometer operating at a proton frequency of 600 MHz. One-dimensional $^{13}C$ spectra were acquired using a cross-polarization (CP) sequence with 1 ms contact time and spectral width of 100 kHz. The sample was spun at 8 kHz and the temperature was kept at 37 ºC. Chemical shifts were assigned using refocused Insensitive Nuclei Enhanced by Polarization Transfer (rINEPT) and Total Through Bond Correlation Spectroscopy (TOBSY) experiments acquired using a BioMAS probe. Pulse widths were 5.5 µs ($^{13}C$, $^{15}N$), 2.5 µs ($^{1}H$) with 100 kHz (direct $^{13}C$ dimension) and 3.33 kHz (indirect $^{1}H$ dimension) spectral widths. Typically, a total of 128 scans with 30 increments in the indirect dimension were acquired. The data were processed using NMRPipe and analyzed with Sparky software.

*Secondary Structure Prediction.* To analyze the secondary structure propensity of TLQP21 two programs were used: PredictProtein and JUFO. PredictProtein (www.predictprotein.org) is an automatic Internet service that includes software for the prediction of protein structure and function. The JUFO (http://www.meilerlab.org/index.php/servers/show?s_id=5) server provides a simultaneous prediction of secondary structure and trans-membrane spans from the protein sequence. It uses an Artificial Neural Network trained on databases of membrane proteins and soluble proteins.

**Splenocyte isolation**

Three to five C3aR1 knockout (Jackson Laboratory, C.129S4-C3ar1tm1Cge/J, stock number 005712) and specific wt BALB/cJ mice were euthanized with $CO_2$ and spleens were harvested. Spleens were placed in complete media (RMPI with 10% FBS, 1% 2-mercaptoethanol and 1% penicillin/streptomycin) and filtered through a 100µm, then 70µm mesh nylon screen to yield a single-cell suspension. Red blood cells were removed with 5ml of ACK lysis buffer (150mM NH4Cl, 10mM $KHCO_3$, 0.1mM $Na_2EDTA$, pH 7.4) and incubated for 5 minutes. 10ml of complete media was added to wash cells; cells were centrifuged (10min at 200x g) and supernatant was discarded. The splenocytes were washed two additional times with complete media. Splenocytes were seeded at $1x10^6$ cells/ml and stored in an incubator (37°C, 5% $CO_2$) for 4 hours until NMR sample preparation. All animal experiments were approved by the IACUC, University of Minnesota.

**Gastric contraction assay**

Wistar female rats (250-350 g; Charles River) were euthanized by inhalation of 75% $CO_2$ in air. The stomach was removed and washed in fresh Tyrode's solution as previously described (Severini et al., 2009). Longitudinal strips were obtained from the rat longitudinal forestomach (RLF) musculature and mounted vertically in a 5 ml organ bath in oxygenated (95% $O_2$ and 5% $CO_2$) Tyrode's solution at 37 °C. Responses were recorded isotonically by a strain gauge transducer (DY 1, Basile, Milan, Italy) and displayed on a recording microdynamometer (Unirecord, Basile. Milano, Italy). Tissues were allowed to equilibrate for about 60 min and the superfusion buffer was changed every 10 min. Saturating concentrations of acetylcholine (ACh, 25 μM) were added every 20 min, washing the tissue after 1 min contact time, until reproducible contractile responses were obtained. After 30 min

equilibration time, peptide activity was tested, washing the tissue as soon as the contraction peak had developed, after a contact time with muscle strips of 1-3 min. Since we demonstrated that an interval of 20 min was necessary to obtain a complete recovery, this interval was used for every peptide addition. Peptides were purchased from Primm (Milano, IT) C3a70-77 for Anaspec (USA) and C3aR1 antagonist from Calbiochem (USA). Data were analyzed with unpaired t-tests. All animal experiments were approved by the Ethics Committee of the Italian Ministry of Health.

**Receptor cross-linking experiment**

Crosslink peptide with N-terminal biotin and benzoylphenylalanine (Bpa) substitution of H12 was purchased from AAPPTec (Louisville, KY), purified by HPLC as the acetate salt, and verified by mass spectrometry.

*Membrane preparation:* Confluent CHO and 3T3 cells were washed twice with cold PBS before collecting the cells by scraping into cold Homogenization Buffer (20 mM HEPES, 1 mM EDTA, 255 mM sucrose, pH 7.6). Cells were briefly sonicated to lyse then centrifuged 20 min at 10,000 × g, 4 ºC. The precipitated membranes (P1) were resuspended in resuspension Buffer (20 mM HEPES, 1 mM EDTA, pH 7.6). The supernatants were transferred to fresh tubes and centrifuged 60 min at 41, 000 × g, 4 ºC. These precipitated membranes (P2) were also resuspended in resuspension Buffer. Both membrane protein concentrations were determined by BCA assay (Pierce).

*Crosslinking:* 3T3 and CHO membranes were diluted with PBS to 0.5 mg/mL protein. 1 mL of diluted membranes was aliquoted into a 96-well plate. An equivalent volume of TLQP-21 crosslink peptide was added to the diluted membranes and incubated for 10 min at room temperature. The 96-well plate was then placed on ice and transferred to the cold room for crosslinking. Crosslinking was achieved by a UV lamp (8 watt, 365 nm) for 30 min. Aliquots were collected from the 96-well plate and combined. In some cases (P2ppt), proteins were precipitated through addition of trichloroacetic acid to achieve a 6% solution. After 30 min incubation on ice, the samples were centrifuged to isolate the protein pellets. The protein pellets were washed twice with cold acetone and then resuspended in RIPA buffer (25 mM Tris base, 150 mM NaCl, pH 8.0, 1% deoxycholic acid, 1% Triton X-100).

*Western Blotting:* Aliquots of either the crosslinked P1 or P2 membrane solution or the solubilized precipitated membrane solution (P2ppt) were loaded onto

4-12% bis-TRIS gels and separated with MOPS buffer (Invitrogen) before transfer to nitrocellulose membranes. After blocking for 1 h in 5% milk in TBS-T, the membranes were washed 4 × 10 min with TBS-T and blotted with guinea pig anti-TLQP21 antibody [Possenti R et al., 2012]; 1:10,000 5% BSA) for 72 h at 4 ºC, and then 90 min in anti-guinea pig IRDye 680RD (Li-Cor, 926-68077). The membranes were then scanned by Li-Cor Odyssey.

**GPCR β-arrestin recruitment assay: G-protein independent**

The assay was done as previously reported [Lin et al., 2013]. Briefly, HTLA cells (an HEK293 cell line stably expressing a tTA-dependent luciferase reporter and a β-arrestin2-TEV fusion gene) were cultured in DMEM supplemented with 10% FBS and 5 µg/ml. Puromycin and 100 µg/ml Hygromycin. HTLA cells were transfected with C3aR-tTA construct using the calcium phosphate method and incubated overnight at 37°C. Cells were plated in Poly-L-Lys (PLL) coated 384-well white clear bottom cell culture plates at a density of 15,000 cells in 50 µl per well of DMEM with 1% dFBS and incubated overnight. Drug solutions were prepared in sterile 1XHBSS, 20 mM HEPES, pH 7.4 (assay buffer) at 6x dilution and added to cells (10 µl per well) for overnight incubation at 37°C. The following day, the medium was replaced by 20 µl per well of BrightGlo reagent (diluted 10-x with assay buffer). Plates were incubated for 20 minutes at room temperature in the dark before being counted on a luminescence counter.

# 2.4 RESULTS

## TLQP-21 targets the C3aR1 receptor

To establish the selective binding of the TLQP-21 to the C3aR1 receptor, we carried out photoaffinity labeling experiments. First, we synthesized a biotin-conjugated TLQP-21 peptide, substituting F13 with a benzophenone derivative; we then incubated the peptide with both 3T3L1 and CHO cells which express the C3aR1 (**Figure S2.1** and [Possenti et al., 2012, Choy et al., 1995, Cassina et al., 2013]). Upon UV irradiation of the reaction mixture, the modified peptide consistently cross-linked with a protein running at approximately 55 kDa on the SDS-PAGE, corresponding to the nominal molecular weight of the C3aR1 receptor [Klos et al., 2013, Roglic et al., 1996] (**Figure 2.1A**). To test the binding specificity of the TLQP-21 for the C3aR1 receptor, we carried out the same reaction in the presence of SB290157, a well-documented C3aR1antagonist [Ames et al., 2001]. In the presence of the antagonist, we observed a substantial reduction in cross-linking efficiency (**Figure 2.1B**), indicating that SB290157 competes with TLQP-21 binding to the C3aR1 receptor.

To provide additional evidence that TLQP-21 targets the C3aR1, we used a β-arrestin recruitment assay in HTLA cells transfected with the C3aR1 receptor [Lin et al., 2013]. We found that the $EC_{50}$ for mouse TLQP-21 is approximately 3 times lower than that of C3a and the $EC_{50}$ for the human TLQP-21 is approximately 22 times lower than C3a (**Figure 2.1C;** $EC_{50}$, C3a=3.0μM; mouse TLQP-21=10.3μM; human TLQP-21=68.8μM), indicating that both human and mouse TLQP-21 species are active toward human C3aR1, although with different potency.

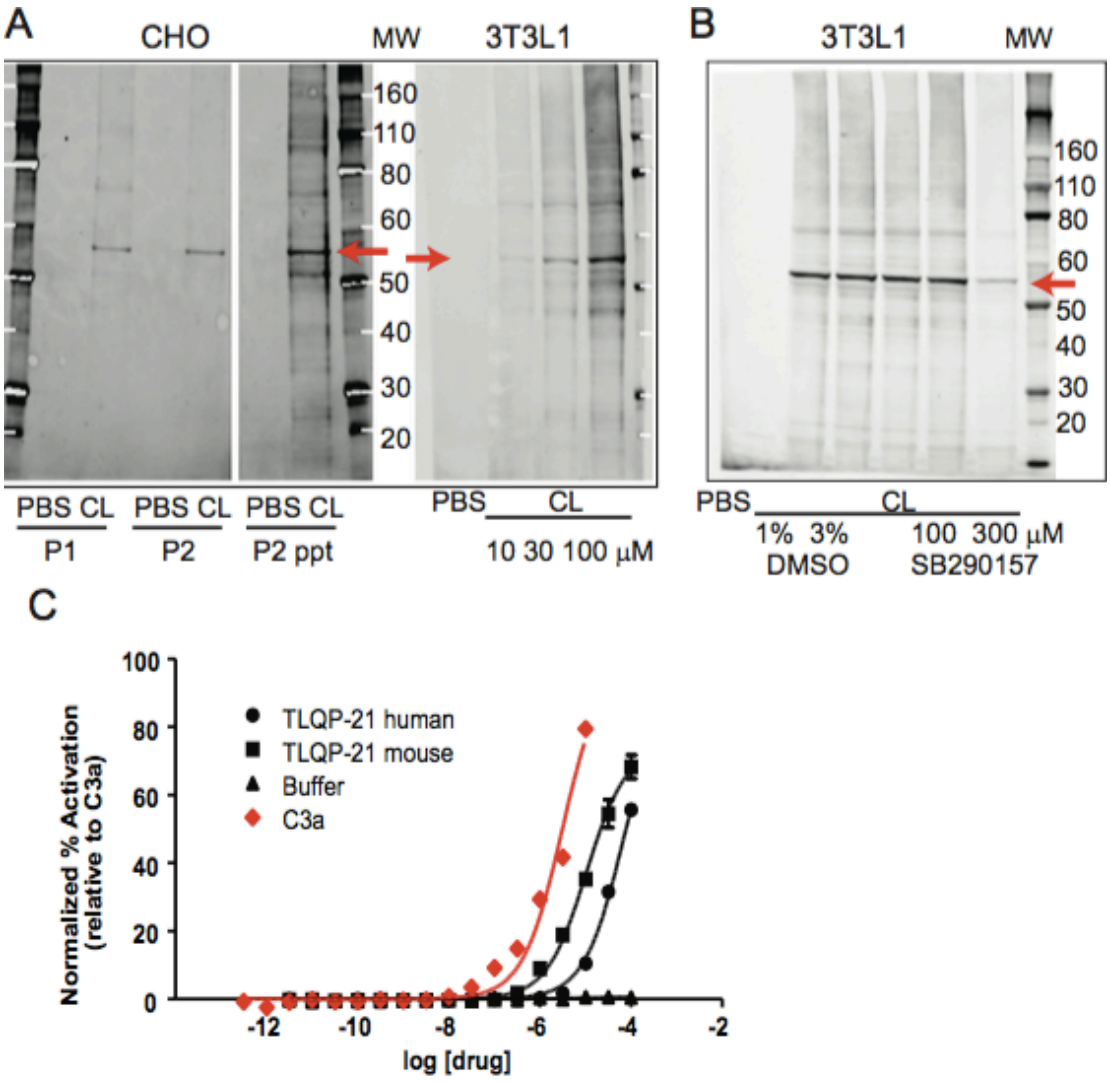


**Figure 2.1. TLQP-21 binding in 3T3L1 and CHO cells and activity at the C3aR1.** **A**) Photoactivated crosslinking of a modified TLQP-21 peptide (CL) in CHO and 3T3 cells. CHO membranes were treated with PBS or CL (100 μM). A band of ~56 kDa was observed with anti-TLQP21 in membrane fractions P1and P2 from CL-treated but not PBS-treated membranes. Labeling remained in the protein pellet when P2 membranes were TCA-precipitated (P2 ppt). P2 membranes from 3T3 cells were treated with PBS or increasing concentrations of CL. **B**) Crosslinking of a modified TLQP-21 peptide (CL) to membranes prepared from 3T3L1 cells is reduced in the presence of the C3aR1 antagonist SB290157. Lanes 2 and 3 show that crosslinking is not affected by DMSO used to dissolve SB290157. **C**) The β-arrestin recruitment assay showed that TLQP-21 is an agonist for the human C3aR1, similarly to the human C3a peptide. The mouse TLQP-21 has higher potency than the human TLQP-21.

## TLQP-21 undergoes a *disorder-to-order* transition upon binding C3aR1

Secondary structure predictions showed that the TLQP-21 sequence has a low propensity to form a well-order $\alpha$-helix [Garcia et al., 2005] (**Figure S2.2**). Accordingly, solution NMR experiments in aqueous solutions showed that the peptide is essentially unstructured, with a chemical shift index typical of random coil conformations (**Figure S2.2**). Addition of the helical-promoting solvent trifluoroethanol or dodecyl phosphocholine micelles left the resonances of the peptide essentially unperturbed, excluding its propensity to adopt an ordered conformation in membrane mimicking environments (**Figure S2.2**). We then tested the peptide's interactions with lipid membranes using magic angle spinning (MAS) solid-state NMR spectroscopy. To visualize the peptide, we synthesized three different TLQP-21 analogs with $^{15}N$, $^{13}C$ labels interspersed throughout its primary sequence: TLQP-21-*ALP,* labeled at $A_{16}$, $L_{17}$, $P_{18}$; TLQP-21-*PAR*, labeled at $P_4$, $A_6$, $R_9$; and TLQP-21-*PARRPA*, labeled $P_4$, $A_6$, $R_9$, $R_{11}$, $P_{19}$, $A_{20}$. (**Figure S2.3**). We performed two different experiments: the refocused INEPT (rINEPT) experiment, which is sensitive to more dynamic regions of proteins (Fyfe et al., 1995), and cross-polarization (CP) experiments [Engelke and Steuernagel 2007], which detects more rigid domains (**Figure S2.3**). The peptide was reconstituted with large unilamellar vesicles of DOPC:DOPE. Under these conditions, we did not observe any peptide resonances in the CP spectra, excluding a strong binding of the peptide to the membrane vesicles, and at the same time supporting the dynamic nature of the peptide. In contrast, the rINEPT experiment detected essentially all of the labeled sites, displaying a well-resolved spectrum of TLQP-21 with chemical shift values corresponding to the tabulated random coil values (http://www.bmrb.wisc.edu) (**Figure 2.2A,C,E** and **Figure S2.2D**). Taken with the solution NMR experiments, the solid-state NMR spectra showed that the peptide is intrinsically disordered in solution and does not have a strong tendency to associate with lipid bilayers.

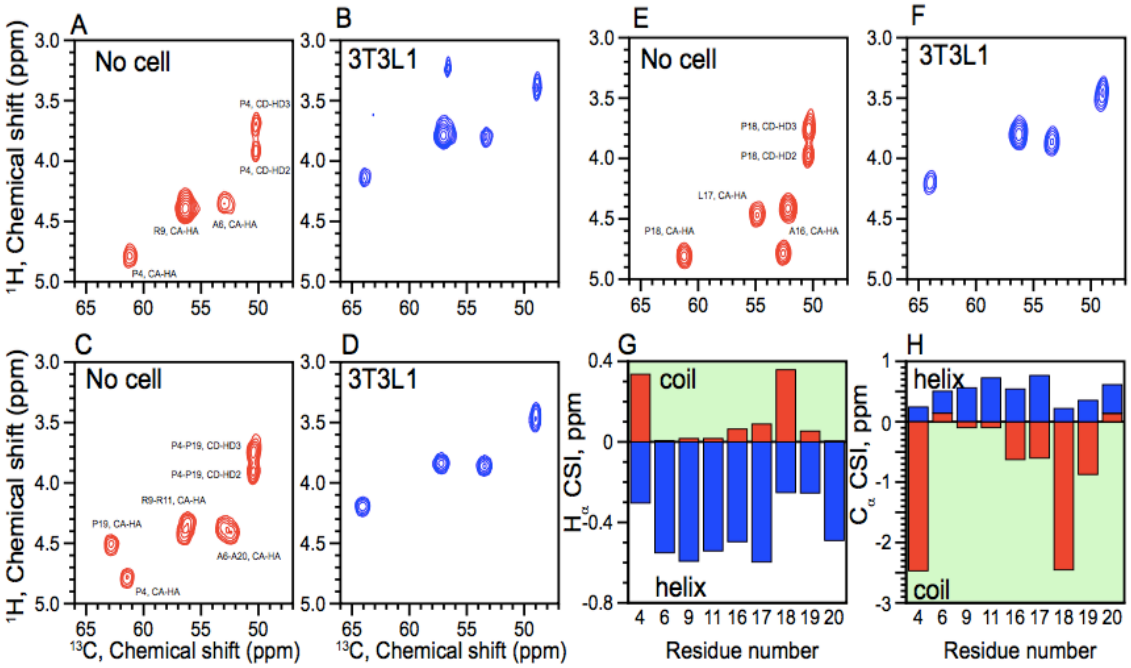


**Figure 2.2. Structural analysis of TLQP-21 in presence of target 3T3L1 cells.** Overlay spectra of refocused INEPT spectrum of TLQP-21 $^{13}$C and $^{15}$N labeled at $P_4$-$R_6$-$A_9$ (**A,B**), $P_4$-$A_6$-$R_9$-$R_{11}$-$P_{19}$-$A_{20}$ (**C,D**) or $A_{16}$-$L_{17}$-$P_{18}$ (**E,F**) with resonance assignments indicated. Experiments were performed in buffer (**A,C,E**) or in the presence of 3T3L1 cells after 24 hour incubation at 37ºC (**B,D,F**). **G,H**. Chemical shift index of TLQP-21 in buffer (red) or in the presence of 3T3L1 cells (blue) (Schwarzinger, et al., 2000).

To test TLQP-21 binding under the native conditions rather than in a reconstituted system, we probed the peptide-receptor interactions by incubating the peptide with 3T3L1 cells that express C3aR1 (**Figure S2.1**). Under these conditions, TLQP-21 underwent a *disorder-to-order* transition (**Figure 2.2B,F,D**). Specifically, the chemical shifts of the Cα-Hα resonances changed significantly (**Figure 2.2G,H**), consistent with a structural transition from random coil to α-helical conformation (**Figure 2.3**). The experiment was repeated for three labeled TLQP-21 analogs spanning the core sequence, and in all cases we observed the same chemical shift transitions from random coil to helix (**Figure 2.2**).

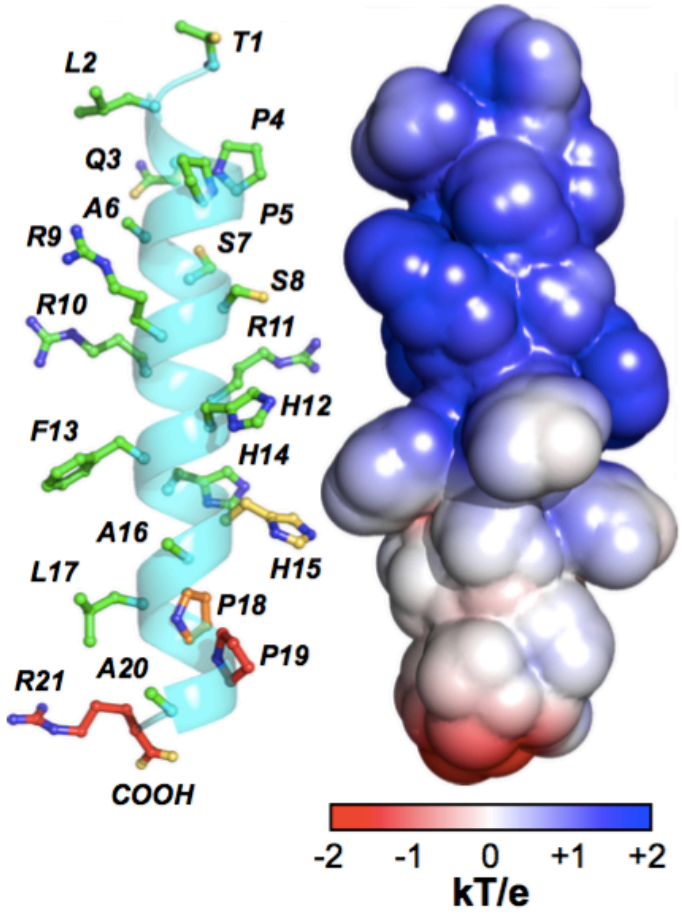


**Figure 2.3. A structural model of TLQP-21 upon receptor binding**. The backbone conformation was obtained with XPLOR-NIH software (Schwieters et al., 2003) constraining the dihedral angles of the residues showing helical chemical shifts. The conformation of the side chains is arbitrary. Electrostatic surface calculated with APBS (Baker et al., 2001) illustrates the positively charged N-terminal domain of TLQP-21 and primarily neutral C-terminal domain.

To confirm the specificity of the binding under NMR conditions, we analyzed TLQP-21 binding in the presence of $N^2$-[(2,2-Diphenylethoxy)acetyl-L-Arginine (or SB290157), a potent inhibitor of C3aR1 that does not antagonize either C5aR or other GPCRs [Ames et al., 2001]. Since the concentration of the receptor is unknown, we used 5 μM of the inhibitor. In the spectrum of *TLQP-PAR* (**Figure 2.4C**) we detected two conformations of the peptide: one with chemical shifts corresponding to the unfolded peptide, and a weaker set matching the helical structure. These data indicate that there is only a partial saturation of the receptor on the adipocytes with the SB290157 inhibitor. To circumvent this issue, we used splenocytes derived from either wild type mouse expressing C3aR1 receptor [Kwan et al., 2013], or from a C3aR1 knockout mouse. Again, for the wild type cells we

observe the backbone chemical shifts matching those of the folded helical conformation (**Figure 2.4E**). Conversely, TLQP-21 incubated with the C3aR1 knockout splenocytes exhibits chemical shifts those of the unfolded structure (**Figure 2.4F**). Finally, although the N38 cell line has been proposed as a negative control for TLQP-21 activity [Cassina et al., 2013], we detected significant expression of the C3aR1 receptor using QPCR (**Figure S2.1**). As a result, we have observed binding of the TLQP-21 peptide to the receptor with concomitant transitions from disordered to helical conformation (**Figure S2.4**).

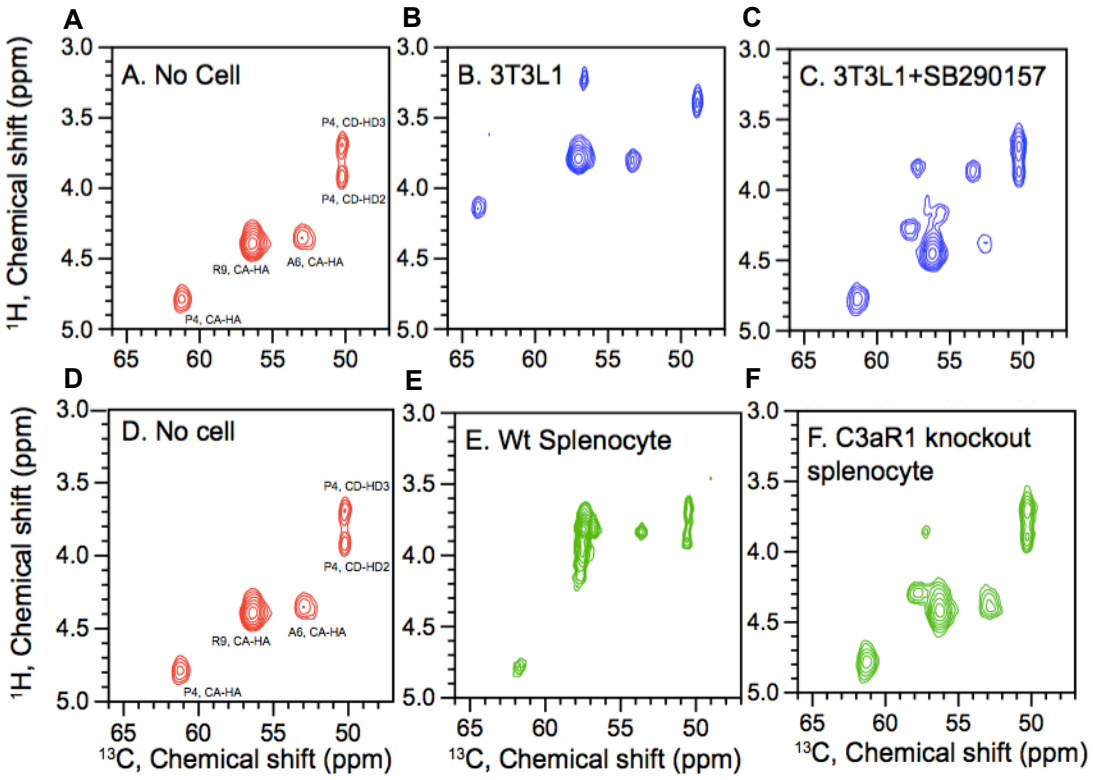


**Figure 2.4. Structural analysis of TLQP-21 in presence of C3aR1 knockout cells and a C3aR1 antagonist.** Refocused INEPT spectra of TLQP-21, labeled with $^{13}$C and $^{15}$N at $P_4$-$A_6$-$R_9$ with resonance assignments indicated. Experiments were performed in buffer (**A,D**), in the presence of 3T3L1 cells (**B**), in the presence of 3T3L1 cells incubated with the C3aR1 antagonist SB290157 (**C**), in the presence of splenocytes derived from wild type (**E**) or in the presence of splenocytes derived from a C3aR1 knockout mice (**F**).

## Determination of the hot spots for TLQP-21 biological function

After establishing the structural determinant of TLQP-21 binding to C3aR1, we sought to identify the hot spots for the peptide activity. The primary amino acid sequence of murine TLQP-21 (TLQPPASSRRRHFHHALPPAR) corresponds to amino acids 556–576 of the VGF pro-peptide [Bartolomucci et al., 2006, 2011]. One of the best characterized bioassays for TLQP-21 activity is the contraction of stomach fundus strips [Severini et al., 2009]. At a dose of 3μM TLQP-21 induces up to ~69% of the corresponding contraction promoted by acetylcholine. To elucidate the hot spots responsible for optimal biological activity, we synthesized and tested the biological response of two truncated analogs of the TLQP-21 peptide: one without the C-terminal sequence (TLQP-11), and the second without the N-terminus (HFHH-10). We found that TLQP-11 is essentially inactive, with zero response at concentrations up to 10μM (**Table 2.1**), while HFHH-10 induced a modest biological activity, with ~3% response at a concentration of 3μM**,** 62% at 6μM, and 75% at 10μM. These experiments suggest that the hot spots for biological activity are situated at the C-terminus, and demonstrate that the entire peptide sequence is required for its optimal activity. We next performed Ala-scanning mutagenesis [Morrison and Weiss 2001] on the C-terminal portion of TLQP-21 We found that mutations of endogenous amino acids with Ala had no significant effects, with the exception of the four C-terminal amino acids. Specifically, the P18A mutant showed partial biological function with ~65% activity at 3μM. The P19A mutant showed only residual activity with 19% at 3μM (and 35% at 6μM) (**Table 2.1; Figure S2.5**). Interestingly, the human TLQP-21, in which Ser is in position 20 (Ala for the rodent sequence), showed limited biological activity toward the rodent receptor with ~20% at 3μM compared to the mouse sequence (**Table 2.1**), a finding which is in line with the β-arrestin activity assays reported in **Figure2.1C**. Importantly, the R21A mutant resulted in a complete loss of activity (**Table 2.1; Figure S2.5**), even after increasing the dose up to 10μM. The inactive R21A mutant does not block the activity of a subsequent infusion of TLQP-21, suggesting that it does not behave as a C3aR1 antagonist (**Table 2.1; Figure S2.5**). Note that under our conditions the biological activity elicited by TLQP-21 is similar to that of the C3aR1 agonist $C3a_{70-77}$ [Hugli and Erickson 1977], with 3μM TLQP-21 and $C3a_{70-77}$ causing approximately 69% and 55% contraction of fundus strips, respectively, relative to acetylcholine (**Figure S2.5**).

Finally, we investigated the effects of capping the TLQP-21 C-terminus via amidation. Although this post-translational modification is not observed for the TLQP-21 peptide *in vivo* [Bartolomucci et al., 2006], it represents a pre-requisite for the activity of several other hormonal peptides such as CRH [Vale et al., 1981], and it increases the stability of several synthetic peptides [Adessi and Soto 2002]. Upon C-terminal amidation, the TLQP-21 peptide is completely inactivated (**Table 2.1**), suggesting that the free carboxylic group is necessary for activity.

| Peptide | Activity % of TLQP-21 (average ± SEM) |
|---|---|
| TLQPPASSRRRHFHHALPPAR | 100 |
| TLQPPASSRRR | inactive |
| HFHHALPPAR | 2.6±4*** |
| TLQPPASSRRR**A**FHHALPPAR | 95±4 |
| TLQPPASSRRRH**A**HHALPPAR | 88±9 |
| TLQPPASSRRRHF**A**HALPPAR | 91±5 |
| TLQPPASSRRRHFH**A**ALPPAR | 84±10 |
| TLQPPASSRRRHFHHAL**A**PAR *(P18A)* | 65±7 * |
| TLQPPASSRRRHFHHALP**A**AR *(P19A)* | 19±4 *** |
| TLQPPASSRRRHFHHALPPA**A** *(R21A)* | inactive |
| TLQPPASSRRRHFHHALPPAR-**NH2** | inactive |
| TLQPPSALRRRHYHHALPP*S*R *(human)* | 20±9** |

*p>0.5, **<0.01, **<0.001.

**Table 2.1. Contractile activity on rat stomach fundus exerted by TLQP-21 mutants** (mutations highlighted in bold).

Importantly, NMR spectra of the R21A mutant (labeled with $^{13}C$ and $^{15}N$ at $A_{16}$, $L_{17}$ and $P_{18}$) in the presence of 3T3L1 cells show a conformational transition similar to that of the wild-type peptide (**Figure 2.5**). Therefore, the loss-of-function character of the inactive mutant is probably due to changes in the electrostatic interactions at the C-terminal portion of the peptide. The latter is supported by the chemical structure of C3a [Hugli and Erickson 1977], by the analogous mutations at R77 of C3a

[Nattesheim et al., 1988], as well as the chemical structure of the C3aR1 antagonist SB290157, which includes a hydrophobic N-terminal diphenylethoxy group linked to the acetyl-L-Arg moiety [Ames et al., 2001] that closely mimics the C-terminal residues of the TLQP-21 peptide.

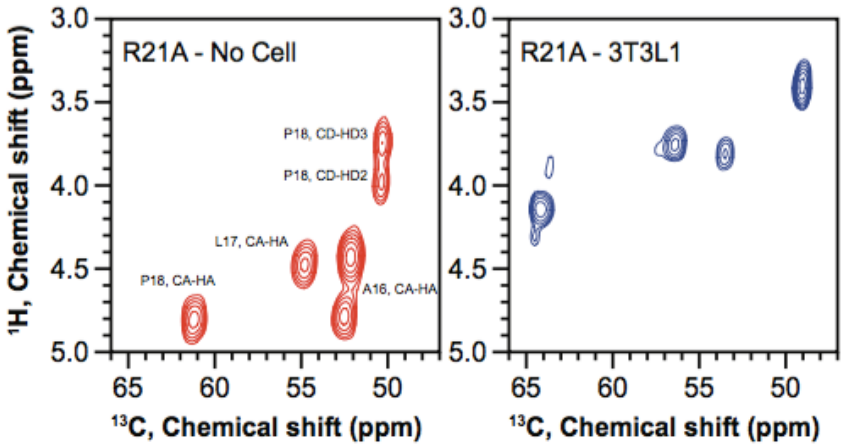


**Figure 2.5. Structural analysis of mutant R21A in presence of target 3T3L1 cells.** Refocused INEPT spectra of R21A mutant, labeled with $^{13}$C and $^{15}$N at $A_{16}$-$L_{17}$-$P_{18}$ with resonance assignments indicated. Experiments were performed in buffer (left panel) or in the presence of 3T3L1 cells (right panel).

## 2.5 DISCUSSION

The role of the TLQP-21 neuropeptide in the pathophysiology of gastrointestinal and metabolic functions has been recognized by several independent studies [Bartolomucci et al., 2011]. Despite this, the molecular mechanisms for eliciting TLQP-21 function have remained elusive until a recent study identified the C3aR1 receptor as the target for TLQP-21 [Hannedouche et al., 2013]. Indeed, our photoaffinity labeling and β-arrestin assays (**Figure 2.1**) data support these previous studies, showing that TLQP-21 cross-links with the C3aR1 receptor selectively. A second putative receptor for TLQP-21, the globular head of C1q has been recently described [Chen et al., 2013]. Published [Possenti et al., 2012, Hannedouche S et al., 2013, Passina et al., 2013] and current data do not support a second binding site in either CHO or 3T3L1 cells (**Figure 2.1**) and there is no apparent structural/functional similarity between TLQP-21 and the predicted C1q ligands [Gaboriaud et al., 2003].

Importantly, the NMR measurements demonstrated that the peptide is intrinsically disordered in solution and does not assume an ordered conformation upon addition of helical-inducing environments. However, when incubated with cells expressing C3aR1, the TLQP-21 peptide undergoes a folding-upon-binding transition, adopting a well-defined α-helical conformation (**Figure 2.3**). This structural transition does not occur in the presence of C3aR1-knockout cells and can be inhibited upon treatment of 3T3L1 cells with a selective and competitive antagonist of the C3aR1 receptor [Ames et al., 2001].

Transition from a random coil to helix is a common mechanism for activating GPCRs of the secretin family [Shoichet and Kobilka 2012; Hollenstein et al., 2014; Parthier et al., 2009; Kamik et al., 2003]. For these receptors, the ligand peptides have been found to be disordered in aqueous solutions, but adopted a structured helical conformation upon binding the extracellular domains of the receptors. The driving force for their binding and folding is the formation of amphipathic helices in which the hydrophobic residues embed into the binding site. At least six different examples have been reported in the literature, e.g. CRH, PACAP, Glucagon, GLP-1 etc, where the high-resolution structures have been solved by either NMR or X-ray crystallography [Pal et al., 2012]. While the apparent mechanism of TLQP-21 helix folding is reminiscent of these peptide hormones, the chemical nature of this VGF-

derived peptide is rather different, as TLQP-21 sequence is flanked by two pairs of proline residues at both termini. In the structural model derived from our chemical shift measurements, hydrophobic and hydrophilic residues are not segregated into two distinct faces of the helix; rather, the charges are interspersed throughout the peptide sequence (**Figure 3**). This suggests a mechanism of recognition by the cognate receptor that is different from that of other peptide hormones for which a structural analysis has been conducted [Parthier et al., 2009]. Furthermore, the C-terminus of peptides active at class B GPCR act as a docking site to initiate the helix formation, and the N-terminal residues are responsible for the activation of the receptors [Parthier et al., 2009; Karnik et al., 2003]. Conversely peptides active at class A GPCR (including the C3aR1) [Beck-Sickinger et al., 1994; Neelamkavil, et al., 2005] as well as other peptides of the granin family [Bartolomucci et al., 2011] do not show a common binding mechanism. The hot spots for TLQP-21 activity reside at the C-terminus. In fact, alanine-scanning mutagenesis and the bioassay of fundus strip contraction showed that the C-terminal sequence (-$PPAR_{21}$) is central to TLQP-21 biological activity (**Table 2.1**). A similar situation is found for the C3a peptide, the first ligand ever identified for the C3aR1 [Nettesheim et al., 1988]. In the absence of the receptor, the C3a peptide is organized in helical segments interrupted by short flexible loops that become less defined at residue 66 [Klos et al., 2013], while they adopt a significantly more ordered helical conformation in the crystal lattice [Nettesheim et al., 1988]. As with TLQP-21, the C3a peptide's hot spots are located at the C-terminus, with R77 playing a critical function [Ames et al., 2001; Hugli and Erickson 1977; Nettesheim et al., 1988]. By deleting the C-terminal $R_{77}$ of C3a it is possible to ablate the peptide's function at C3aR1 completely, although the deletion mutant is still able to form an ordered helix [Nettesheim et al., 1988]. A very similar result was obtained with TLQP-22.1 The R21A mutant of TLQP-21 is inactive while still undergoing an $\alpha$-helix conformational change. A full understanding of the similarities in the mechanism of action of TLQP-21 and C3a is currently lacking. In CHO and HeK239 cells transfected with C3aR1, TLQP-21 binds the receptor with 100 fold lower affinity than C3a [Hannedouche et al., 2013], while both these ligands induce a similar contraction of gastric fundus strips (present data) and insulin release (Stephens et al., 2012; Lo et al., 2014). Conversely, mouse TLQP-21 enhances isoproterenol induced in mouse adipocytes [Possenti R et al., 2012], while in an heterologous system Lim et al (2013) showed that human serum C3a exerts the opposite effect in murine 3T3L1 cells. Finally, using mouse genetic it has been

demonstrated that C3aR1 knockout mice are transiently resistant to diet-induced obesity and are protected from insulin resistance and liver steatosis [Mamane et al., 2009], similar to VGF knockout mice [Hahm et al., 1999, 2002]. In conclusion, although the mechanism of binding to the C3aR1 receptor may appear similar for both TLQP-21 and C3a, differences in their primary sequences might account for the non-fully overlapping biological actions.

Another important finding of our investigation relates to the different function between human and rodent TLQP-21 sequences. A recent study reported that the human TLQP-21 sequence is 5-fold less potent toward the rodent C3aR1 than the corresponding rodent sequence [Hannedouche et al., 2013]. Here, we tested the potency of these two peptides toward the human C3aR1 receptor and found that both human and mouse TLQP-21 sequences target the human receptor with different potency. Specifically, we found an $EC_{50}$ for the mouse TLQP-21 approximately 3 times lower than the C3a peptide, while the corresponding $EC_{50}$ for the human TLQP-21 is approximately 22 times lower (**Figure 2.1C**). The rodent (rat and mouse) and primate (human, chimpanzee, and macaque) TLQP-21 sequences differ by four amino acids [Bartolomucci et al 2011]. However, Ser20 substitutes Ala20 at the C-terminus of the rodent peptide in the human sequence (**Table 2.1**), resulting in a mutation leading to a peptide with lower potency toward the primate and the rodent C3aR1. In support, mutations at the C-terminus of C3a reduce the affinity toward the human receptor [Klos et al., 2013]. Interestingly, casoxin C (Tyr-Ile-Pro-Ile-Gln-Tyr-Val-Leu-Ser-Arg) and Oryzatensin (Gly-Tyr-Pro-Met-Tyr-Pro-Leu-Pro-Arg) are short bioactive peptides with sequence analogy with the human complement C3a(70-77) and substitution of Ala76 in C3a with either Ser or Pro respectively [Takahashi et al., 1996,1997]. The biological activity of casoxin C and oryzatensin in the ileum-contraction assay is similar to $C3a_{70\text{-}77}$ but with lower potency [Takahashi et al., 1996, 1997]. Overall these data suggests that, unlike the mutation of the Arg77/Arg21 which abrogate activity at the C3aR1 (see above), mutating the Ala76 in C3a and Ala20 in TLQP-21 could reduce their biological activity.

The lower potency of the human TLQP-21 peptide might reduce the lipolytic potential of humans and may constitute one of the factors explaining human vulnerability to obesity. Conversely, the rodent peptide could represent a gain of function mutation with respect to the basal TLQP-21 activity toward the C3aR1 receptor and suggests possible point mutations for augmenting or reducing TLQP-21 potency in humans. Synthetic molecules designed to target GPCRs have already

been developed into potent agonists and antagonists by engineering lactam-bridges promoting $\alpha$-helical structures [Neelamkavil et al., 2005; Ammoun et al., 2003; Grace et al. 2007; Murage et al., 2008; Pellecchia et al., 2008]. The mouse TLQP-21 sequence represents a molecular template for designing new analogues of this peptide that can serve as agonists or antagonists for C3aR1 having important implication for obesity [Possenti et al., 2012], diabetes [Stephens et al., 2012], hypertension [Fargali et al., 2014], pain [Fairbanks et al., 2014] and potentially immune functions.

In summary, our results show a folding-upon-binding mechanism for TLQP-21 that activates the cognate C3aR1 receptor. Using a combination of spectroscopic and biological assays, we identified the hot spots for TLQP-21 function as residing at the C-terminal sequence of the peptide. C-terminal amidation or mutation of the basic arginine 21 residue obliterates peptide function, suggesting that both positive and negative electrostatic interactions at the C-terminus are necessary for biological activity.

This study represents a major step toward understanding the molecular mechanism for activation of TLQP-21 and paves the way for designing new agonists/antagonists to modulate the function of the C3aR1 receptor [Reid et al., 2013].

## ACKNOWLEDGMENTS

Supported by the Minnesota Partnership for Biotechnology and Medical Genomic, Decade of Discovery in Diabetes Grant (AB), NIH/DK10249601 (AB), NIH R01DE021996 and NIH R21DA025170 (LV) and the NIMH Psychoactive Drug Screening Program (BLR and MFS). NMR experiments were carried out at the Minnesota NMR Center. 3T3L1 cells were provided by The Molecular & Cellular Basis of Obesity Core, Minnesota Obesity Center (5P30DK050456-18).

## 2.6 SUPPLEMENTARY FIGURES

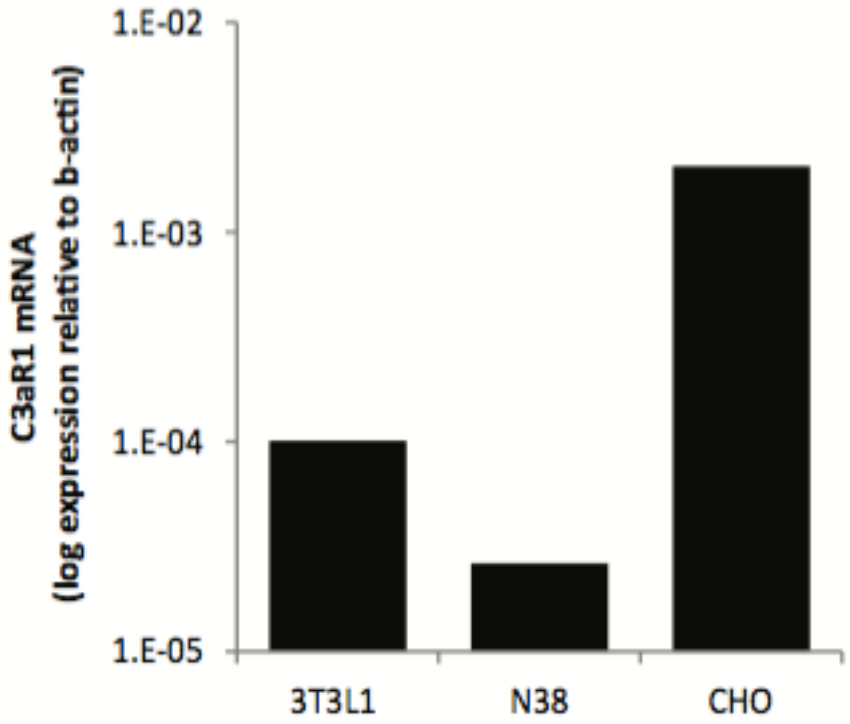


**Figure S2.1, related to Figure 2.1. and Figure S2.4. Gene expression of C3aR1.** C3aR1 mRNA was measured by real time QPCR in 3T3L1, N38 and CHO cells and normalized over β-actin expression.

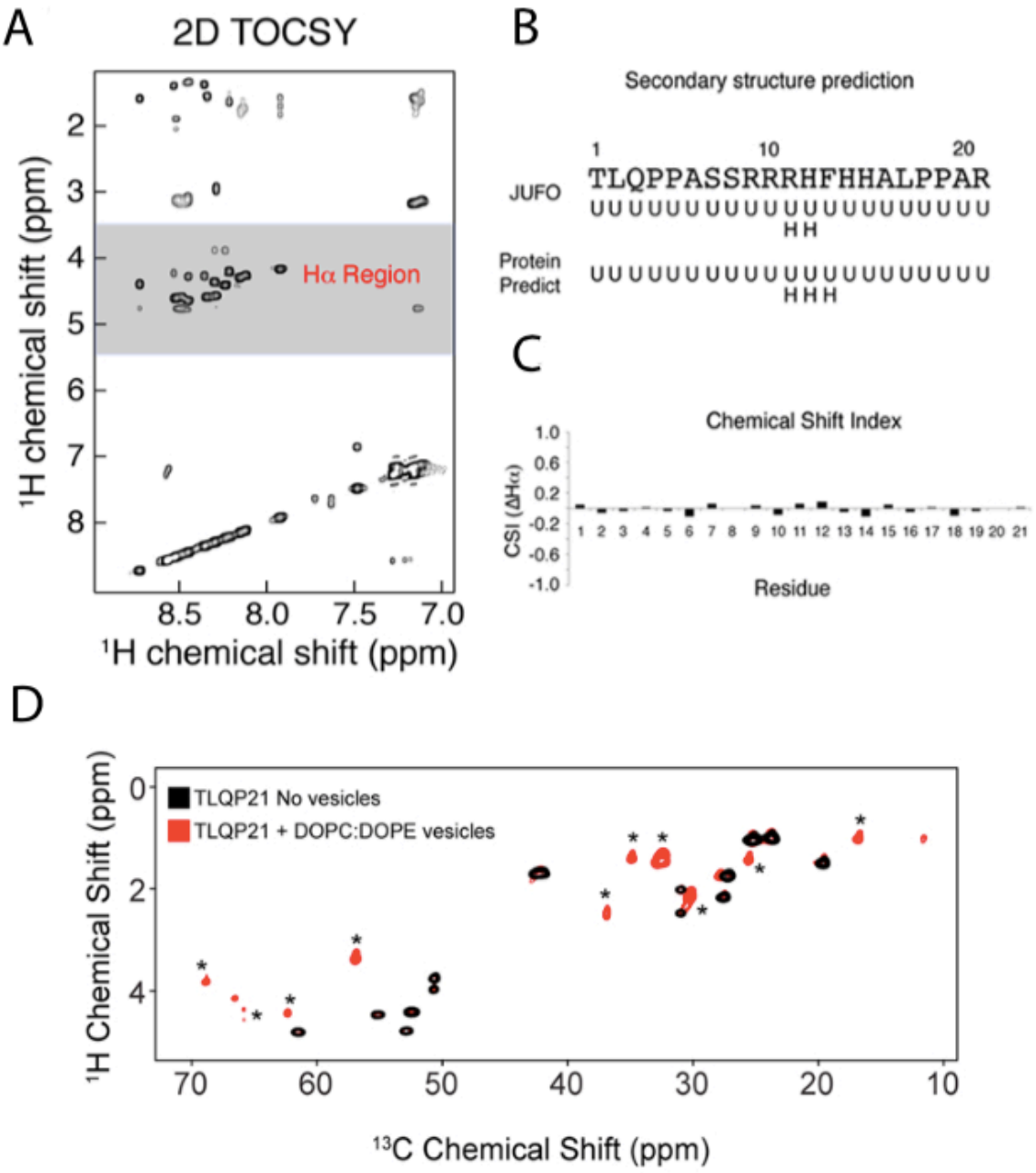


**Figure S2.2, related to Figure 2.2. Software prediction and secondary structural characterization of free TLQP-21.** **A**) Two dimensional total correlation spectroscopy spectrum of TLQP-21 dissolved in NMR buffer at acquired at 37ºC. Only the amide region (~7-9ppm) is shown for clarity. **B**) Secondary structural prediction of TLQP-21 using JUFO and PredictProtein software. **C**) Chemical Shift index ($\Delta H\alpha$) of TLQP-21 using assigned $H\alpha$ chemical shift in (**A**). **D**) Overlay of TLQP-21 rINEPT in the absence (black) and presence (red) of small unilamellar vesicles composed of DOPC/DOPE lipids. No changes in chemical shift are detected when TLQP21 interacts with SUVs. Asterisks indicate natural abundance 13C of lipid molecules.

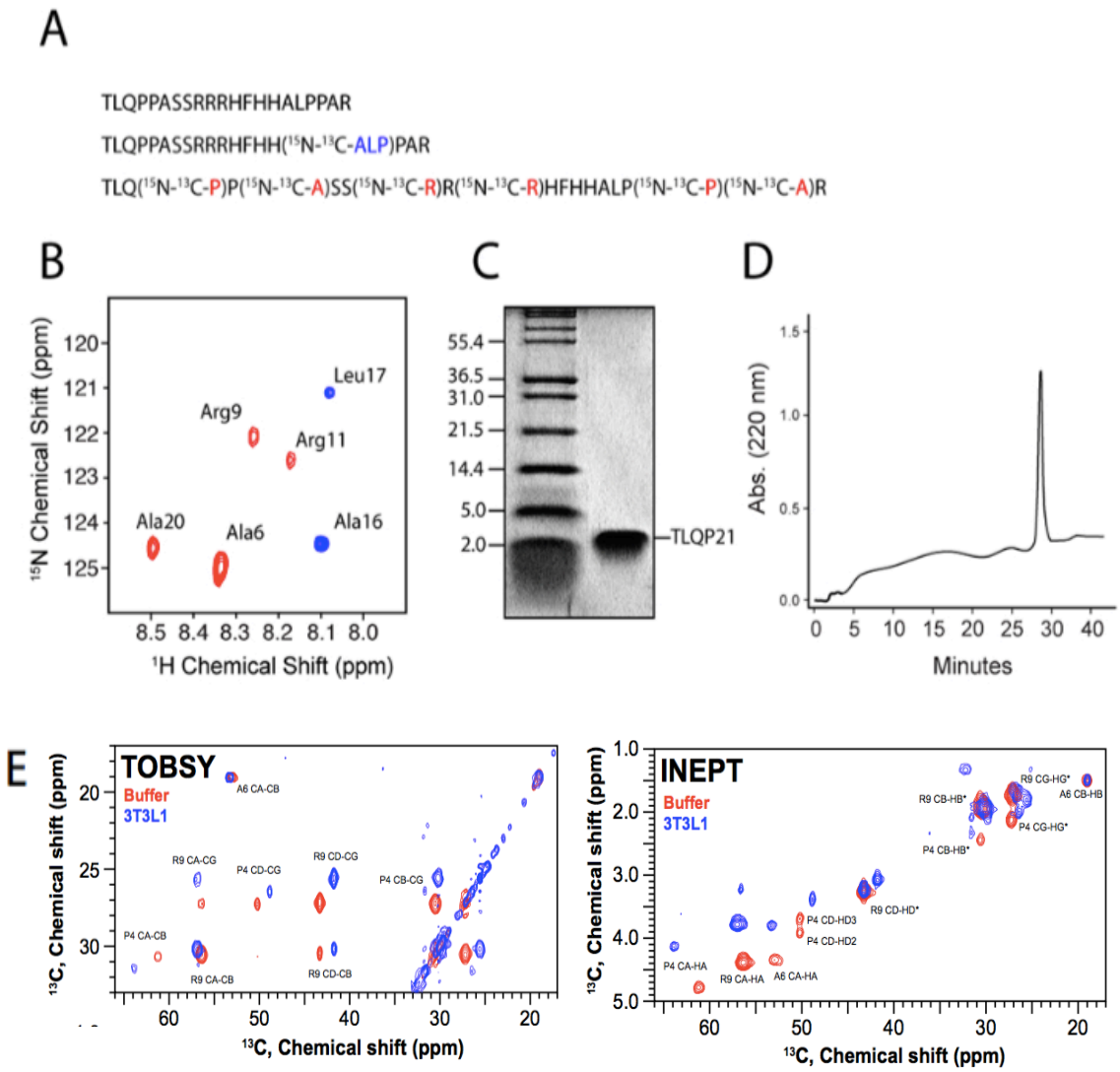


**Figure S2.3, related to Figure 2.2. TLQP-21 peptide synthesis and chemical characterization**. **TOBSY and INEPT spectra. A**) Sequences of TLQP21 mouse isoform with the location of isotopic labeling. **B**) Overlay of two 15N-HSQC fingerprinting spectra of TLQ-P21 corresponding to the isotopic labeled peptides (blue = ALP labeling, red=PARRPA labeling). **C**) SDS-PAGE of purified synthetic TLQP21 stained with Coomassie. **D**) Analytical HPLC trace showing single peak corresponding to pure TLQP-22.1 **E**) TOBSY and INEPT spectra of $^{13}C/^{15}N$ TLQP-21 (P4-A6-R9) in buffer (red) or in presence of 3T3L1 cells (blue) illustrating the assignment of the resonances. INEPT spectrum contains only signals from 13C-1H pairs. TOBSY spectrum contains the signals from the adjacent $^{13}C$-$^{13}C$ groups, allowing for the spin system assignment.

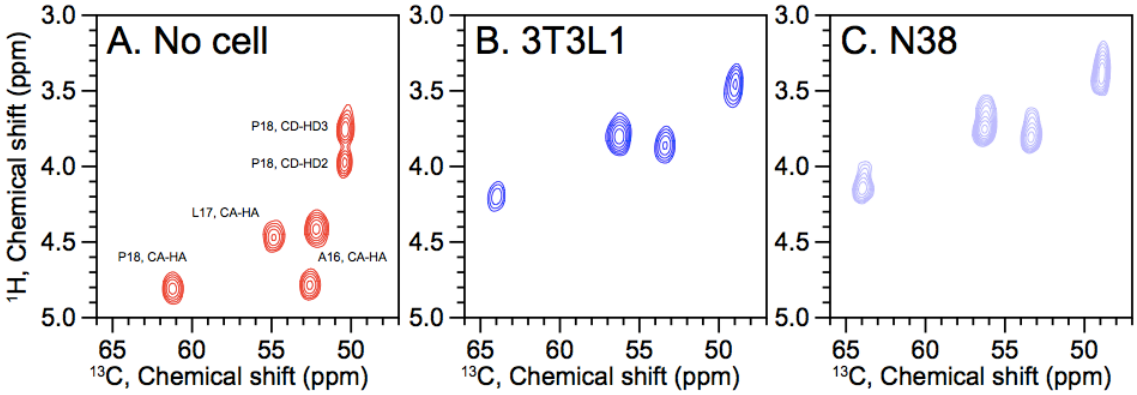


**Figure S2.4, related to Figure 2.4**. **Structural analysis of TLQP-21 in presence of N38 cells.** Refocused INEPT spectra of TLQP-21, labeled with $^{13}$C and $^{15}$N at $A_{16}$-$L_{17}$-$P_{18}$ with resonance assignments indicated. Experiments were performed in buffer (**A**), in the presence of 3T3L1 cells (**B**) or in the presence of N38 cells (**C**)

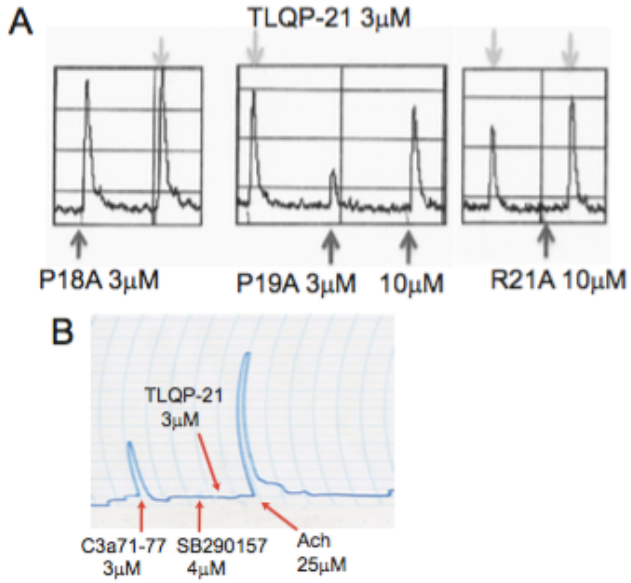


**Figure S2.5, related to Table 2.1 Gastric fundus strip contraction assay**. (**A**) Graphs show example of the contractile responses evoked by TLQP-21 (top arrows) and the C-terminal mutants P18A, P19A and R21A. (**B**) The C3a71-77 induces a contraction similar to TLQP-21 while the C3aR1 antagonist SB290157 antagonizes TLQP-21-induced contraction of stomach fundus strips. *p>0.5, **<0.01, **<0.002.1

# Chapter Three

# TLQP-21 enhances βAR-induced lipolysis via increased $[Ca^{2+}]_i$ and ERK phosphorylation

Cheryl Cero[1], Rana Mohammed[1], Allison Gurney[1], Nathan Zaidman[2], Scott O`Grady[2], Alessandro Bartolomucci[1]

[1] Department of Integrative Biology and Physiology, University of Minnesota, Minneapolis, MN 55455, USA

[2] Department of Animal Science, Integrative Biology and Physiology, University of Minnesota, 480 HaeckerHall, 1364 Eckles Avenue, St Paul, MN 55108, USA

This chapter in part contains data from an original article previously published in:

**Structure. 2014 Dec 2;22(12):1744-53.**

Reproduced with permission From Structure, Cell.

Copyright Clearance Obtained Sep 01 2015.

## 3.1 SUMMARY

The VGF-derived TLQP-21 peptide has been shown to bind to the Complement 3a Receptor (C3aR1) on adipocytes membranes and to increase ISO (isoproterenol)-induced lipolysis in adipocytes. However, the molecular mechanisms are still largely unknown. This study aimed to delineate the mechanism of action of TLQP-21-induced lipolysis using 3T3L1 and mouse adipocytes as a model. TLQP-21 was unable to induce lipolysis but enhanced ISO-induced lipolysis in 3T3L1 adipocytes. Furthermore, we showed that TLQP-21 increased the cAMP activator forskolin-induced lipolysis in 3T3L1 cells as well as in β1, β2, β3-AR knockout adipocytes suggesting that increased $[cAMP]_i$ exerts a permissive effect on TLQP-21-induced lipolysis. Additionally, we directly demonstrated that TLQP-21 pro-lipolytic effect is mediated by increased $[Ca^{2+}]_i$ and phosphorylation of MAPK/ERK. These results indicate a novel mechanism of TLQP-21 induced lipolysis in 3T3L1 cells and this study has important implications to design innovative pro-lipolytic pharmacological agents.

## 3.2 INTRODUCTION

Lipolysis is a complex and tightly regulated multistep process mostly stimulated by catecholamine hormones Briefly, norepinephrine (NE), released by the postganglionic sympathetic neurons innervating adipose fat depots, stimulate lipid mobilization via activation of β-adrenoreceptors (β-ARs) on adipocyte membranes [Jocken and Blaak, 2008]. In response to the adrenergic stimulation, adenylate cyclase (AC) is activated to generate cyclic AMP (cAMP). cAMP activates protein kinase A (PKA) that catalyzes the phosphorylation of hormone sensitive lipase (HSL) that causes the activation and translocation of this lipase from the cytosol to the lipid droplet [Holm, 2003]. PKA also phosphorylates perilipin that moves away from the lipid droplet increasing the surface area on the droplet for more lipolysis. Aside from HSL, there are other important lipases and proteins involved in the breakdown of triglycerides. The main lipases are, adipose triglyceride lipase (ATGL) that performs the first step hydrolyzing triacylglycerol (TAGs) to generate diacylglycerols (DAGs), hormone-sensitive lipase (HSL) hydrolyses DAGs generating monoacylglycerol (MAG) and lastly monoglyceride lipase (MGL) that cleaves MAG into glycerol and NEFAs [Zimmermann et al., 2004; Lass et al., 2006; Duncan et al., 2007]. As an end result of lipolysis, NEFAs and glycerol are released from adipocytes and delivered to peripheral tissues [Lass et al., 2011; Ahmadian et al., 2009; Duncan et al., 2007]. Overeating and obesity compromises the normal physiological regulation of lipolysis leading to decreased catecholamine-induced lipolysis in obese patients [Arner, 1992; Large et al., 1999]. Therefore, identifying new drugs that could finely tune lipolysis would be extremely helpful for obese patients by directly targeting excessive fat mass.

The TLQP-21 peptide spans from residue 556 to residue 576 of the rodent VGF precursor sequence [Bartolomucci et al., 2006]. Originally identified in rat brain tissue extracts [Bartolomucci et al., 2006], TLQP-21 is a multifunctional peptide important in many physiological states [Bartolomucci et al., 2006; Sibilia et al., 2010; 2012; Brancia et al., 2010; Rizzi et al. 2008; Fairbanks et al., 2014; Fargali et al., 2014]. TLQP-21 is expressed in sympathetic nerve terminals innervating white adipose tissue (WAT) and binds to C3aR1 expressed on the adipocyte membrane thereby increasing ISO-induced lipolysis [Hanneduche et al., 2012; Cero et al., 2014].

The Complement 3a, a potent anaphylatoxin, product of adipsin cleavage of C3 [White et al., 1992; Choy and Spiegelman, 1996; Lo et al., 2014] was the first

ligand characterized for C3aR1 [Markiewski et al., 2007] and its role in adipocyte function remains poorly characterized. Similarly the cell signaling cascade activated by C3aR1 activation is poorly characterized [Lo et al., 2014]. We have previously shown that TLQP-21 increases phosphorylation of AMPK, ERK and not PKA substrates [Possenti et al., 2012]. In presence of ISO, TLQP-21 increased the phosphorylation of AMPK, ERK as well as HSL and enhances ISO-induced lipolysis in mature murine adipocytes. The exact mechanism of TLQP-21-induced lipolysis is still unclear. TLQP-21 treatments increased intracellular $Ca^{2+}$ concentration ($[Ca^{2+}]_i$) in several cell lines including cerebellar granules [Severini et al., 2008], GH3 [Petrocchi et al., 2013], brain and spinal cord-derived primary microglia [Chen et al., 2013], and insulinoma cell lines [Petrocchi et al., 2015]. Importantly, in hamster CHO-K1 cell line and rat ovary cell line O-342, the cell signaling cascade activated by TLQP-21/C3aR1 seemed dependent upon ATP priming that led to increased $[Ca^{2+}]_i$ and sensitive to pertussotoxin, suggesting the C3aR1 receptor to either be a $G_{i/o}$ coupled receptor [Hanneduche et al., 2012].

Based on these findings the working hypothesis in this current study was that TLQP-21 pro-lipolytic effect requires increased $[cAMP]_i$ and is mediated by increased $[Ca^{2+}]_i$ and downstream phosphorylation of the MAPK/ERK pathway.

## 3.3 EXPERIMENTAL PROCEDURES

**Peptide Synthesis**

*For methods refer to Chapter 2.*

**Cell culture**

3T3-L1 cells were plated on 6 wells plates and maintained in DMEM with supplemented with 10% fetal calf serum (Lonza) and with penicillin/streptomycin 100units/ml (Invitrogen, Carlsbad, CA) in a humidified atmosphere of 5% $CO_2$ at 37°C. Media was changed every other day until cells were confluent. Once confluent, differentiation into adipocytes was initiated by using a differentiation cocktail containing 10% fetal bovine serum (FBS) (Atlas) 0.5mM methylisobutylxanthine (Sigma Aldrich, Saint Louis, MO), 10μg/ml insulin (Sigma Aldrich, Saint Louis, MO), and 0.25μM dexamethasone (Sigma Aldrich, Saint Louis, MO). After 48 hours, the media was replaced with FBS medium supplemented only with 10μg/ml insulin, which was removed after 2 day. Thereafter, the differentiated cells were maintained in DMEM with 10% FBS and media changed every other day used in experiments 8-9 days after induction.

**Primary adipocytes isolation**

Epidydimal fat pads (eWAT) from wild type and β-less mice were dissected under sterile conditions and washed in KRH buffer + 1% BSA fatty acid free (Roche). After finely mincing and digesting the tissue using collagenase type II (Sigma) for 30 minutes at 37°C in KRH buffer + 1%BSA, the digestion was then stopped by adding KRH + 1% BSA and the cell suspension centrifuged at 1240 rpm (or 200g) for 3 minutes to separate mature single adipocytes from the stromal vascular fraction. Adipocytes cell suspension was extensively washed and passed throw a 100μm cell strainer to separate single cells.

**Pre-adipocytes isolation, culture, differentiation**

A similar protocol was used for the isolation of pre-adipocytes, HBSS was used instead of KRH for the isolation process. Cell suspension was filtered through a 25μm mesh to remove endothelial cell and isolate stromal vascular fraction. The stromal vascular fraction was plated onto 12-well plates in DMEM/F12+10%FCS at a density of 150.00 cells/$cm^2$. Once confluency was reached, differentiation was

induced by the addition of induction media containing 250μM methylisobutylxanthine (Sigma Aldrich, Saint Louis, MO), 10μg/ml insulin (Sigma Aldrich, Saint Louis, MO), 100nM dexamethasone (Sigma Aldrich, Saint Louis, MO) and 60μM of indomethacin. After 48 hours, the induction media was replaced with insulin containing media, which was removed after 2 days. From that day forward, the maintenance media, DMEM/F12+10%FCS, was replaced every other day and differentiated cells used at day 8-9 after induction.

**Lipolysis assay**

3T3-L1 adipocytes were serum-starved in Krebs-Ringer buffer containing HEPES (KRH buffer) (NaCl at 120mM; KCl at 4.7mM; $CaCl_2$ at 2.2mM; HEPES at 10mM; $KH_2PO_4$ at 1.2mM; $MgSO_4$ at 1.2mM; glucose at 5.4mM) supplemented with 1% bovine serum albumin (BSA) fatty acid free (Roche) for 3 hours. Following starvation the cells were incubated with KRH buffer containing 4% BSA with TLQP-21 (100nM) in presence and absence of Isoproterenol (ISO) (Sigma) concentrations raging from 1nM, 15nM, 50nM, 100nM, 1μM; Forskolin (100nM, 1μM and 10μM) (Sigma) or ethylene glycol tetraacetic acid (EGTA) (1mM).

For the intracellular cheletor 1,2-bis (*o*-aminophenoxy) ethane-*N*,*N*,*N*′,*N*′-tetraacetic acid tetra (acetoxy- methyl) ester (BAPTA-AM) (Sigma) experiments, the differentiated cells were first pre-exposed to BAPTA-AM (5μM) in KRK with 4% BSA for 10 min, the buffer was then removed and replaced with buffer containing different treatments. 1μM and 10μM MEK1/2 inhibitor U0126 (Calbiochem) was used to inhibit the activation of MEK1 and MEK2 that are directly responsible for the activation of ERK.

In the pre-adipocytes' lipolytic experiments, a similar protocol to the 3T3L1 cells was used. For lipolysis in primary adipocytes, 150-200,000 adipocytes were incubated in 1X KRH buffer + 4% BSA fatty acid free (Roche) for 180 minutes at 37°C with Isoproterenol (1nM to 10mM) or Forskolin (10μM).

In all experiments, lipolysis was measured as the rate of glycerol release over a 3h period. Following the 3 hours of incubations with treatments at 37°C and 5% CO2, the media was collected and incubated at 60°C for 20 min to inactivate any enzymes released from the cells. Media was stored at -20°C until the glycerol assay was performed.

For 3T3L1 cells, free glycerol concentration was measured by reacting 80μl of conditioned media with 120μl of Free Glycerol Reagent from the Free Glycerol Determination kit (Sigma) in a flat-bottom 96-well plate. For the primary and pre-adipocytes, 30μl of supernatant was combined to 120μl of free glycerol reagent. All samples were allowed to incubate for 15 minutes at room temperature. Absorbance was measured at 540 OD on a plate reader (Synergy H1, BioTEK) to determine glycerol content and was normalized to total cellular protein content determined with the Bradford Assay (Thermo Scientific). The data were normalized to the control response detected in the same experiment and are expressed as fold change over controls.

**Western blot**

3T3L1 cells were rinsed 3X with cold PBS and harvested in RIPA buffer containing protease (Complete Mini, Roche) and phosphates inhibitors (Thermo Scientific). Lysates were then sonicated and centrifuged at 12,000 rpm for 10 min the protein concentration was determined using Bradford Assay (vendor). Equivalent amount of cell extracts were diluted in sodium dodecyl sulfate (SDS) sample buffer and boiled for 5 min at 95°C. Proteins were resolved by SDS-polyacrylamide gel electrophoresis and transferred to nitrocellulose membranes (Bio-Rad, Hercules, CA Individual proteins were detected with the specific primary antibodies following incubation overnight at 4°C (tubulin, p44/42 and pp44/42 all at 1:1000 from Cell Singnaling). Incubation with peroxidase-coupled secondary goat-anti-rabbit antibodies (1:20.000, LI-COR) was performed at room temperature for 1 h and developed with enhanced chemiluminescence (LI-COR).

**Quantitative Real-Time PCR**

Undifferentiated and differentiated 3T3L1 were harvested in 400μl TRI REAGENT (Molecular Research Center, Inc., Cincinnati, Ohio) and RNA was ISOlated follwing the manufacturer's instructions. Total RNA was digested with Dnase I using DNA-free (Ambion, Austin, TX) and tested for the presence of DNA contamination using PCR. Total RNA concentration and purity was then determined using NanoDrop at the UV absorbency of 260 nm (NanoDrop 2000 UV-Vis Spectrophotometer, Thermo Scientific). 1μg of RNA was converted into cDNA using iScript cDNA Synthesis Kit (Bio-Rad Laboratories, Hercules, CA). The mouse neuronal ion channels PCR array

(Qiagen) was used according the manufactures instructions using the C1000 thermal cycler ™ (Bio-Rad Laboratories, Hercules, CA). The PCR reactions were carried out using IQ™ Syber Green Supermix. Thermal cycling conditions were hotstart for 10 minutes and 40 cycles of 95°C for 15 sec and 60°C for 60 sec with the ramp rate between the 95°C to 60°C sec being 1°C/sec. The results were calculated by the comparative $C_t$ method using β-actin as an endogenous reference gene.

**Fura-2 loading and $Ca^{2+}$ measurements**

3T3-L1 cells grown to confluence and were differentiated in chamber slides (Lab Tex). On day 8 of differentiation, cells were loaded and incubated for 90 minutes with FURA-2 acetoxymethyl ester, then washed in Hanks' balanced salt solution (HBSS, Thermo Scientific) free from $Ca^{2+}$. Single cell fluorescence was visualized using a Nikon UV-fluor 20X or 40X oil-immersion objective. Intracellular $Ca^{2+}$concentration $[Ca^{2+}]_i$ will be measured as the ratio of fluorescence emitted when the cells will be alternately excited at 340 and 380 nm ($F_{340}/F_{380}$). Cells were treated with TLQP-21 in presence or absence of ISO. $[Ca^{2+}]_i$ and prostaglandin $F_{2\alpha}$ ($PGF_{2\alpha}$) known to be responsible for calcium mobilization in 3T3-L1 cells used a positive control. Image acquisition and data analyses were performed using Image-1 MetaMorph software running on a Dell Optiplex 760 microcomputer. $[Ca^{2+}]_i$ was measured as the ratio of fluorescence emitted at 510 nm when the cells were alternately excited at 340 nm and 380 nm [$F_{340}/F_{380}$)]. $[Ca^{2+}]_i$ was calculated following calibration using the Fura-2-AM calcium imaging calibration kit (Life Technologies).

**Statistical Analysis**

Statistical Analysis was evaluated using the analysis of variance (ANOVA) using Statistica 12. After a statistically significant ANOVA result, we performed between-group comparisons using the Tukey *post hoc* analysis for comparisons of all means. The data are reported as the means ± SEM from at least 2-5 independent experiments with n=3 for each experiment. Graphs were performed with Graphpad Prism, version 5.

## 3.4 RESULTS

### TLQP-21 potentiates lipolysis

3T3L1 adipocytes were incubated with TLQP-21 ranging from 50nM to 1μM and ISO ranging from 1nM to 1μM. As expected, ISO-induced a dose-dependent increase in lipolysis starting from 10nM [$F(8,79)=29.1$, $p<0.00001$]. Conversely, treatment with TLQP-21, even in the micro molar range, did not affect lipolysis, a finding in line with previous results obtained with mice mature adipocytes [Possenti et al., 2012].

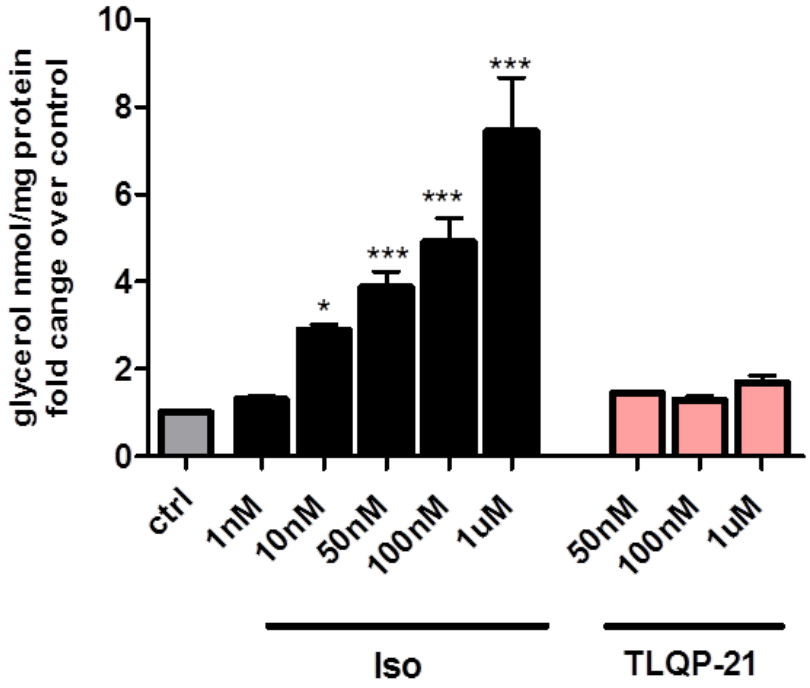


**Figure 3.1. ISO but not TLQP-21 dose dependently induced lipolysis in 3T3L1 cells.** Dose response study of ISO and TLQP-21 in 3T3L1 adipocytes. Treatments: ISO at 0 nM, 1nM, 10nM, 50nM, 100nM and 1μM; TLQP-21 at 50nM, 100nM and 1μM. TLQP-21 does not induce lipolysis per se. *p<0.001, **p<0.001, *** p<0.0001.

Subsequently, we co-incubated the adipocytes with ISO and TLQP-21 and found that TLQP-21 potentiated lipolysis induced by the β-adrenergic receptor agonist isoproterenol [$F(5,65)=62.1$, $p<0.0001$] (**Figure 3.2A)**. Moreover, 3T3L1 cells incubated with 50nM ISO and increasing doses of TLQP-21 displayed an initial increase in glycerol which plateaued at 100nM [$F(5, 38)=101.8$, $p<0.00001$] (**Figure**

**3.3B**). These data suggest that in 3T3L1 cells the target receptor for TLQP-21, C3aR1, could get saturated around 100nM.

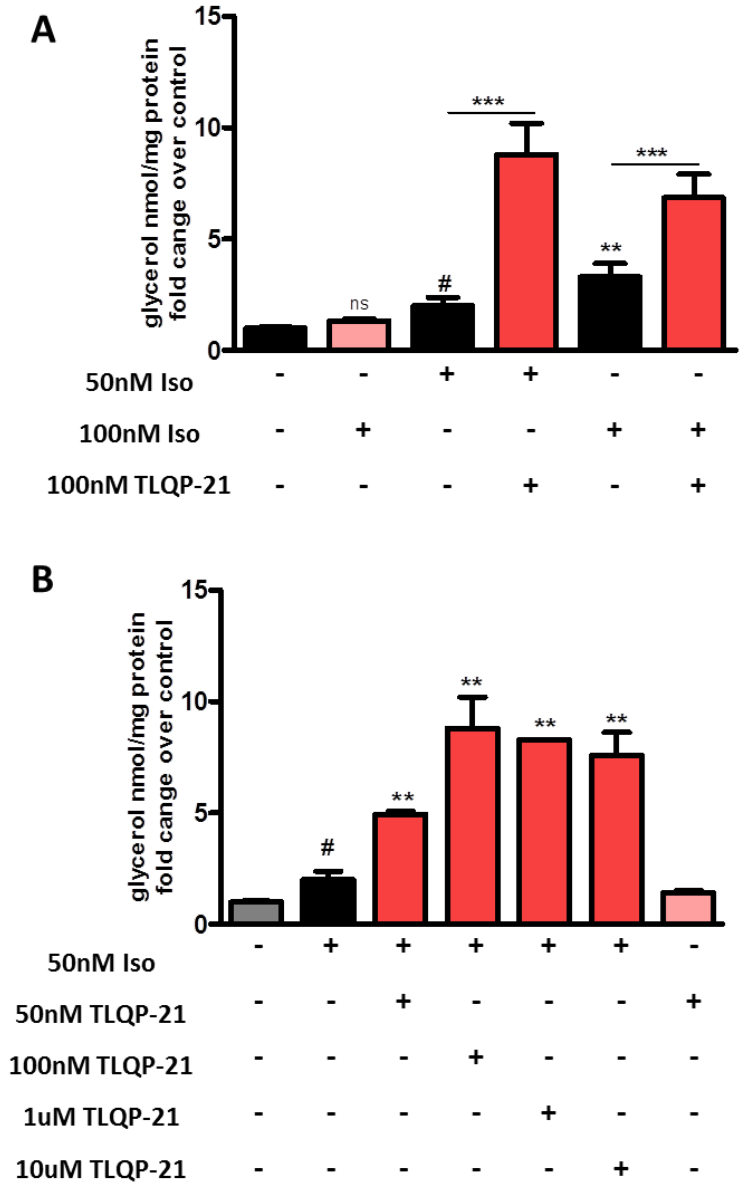


**Figure 3.2. TLQP-21 potentiates ISO-induced lipolysis.** Dose response study to ISO at 0 nM, 50nM and 100nM and TLQP-21 at 100nM in 3T3L1 adipocytes. Dose response study to TLQP-21 at 50nM, 100nM, 1μM and 10 μM and 50nM ISO. **p<0.001

Furthermore, to examine whether TLQP-21-mediated pro-lipolytic effects requires NE (or ISO) induced priming or the permissive action of increased $[cAMP]_i$,

3T3L1 cells were incubated with adenylate cyclase (AC) activator Forskolin (Forsk) that increase intracellular cAMP without the activation of the β-ARs. As expected [Schimmel, 1984], Forsk induced a dose-dependent increase of glycerol release from adipocytes (**Figure 3.3**) [**Figure 3.3A**; $F(4,19)=695.64$, $p<0.00001$] with TLQP-21 potentiating lipolysis induced by a maximal (10μM) but not a sub-maximal (100nM or 1μM) dose of Forsk [**Figure 3.3B**; $F(7,28)=211.01$, $p<0.0001$]. Overall, suggesting that the 10μM Fosrk increases intracellular cAMP and lipolysis to an extent that is similar to Iso 50-100nM.

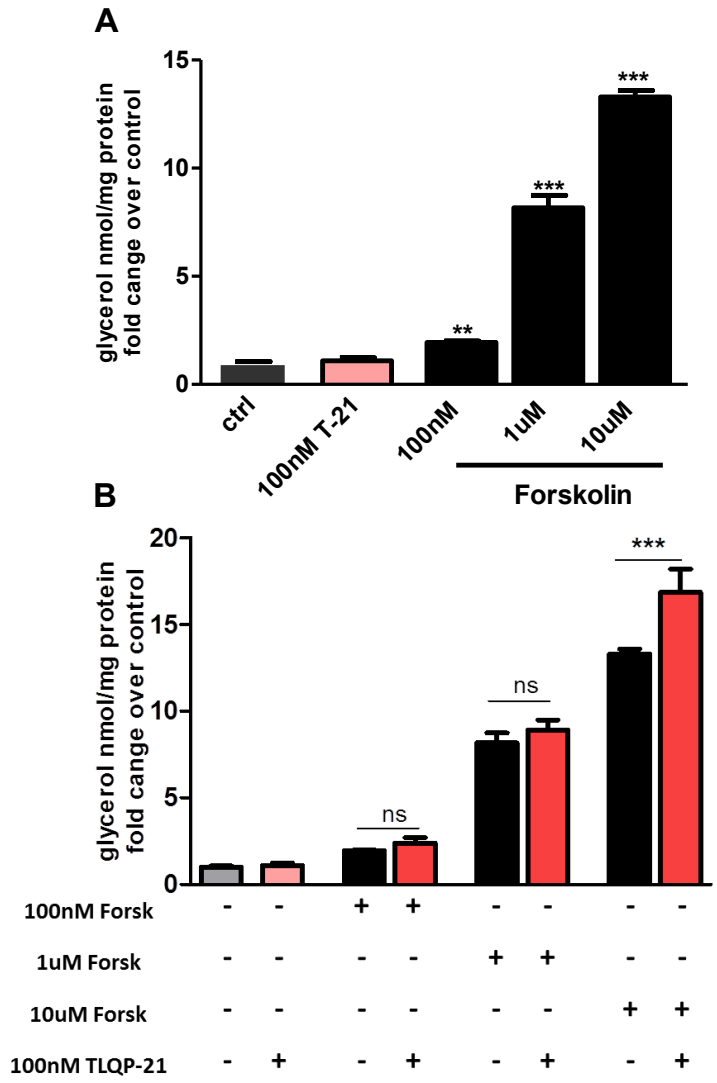


**Figure 3.3. TLQP-21 enhances Forskolin-induced lipolysis in 3T3L1.** TLQP-21 requires cAMP to lipolysis in 3T3L1 adipocytes. **p<0.001; ***p<0.0001.

We next used β-less adipocytes to further characterize the pro-lipolytic mechanism of TLQP-21. As predicted, mature adipocytes collected from β-less mice and stimulated in vitro were unresponsive to ISO treatment but were responsive to Forsk [F(2,8)=17.8, p<0.001] indicating that the lipolytic pathway downstream of β-AR is maintained (**Figure S3.1**). We next isolated, cultured and differentiated β-less pre-adipocytes into mature adipocytes and treated with Forsk (1μM or 10μM) in presence or absence of TLQP-21 (100nM or 1μM). TLQP-21 potentiated Forsk-induced lipolysis in β-less adipocytes although with a slightly different pharmacology compared to 3T3L1 that can be explained by the altered signaling and biogenesis characteristic of this mutant strain [Bachman et al 2002; Tavernier et al., 2005] [F(4,15)=9.4, p<0.0005] (**Figure 3.4).** Altogether, these data demonstrate that increased cAMP exerts a permissive action for TLQP-21-induced lipolysis.

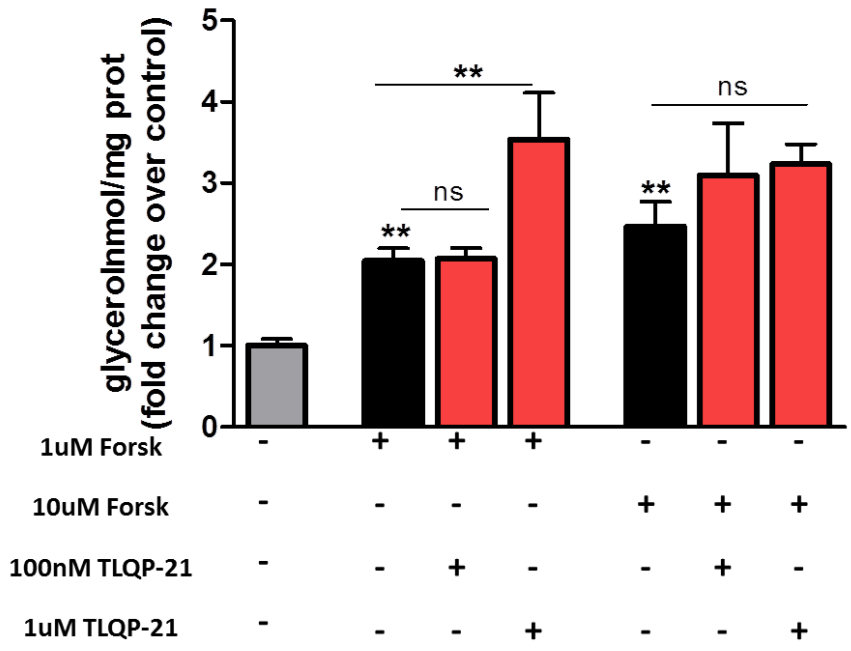


**Figure 3.4. TLQP-21 requires cAMP to induce lipolysis.** TLQP-21 stimulates Forsk-induced lipolysis in β-less pre-adipocytes **p<0.001.

## TLQP-21 pro-lipolytic effects are mediated by C3aR1 activation

We next examined the effect of C3a on lipolysis in 3T3L1 adipocytes. We used an murine octapeptide containing the C-terminal fragment of the C3a anaphylatoxin peptide, the $C3a_{70-77,}$ a well established C3aR1 agonist [Hugli and Erickson, 1977]. Similarly to TLQP-21, $C3a_{70-77}$ did not modulate lipolysis in absence of isoproterenol (**Figure 3.5A**), while enhanced ISO-induced lipolysis [F(5,26)=64.8, p<0.000001](**Figure 3.5**).

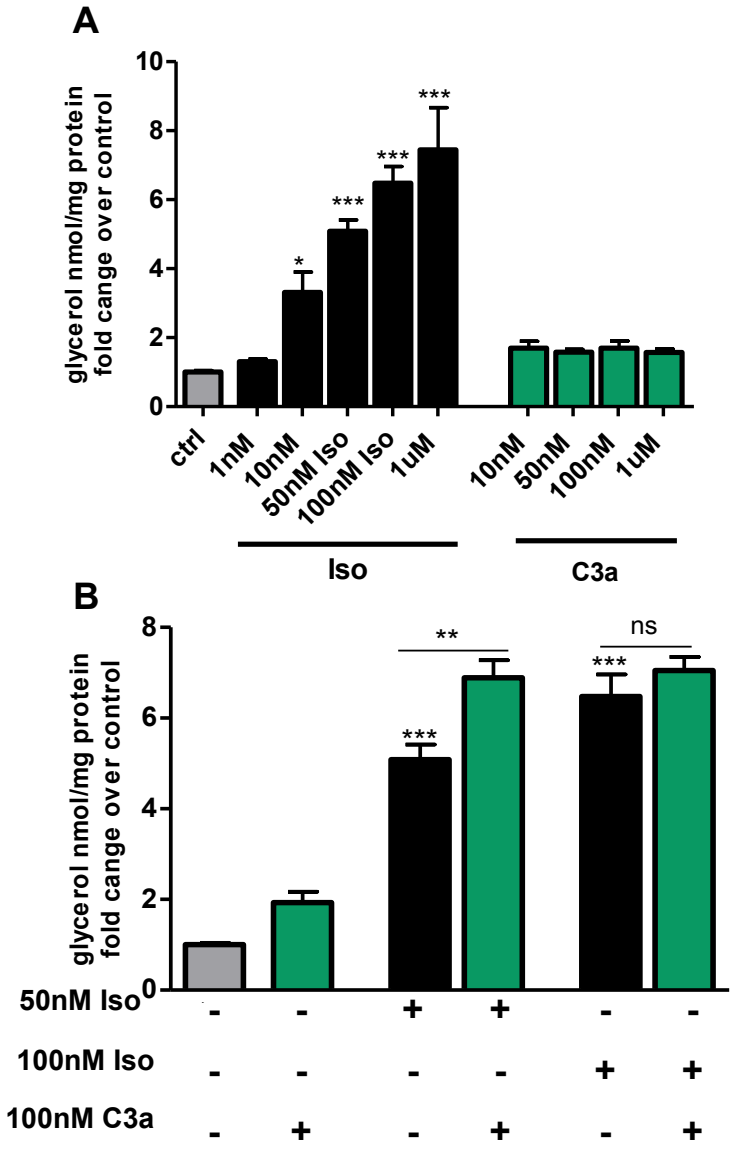


**Figure 3.5. $C3a_{70-77}$ enhances lipolysis in 3T3L1.** Similar to TLQP-21, C3a70-77 peptide potentiates ISO-induced lipolysis in 3T3L1 adipocytes. ***p<0.0001.

Furthermore, we recently established that the C-terminal arginine at position 21 in the TLQP-21 peptide sequence is required for C3ar1 activation [Cero et al., 2014; **Chapter 2**]. Specifically, an R21A mutant is deprived from its biological activity in the stomach fundus strip contraction assay [Cero et al., 2014]. These findings led us to investigate whether the R21A peptide modulates lipolysis in 3T3L1 adipocytes. In marked contrast with the pro-lipolyitic activity of TLQP-21, equimolar concentration of R21A mutant peptide did not potentiate ISO-induced lipolysis [$F(5,65)=33.4$, $p<0.00001$] (**Figure 3.6A**). Moreover, contrarily to TLQP-21, the R21A mutant did not increase the phosphorylation of AMPK **(Figure 3.6B**). Overall, these results highlight the critical role of Arg-21 for activating C3aR1-induced lipolysis.

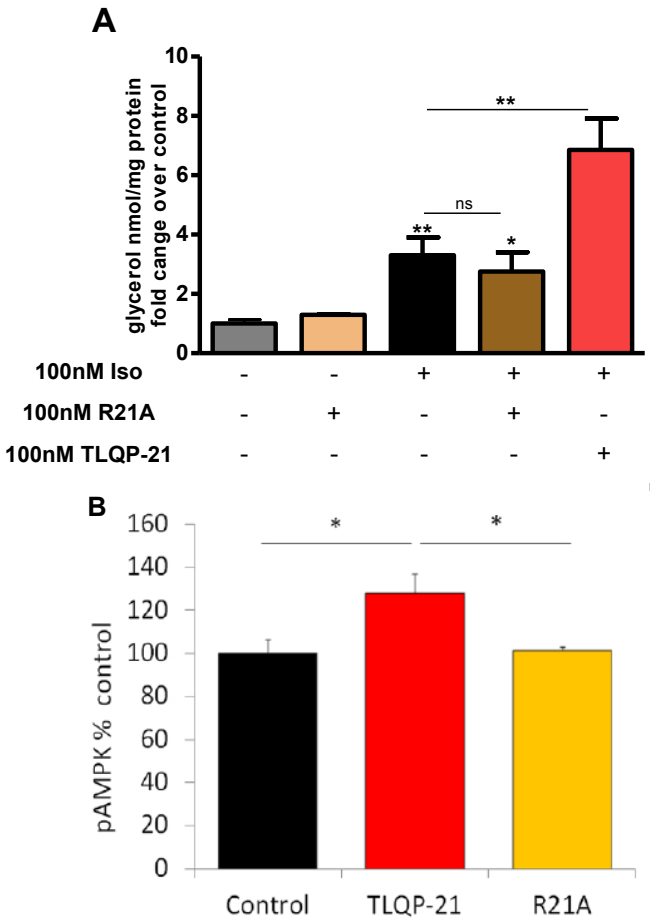


**Figure 3.6. TLQP-21 but not R21A mutant enhances lipolysis in 3T3L1.** Unlike TLQP-21, the R21A mutant peptide does not potentiate ISO-induced lipolysis in 3T3L1 adipocytes. *p<0.001, **p<0.001.

## TLQP-21 increases lipolysis with a mechanism dependent upon increased $[Ca^{2+}]_i$.

Based on previous work [Severini et al., 2008; Petrocchi et al., 2013; Chen et al., 2013; Petrocchi et al., 2015], we hypothesized that TLQP-21 increases $[Ca^{2+}]_i$ to promote ISO-induced lipolysis. To test this hypothesis, 3T3L1 adipocytes were pre-treated with the intracellular $Ca^{2+}$ chelator BAPTA-AM, a cell-permeable molecule that is enzymatically converted to the non cell-permeable calcium chelator BAPTA once within the cell, and performed our lipolyistic experiments in presence of 100nM ISO with or without equimolar concentration of TLQP-21. BAPTA-AM pre-treatment prevented TLQP-21-induced enhancement of ISO-induced lipolysis [$F(5,141)=30$, $p<0.0001$] (**Figure 3.7A)**. Additionally, to determine if increased $[Ca2+]_i$ is mobilized from intracellular or intracellular compartments we also used the extracellular $Ca^{2+}$ chelant EGTA. Similarly to BAPTA, EGTA pretreatment prevented TLQP-21 induced lipolysis [$F(5,155)=33$, $p<0.0001$] (**Figure 3.7B)**. Together, our data demonstrate that calcium mobilization is required for TLQP-21 enhanced lipolysis (**Figure 3.7C**), possibly via activation of the highly expressed membrane transient receptor potential (TRP) TRPC1 and TRPM2 (**Table S3.1**).

We next aimed to provide a direct evidence in support of TLQP-21-increased $[Ca^{2+}]_i$ by using FURA2-AM, a membrane permeable ratiometric florescent dye that binds to free intracellular $Ca^{2+}$ thus allowing to determine global cytosolic changes in its concentration [Gericke et al., 2009]. Surprisingly, TLQP-21 alone or after ATP and UTP priming [Hanneduche et al., 2012] did not lead to an appreciable increase in $[Ca^{2+}]_i$ (**Figure S3.4**) in our experimental conditions. The absence of FURA-detectable increase in $[Ca^{2+}]_i$ is compatible with a local membrane event [Pedersen et al., 1997] or suggestive of a permissive effect of calcium on TLQP-21-induced lipolysis.

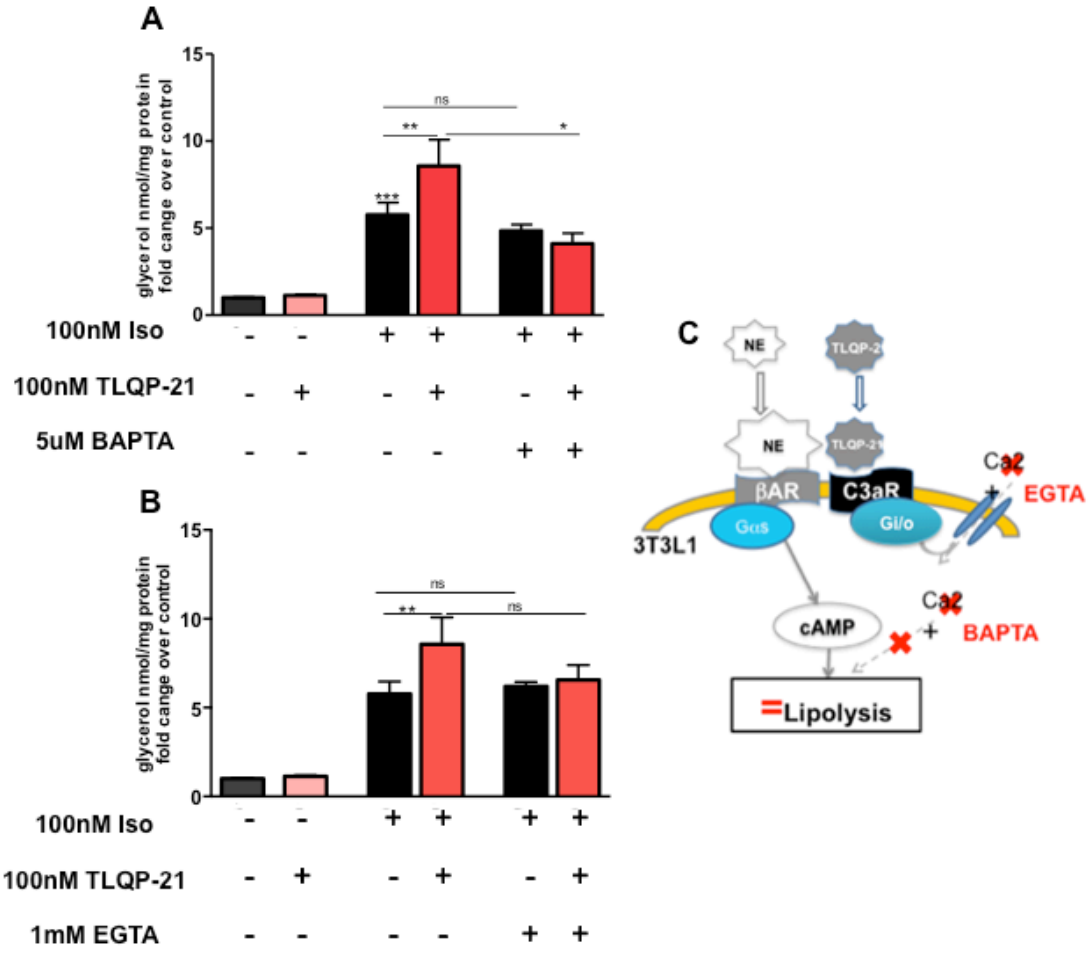


**Figure 3.7. TLQP-21 induced lipolysis is dependent on the rise of free intracellular $Ca^{2+}$.** (**A**) TLQP-21 potentiation of lipolysis is blocked by the intracellular $Ca^{2+}$ chelator BAPTA-AM and (**B**) prevented by the extracellular $Ca^{2+}$ chelant EGTA. (**C**) Schematic representation of proposed mechanism.

## TLQP-21 activates the MAPK/ERK pathway to promote lipolysis

After establishing that TLQP-21 requires $Ca^{2+}$ mobilization to promote lipolysis and based on the evidences that i) TLQP-21 increase the phosphorylation of ERK and increases ISO-induced phosphorylation of ERK and HSL [Possenti et al., 2012] and ii) that ERK has been shown to phosphorylate HSL thereby inducing lipolysis [Greenberg et al., 2001], we hypothesized that TLQP-21 activation of C3aR1 could signal via the MAPK/ERK pathway.

We first assessed the effects of Iso and TLQP-21 on ERK phosphorylation in presence and absence of the MAPK inhibitor U0126. Following 3h of incubation, as previously shown [Greenberg et al., 2001], U0126 10μM decreased β-adrenergic stimulated pERK (**Figure S3.5**). TLQP-21 enhanced Iso-induced ERK phosphorylation and partially restored the inhibitory effects of U0126 on ISO-induced pERK (**Figure S3.5**).

We next tested the effects of a lower dose of U0126 on TLQP-21 mediated lipolysis (the 10μM dose dramatically inhibited spontaneous and ISO-induced lipolysis, data not shown). Pre-incubating 3T3L1 adipocytes with 1μM U0126 completely prevented TLQP-21 pro-lipolytic effect without affecting ISO-induced lipolysis [$F(10,22)=43.7$, $p<0.000001$] (**Figure 3.8**). Overall these and previous data demonstrate that TLQP-21 pro-lipolytic effect is mediated by MAPK/ERK activation.

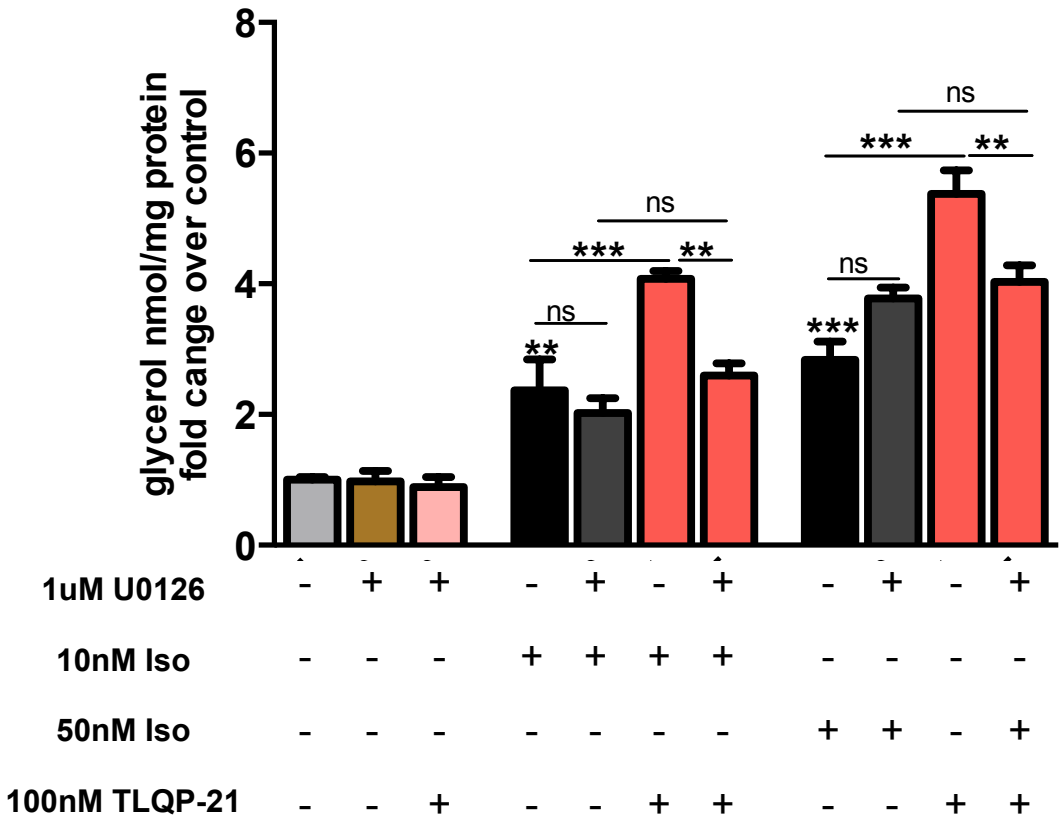


**Figure 3.8. TLQP-21 lipolysis is mediated by the activation of MAPK/ERK pathway.** 1h pre-incubation with MEK1/2 kinase inhibitor U0126 completely blocks TLQP-21 lipolysis in fully differentiated 3T3L1 cells. **p<0.001; ***p<0.0001.

## 3.5 DISCUSSION

In this study we investigate the molecular mechanism of TLQP-21 mediated lipolysis in adipocytes. Here we demonstrate the ability of TLQP-21 to enhance catecholamine and cAMP-stimulated lipolysis in adipocytes. Moreover, we demonstrated that TLQP-21 mediated lipolysis requires increased intracellular cAMP and $Ca^{2+}$ mobilization and is mediated by MAPK/ERK activation.

We demonstrate that in 3T3L1 adipocytes, TLQP-21 stimulates β-AR's-activation-induced lipolysis, as well as lipolysis induced by the adenylate cyclase (AC) activator Forskolin (Forsk). TLQP-21 does not compete with catecholamines to bind to β-ARs; instead it specifically binds to the C3aR1 [Possenti et al., 2012; Hanneduche et al., 2012; Cero et al., 2014]. cAMP signaling is the major pro-lipolyitic pathway in adipose tissue, where cAMP activates PKA that consequently activates HSL by phosphorylation finally resulting in DG hydrolisis [Kolditz et al. 2010]. Catecholamine-stimulation leads to higher concentrations of total cAMP compared to Forsk [Litosch et al., 1982], therefore higher concentration of Forsk were required to detect the pro-lipoltytic effects of TLQP-21 in 3T3L1 cells. Importantly, we showed in 3T3L1 cells that at a submaximal dose of ISO, increasing concentrations of TLQP-21 produces higher lipolytic effects until it reached a plateau (100nM) (**Figure 3.2B**). These results suggest that in 3T3L1 adipocytes C3aR1 saturation could be around 100nM, similar to what was found in mature adipocytes [Possenti et al., 2012]. However, in β-less adipocytes stimulated with a submaximal dose of Forsk, a higher concentration of TLQP-21 (1μM) was required to enhance lipolysis (**Figure 3.3B**), suggesting an altered cAMP activation in cells deficient of βARs. Overall, we conclude that increased cAMP exerts a permissive effect on TLQP-21-induced lipolysis while our data do not support the conclusion that signaling molecules should act as primers for C3aR1 activation [Hanneduche et al., 2012]. In contrast to TLQP-21, the null peptide R21A [Cero et al., 2014, **Chapter 2**], does not exert any lipolytic effect, thus identifying the C-terminal arginine of TLQP-21 as the essential amino acid within the TLQP-21 sequence for its pro-lipolytic effect (**Figure 3.6)**.

Being C3a another potent ligand for C3aR1 [Nettesheim et al., 1988; Choy et al., 1996], and having the C3aR1 agonist $C3a_{70-77}$ [Hugli and Erickson 1977] similar contractile activity on fundus strips compared to TLQP-21 (**see Chapter 2**), we assessed the lipolytic effects of $C3a_{70-77}$ on 3T3L1 cells. We observed that similar to TLQP-21, $C3a_{70-77}$ did not exert any pro-lipolytic effects; while when co-incubated

with ISO, the peptide induced a similar lipolyitic effect (**Figure 3.5)**. These data are in contrast with previously published data [Lim et al., 2013] where C3a has been shown to inhibit ISO-induced glycerol release. It is important to note that the C3aR1 agonist used in Lim et al., [2013] was purified human serum C3a used on murine 3T3L1 cells, which suggest a species-specific difference in peptide/receptor activation; a finding consistent with our demonstration that the human TLQP-21 sequence is ~8-fold less potent at the human C3aR1 compared to the rodent TLQP-21 [Cero et al., 2014]. To use a direct loss of function approach we incubated C3aR1 KO adipocytes with ISO in the presence and absence of TLQP-21. In our experiments C3aR1 KO pre-adipocytes were unresponsive to ISO treatments suggestive of altered βAR functions, and therefore we could not observe TLQP-21 potentiation of ISO-induced lipolysis (data not shown). Additionally, we also attempted to use in 3T3L1 adipocytes the C3aR1 antagonist, SB290157 [Cero et al., 2014]. However the antagonist is soluble in DMSO (0.053%), which induced lipolysis per se, thus limiting its validity in our experimental conditions. Overall, despite we lack a direct demonstration that antagonizing C3aR1 is necessary and sufficient to explain TLQP-21 effect, current and previous data strongly are in strong support of the hypothesis that its effect in adipocyte is mediated by C3aR1 (see also **Chapter 2 and 4**).

With our pharmacological approach we demonstrate that TLQP-21 requires mobilization of intracellular $Ca^{2+}$ to improve lipolysis. Indeed, pre-treating differentiated 3T3L1 cells with the intracellular $Ca^{2+}$ chelator BAPTA or with the extracellular $Ca^{2+}$ chelator EGTA, prevented TLQP-21 pro-lipolytic effects (**Figure 3.7)**. Conversely, we were unable to detect the increase of free intracellular $Ca^{2+}$ in the differentiated 3T3L1 cells even after priming the cells with ATP/UTP [Hanneduche et al., 2012] (**Figure S3.4**). A finding in contrast to the observed increased $[Ca^{2+}]_i$ exerted by TLQP-21 in several other cell lines [Severini et al., 2008; Petrocchi et al., 2013; Chen et al., 2013; Petrocchi et al., 2015]. Hence, TLQP-21 binding to C3aR1 receptor in the 3T3L1 cells may not be activating the PLC/PKC pathway which is line with our previously published phosphorylation data where TLQP-21 failed to phosphorylate PKC [Possenti et al., 2012]. Conversely, the lack of increased $[Ca^{2+}]_i$ detection by FURA2-AM is also compatible with a highly localized and transient membrane local increase similarly to other molecules [Pedersen et al., 1997]. We speculate that C3aR1 activation could be coupled to a $Ca^{2+}$ channels, such as the TRP channels, and the quick and transient increase of $[Ca^{2+}]_i$ given by TLQP-21 could be hard to detect in adipocytes having a limited cytoplasmic

compartment. Moreover, since the extracellular physiological level of $Ca^{2+}$ is 4-fold higher than the intracellular milieu (1mM vs 100nM), it is reasonable to conclude that the influx of $Ca^{2+}$, from the extracellular rather than the intracellular compartments, plays a major role in TLQP-21-induced lipolysis.

Increase of intracellular $Ca^{2+}$ levels positively modulates Ras, the small GTPase that activates the Raf/MAPK/ERK pathway [Cullen et al., 2002; Agell et al., 2002], activating the downstream ERK cascade [Greenberg et al., 2001; Chuderland et al., 2008]. ERK has been reported as an alternative-signaling pathway to activate lipolysis in adipocytes by directly activating HSL by phosphorylation [Greenberg et al., 2001; Rapold et al., 2013; Drira et al., 2014]. TLQP-21 phosphorylates ERK and potentiates ISO-induced phosphorylation of ERK and HSL in 3T3L1 cells [Possenti et al., 2012 and present work]. Thus, we postulated that in adipocytes TLQP-21 mobilizing $Ca^{2+}$ to promote lipolysis could consecutively be activating the Ras/Raf/MAPK/ERK pathway. As previously shown [Greenberg et al., 2001], high dose of U0126 (10μM) decrease ISO-induced phosphorylation of ERK; however we observe a partial recovery of ERK phosphorylation in presence of TLQP-21. Moreover, TLQP-21 enhanced ISO-induced lipolysis was blocked by MEK1/2 inhibitor (**Figure 3.8)**. Our data clearly demonstrate that TLQP-21 mediated lipolysis is MAPK/ERK dependent. Because calmodulin (CaM), the calcium binding protein, is the most abundant $Ca^{2+}$ sensor that binds to increased intracellular $Ca^{2+}$ forming the $Ca^{2+}$/Calmodulin that activates CaM kinase (CaMK) prolonging the effects of a transient $Ca^{2+}$ increase, it would be of interest to block CaMK and study TLQP-21 induced lipolysis. Moreover, since the ERK pathway plays a major role in cell proliferation and differentiation, it would also be of interest to investigate whether TLQP-21 affects these cellular processes.

Lipolytic catecholamine resistance is a considered to be hallmark in obesity and metabolic syndrome [Arner, 1999]. Adipose lipolysis is positively regulated by catecholamine and cAMP signaling pathway [Langin, 2006] that decreases with age [Lönngvist et al., 1990] and is impaired in obesity [Reynisdottir et al., 1994; Stallknecht et al., 1997]. Hence, TLQP-21 potentiating lipolysis without causing cardiovascular side effects [Fargali et al., 2014] could be a new drug target worth investigating that for the treatment of obesity (See **Chapter 4**).

In summary, we established that *in vitro* TLQP-21 potentiation of lipolysis in adipocytes requires increased intracellular cAMP rather than priming via β-ARs activation. Moreover, we provide mechanistic insights demonstrating that TLQP-21

mediated lipolysis require an increase in intracellular $Ca^{2+}$ levels that might trigger the activation of the MAPK/ERK pathway enhancing ISO/cAMP-induced HSL phosphorylation (**Figure 3.9**) [Possenti et al. 2012].

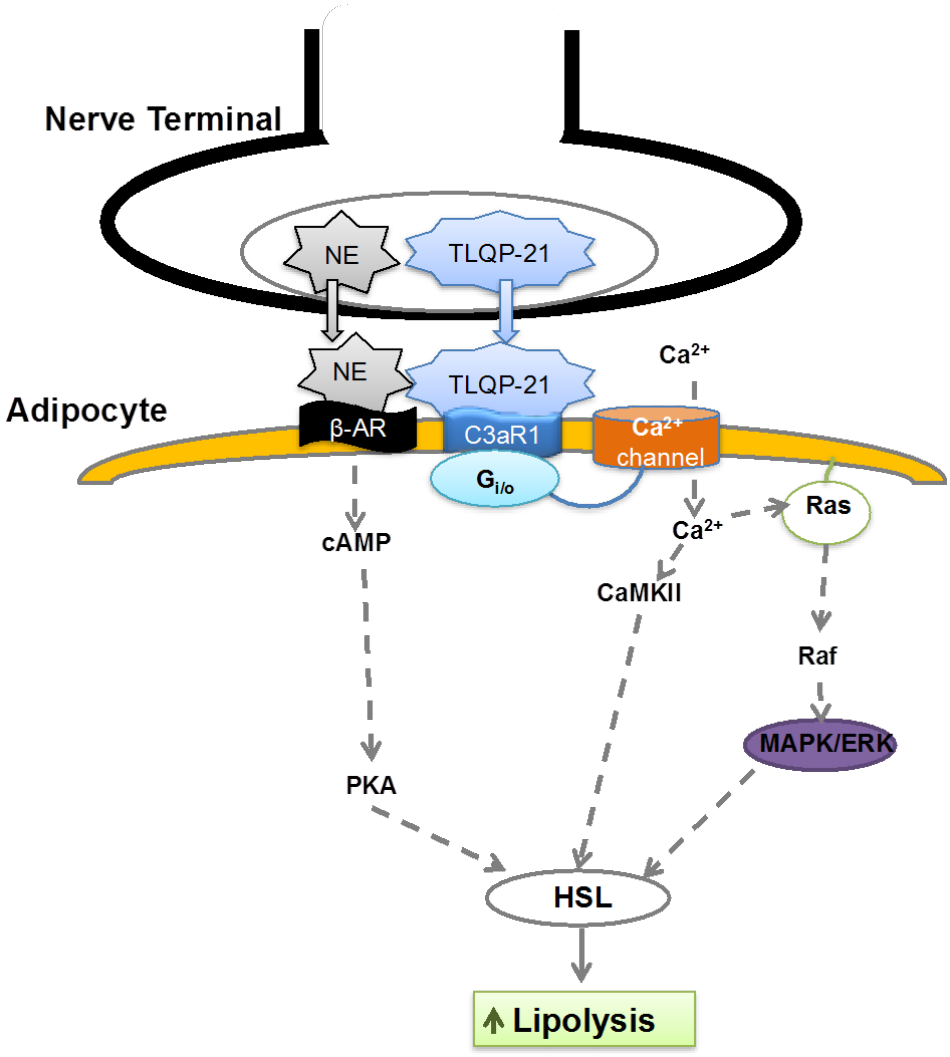


**Figure 3.9. Model of the mechanism activated by TLQP-21 to enhance lipolysis**

# ACKNOWLEDGMENTS

Supported by Minnesota Partnership for Biotechnology and Medical Genomic, Decade of Discovery in Diabetes Grant and NIH/DK102496 (to A.B.). 3T3L1 cells were provided by The Molecular & Cellular Basis of Obesity Core, Minnesota Obesity Center (5P30DK050456-18). We would like to thanks Dr. Veglia and Dr. Verardi for the peptide synthesis. Also, we would like to thank Olufemi Adams, Eric Finnesgard, Lauren Pelkey, Jessica Patricelli and Nick Speilman who have helped with the lipolysis assays.

## 3.6 SUPPLEMENTARY FIGURES

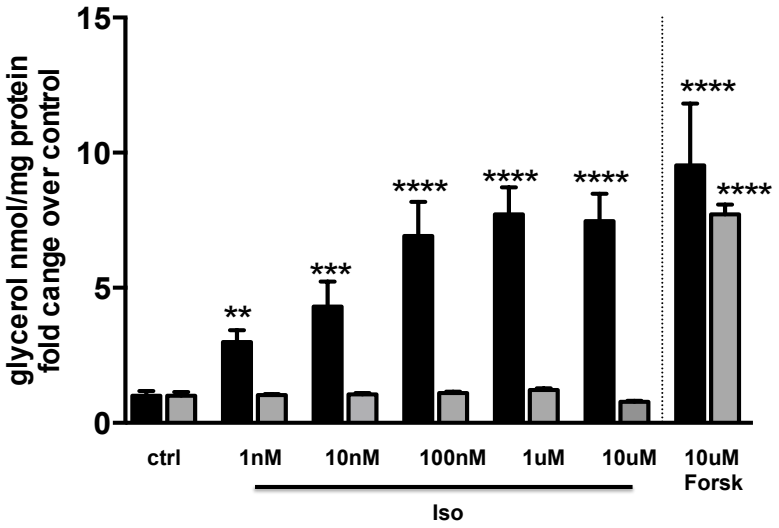


**Figure S3.1. Lipolytic response of primary wt (black) and β-less (grey) adipocytes to ISO and Forsk treatment.** β-less adipocytes undergo lipolysis when treated with Forsk but not with ISO. Treatments: ISO (1nM, 10nM, 100nM, 1μM and 10μM) and Forsk at 10μM **p<0.001, *** p<0.0001, **** p<0.00001 vs control.

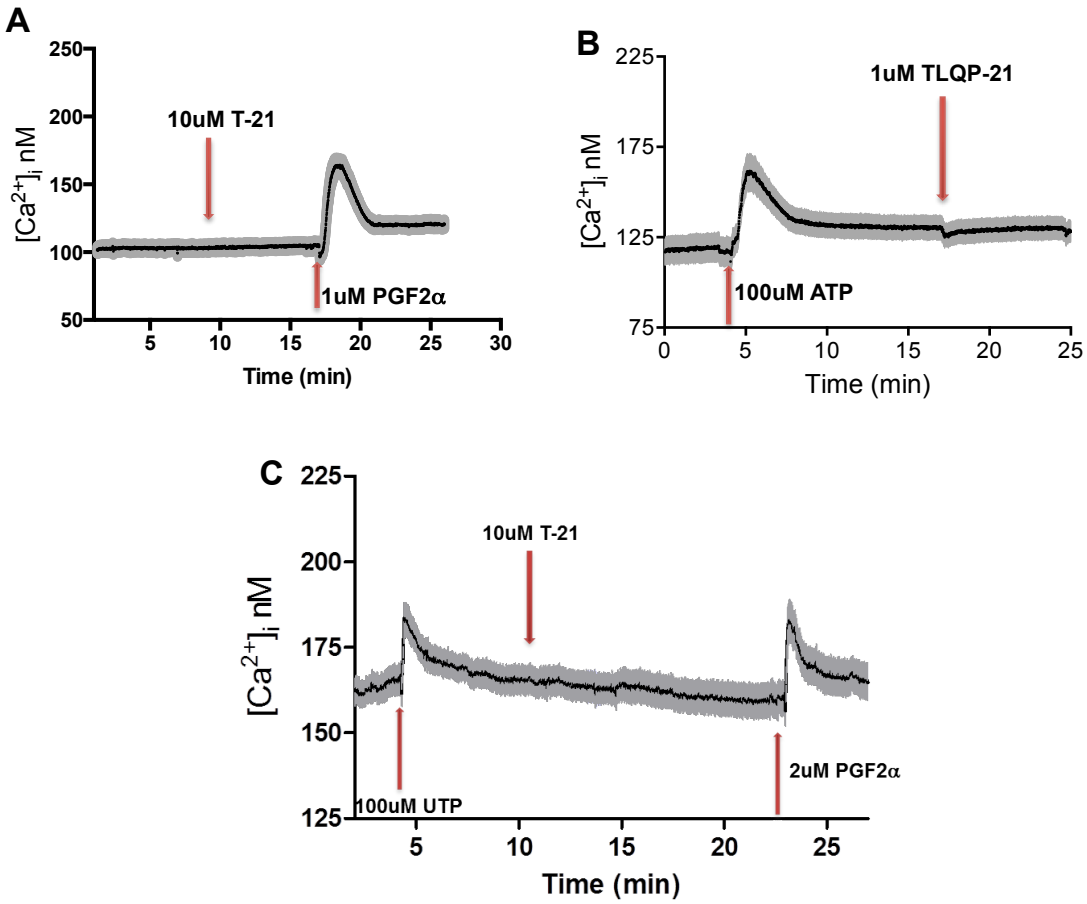


**Figure S3.2. In 3T3L1 cells, nor TLQP-21 alone neither ATP/UTP priming does evoke TLQP-21 induced rise in $[Ca^{2+}]_i$.** Differentiated 3T3L1 cells loaded with Fura2-AM and treated with the indicated pharmacological agents to release calcium. Intracellular calcium release was measured with the membrane-permeable calcium indicator FURA 2-AM (ratiomaetric measurement at 340nm and 380nm, expressed as 340/380. (**A**) TLQP-21 per se does not induce increase of $[Ca^{2+}]_i$. (**B-C**) Priming of the 3T3L1 cell with 100μM ATP or UTP doesn't elicit TLQP-21 to increase $[Ca^{2+}]_i$.

| TRP Gene | Mouse 3T3L1 cell line | |
|---|---|---|
| | Preadipocyte | Adipocyte |
| Trpa1 | 29.3 | 33.4 |
| Trpc1 | 28.8 | 28.9 |
| Trpc3 | 39.9 | 37.7 |
| Trpc6 | NA | NA |
| Trpm1 | 35.2 | 36.0 |
| Trpm2 | 28.2 | 27.2 |
| Trpm6 | 31.2 | 34.2 |
| Trpm8 | NA | 40.1 |
| Trpv1 | 34.8 | 31.8 |
| Trpv2 | 30.5 | 29.1 |
| Trpv3 | 34.6 | 35.9 |
| Trpv4 | 33.7 | 32.1 |
| β-actin | 19.8 | 20.2 |

**Table S3.1. Summary of TRP channels expression** (Ct values) in undifferentiated (preadipocytes) and differentiated (adipocytes) 3T3-L1 cells followed by 40 cycles of amplification.

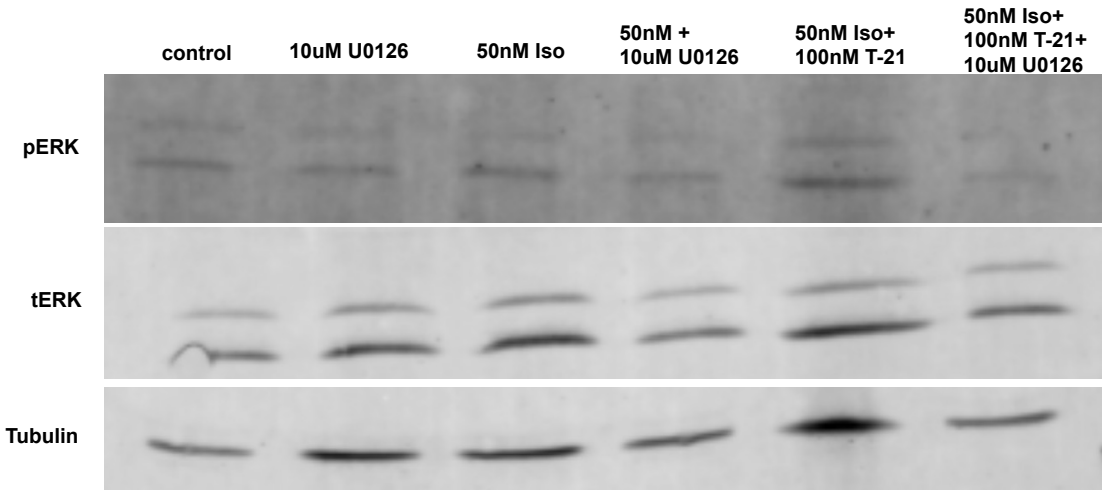


**Figure S3.3. Effects of TLQP-21 on phosphorylation of ERK.** 3h incubation of 50nM ISO in the presence or absence of 100nM and 10μM U0126. TLQP-21 restores the inhibitory effects of MEPP/ERK inhibitor U0126 on the phosphorylation of ERK given by ISO.

# Chapter Four

# TLQP-21 opposes obesity by enhancing β-Adrenergic Receptor-induced lipolysis

***Cheryl Cero[1], Maria Razzoli[1], Allison Gurney[1], Paolo Piaggi[3], Leslie J Baier[3], Gianluigi Veglia[2], ZengKui Guo[4], John M Miles[4], Alessandro Bartolomucci[1]***

[1] Department of Integrative Biology and Physiology, University of Minnesota, Minneapolis, MN 55455

[2] Department of Biochemistry, Molecular Biology and Biophysics, University of Minnesota, Minneapolis, MN 55455

[3] Phoenix Epidemiology and Clinical Research Branch, National Institute of Diabetes and Digestive and Kidney Diseases, Phoenix, AZ

[4] Endocrine Research Unit, Division of Endocrinology, Diabetes, Metabolism and Nutrition, Department of Internal Medicine, Mayo Foundation, 5-194 Joseph, Rochester, MN 55905

***In preparation to be submitted as a manuscript***

## 4.1 SUMMARY

We have previously demonstrated that chronic TLQP-21 treatment decreases adipocyte diameter and induces sympathetic nerve sprouting in white adipose tissue (WAT) of diet-induced obese mice. Mechanistically TLQP-21 enhances beta-adrenergic receptor (β-ARs)-activation induced lipolysis via phosphorylation of hormone sensitive lipase (HSL). The molecular mechanism of action *in vivo* remained so far largely unexplored.

Here, using a pharmacogenomics approach we tested the hypothesis that TLQP-21 anti-obesity effect is mediated by C3aR1 (Complement 3a Receptor 1) and require functional β-ARs. Diet-induced obese wt; $\beta_1$, $\beta_2$, $\beta_3$-adrenergic receptors knockout mice (β-less) and C3aR1 knockout mice were injected i.p. for four weeks with TLQP-21 or vehicle. TLQP-21 decreased weight and fat mass in wt but not in β-less mice. We also established that TLQP-21 anti-obesity effect is due to a low grade pro-lipolytic effect in the absence of changes in food intake. The anti-obesity effect was associated with a healthier metabolic phenotype as demonstrated by a normalization of branch chain amino acids (BBCA) and fed state hyperglycemia in absence of ectopic fat deposition in liver or muscle. Finally, we demonstrated that TLQP-21 activation of C3aR1 is necessary and sufficient to explain its anti-obesity effect. Taken together these results identify TLQP-21 as a novel target for anti-obesity therapies and suggest a possible mechanism of action.

## 4.2 INTRODUCTION

Obesity, a major public health challenge worldwide, is a major risk factor for chronic diseases including, type 2 diabetes, cardiovascular disease and cancer [Gudp et al., 2009]. Despite considerable advances in our understanding of the multiple signaling pathways involved in appetite regulation and energy homeostasis, we currently possess very few safe and effective therapeutic answers to obesity.

The Vgf (not acronymic) gene encodes for a 617 amino acid pre-pro-neurosecretory peptide [Levi et al., 1985, Salton et al., 1991] that is expressed throughout the brain and in several neuroendocrine and endocrine organs [Salton et al., 2000; Levi et al., 2004, Possenti et al., 1999]. The VGF peptide precursor, a member of the chromogranin/secretogranin family [Bartolomucci et al., 2011], undergoes endoproteolytic cleavage by prohormone convertases (PCs) generating several smaller bioactive products stored in secretory granules that are released upon regulated depolarization [Trani et al., 1995]. The implication of *Vgf* in energy homeostasis was first suggested by the evidence that germline deletion of the *Vgf* gene that confers a lean, hyperactive, hypermetabolic and an obese resistant phenotype [Hahm et al., 1999; Watson et al., 2009]. TLQP-21, one of the biologically active VGF-derived peptides, was first identified in rat brain by mass spectrometry and later shown to be expressed in sympathetic nerve terminals innervating white adipose tissue (WAT) as well [Bartolomucci et al., 2006; Possenti et al., 2012]. Complement 3a receptor 1 (C3aR1), a GPCR, has recently been identified as the main target for TLQP-21 [Hannedouche et al., 2013; Cero et al., 2014; See **Chapter 2 and 3**].

We have previously shown that central administration of TLQP-21 increases energy expenditure and prevents early phase of diet induced obesity [Bartolomucci et al., 2006]; while two week of chronic peripheral TLQP-21 delivery with osmotic minipumps in obese mice increased lipolysis, reduced adipocyte diameter and promoted eWAT sympathetic innervation [Possenti et al., 2012]. Remarkably, these physiological effects are paralleled by a normal myocardial morphology [Possenti et al., 2012] and normalized blood pressure [Faragli et al., 2014]. Contrasting data have been reported on the ability of TLQP-21 to enhance glucose-stimulated insulin secretion (GSIS). Stephens et al [2012] showed that TLQP-21 enchases GSIS and protected β-cells degeneration in rats preventing the onset of diabetes [Stephens et al., 2012]. Conversely, more recent work showed no effect of TLQP-21 on insulin

secretion in perfused rats pancreas [Christiansen et al., 2015] or a modest potentiation of glucose-stimulated insulin secretion in insulinoma cell lines [Petrocchi et al. 2015].

Mechanistically, TLQP-21 does not increase lipolysis per se in adipocytes, but it enhances the β-adrenergic receptor induced lipolysis [Possenti et al., 2012; See **Chapter 3**]. However, the potential for TLQP-21 to exert an anti-obesity effect and the exact mechanism of action remains to be identified. The identification of C3aR1 receptor as the target receptor for TLQP-21 and the ability of TLQP-21 to enhance the NE/β-AR induced lipolysis lead us to hypothesize that TLQP-21 anti-obesity effect are mediated by C3aR1 activation and dependent upon functional β-ARs expression.

## 4.3 EXPERIMENTAL PROCEDURES

**Animals Studies**

4-6 weeks old male β-less and their specific wt background strain [Bachman et al 2002], C57Bl6/J, C3aR1 KO and their specific wt background strain BALBc/J (Jackson Labs). Male mice were used in all our studies. All procedure were approved and performed according to Institutional Animal Care and Use Committee, University of Minnesota. Mice housed in same-sex groups of siblings (3-4 per cage) were under standard laboratory conditions at a constant temperature of 22±2°C in a 12h light/ 12h dark cycle, with food and water ad libitum. For the high fat diet induced obesity studies mice were fed a standard diet (STD, D12450B - Research Diets, Inc. 3.85 Kcal/g), and were then switched to a 60% kcal high-fat diet (HFD, D12492, - Research Diets, Inc. 5.24 Kcal/g) for nine weeks to induce a diet-induced obesity phenotype. Food intake and body weight were measured once a week to keep track of the phenotype. For the sub chronic and acute experiments, C3aR1 KO and wt were fed a STD.

**Experimental groups**

After nine weeks on HFD only the obese prone mice were selected for our experiments. Seven days before the beginning of the experiment, all animals were single housed for baseline recording. From day one body weight, food intake were measured every other day while body composition using EcoMRI-100 (QNMR Systems, Houston, TX) was performed on the last day to asses basal body composition. Based on the body weight mice from each genotype were randomized to the following experimental groups: (i) saline group (Con); (ii) 5mg/kg/d of TLQP-21 (iii) 5mg/kg/d R21A treatment.

**Treatment and Experimental Conditions**

TLQP-21 peptide and R21A mutant [Cero et al., 2014] were syntesized using the solid phase peptide synthesis method at the University of Minnesota. Lyophilized TLQP-21 was dissolved in sterile saline. Starting from day 1 of the experiment, a daily intra-peritoneal (i.p.) injection of either saline, TLQP-21 or R21A was administerd to mice alternating sides of injection. During chronic treatment, food intake and body weight were monitored every other day. A whole body composition

scanning was performed weekly. Glucose tolerance test (GTT) was also performed following an overnight fast (12h-14h). Blood glucose levels were measured from tail bleeding 0, 30, 60, and 120 min after an i.p. administration of D-glucose 2g/Kg. Accucheck Aviva glucometer (Roche Diagnostics, Indianapolis, IN, USA) was used to measure glucose (mg/dl).

A week prior to sacrifice, energy expenditure was monitored using indirect calorimetry. At the end of the experimental session, all mice were deeply anesthetized with $CO_2$ and were sacrificed by decapitation.

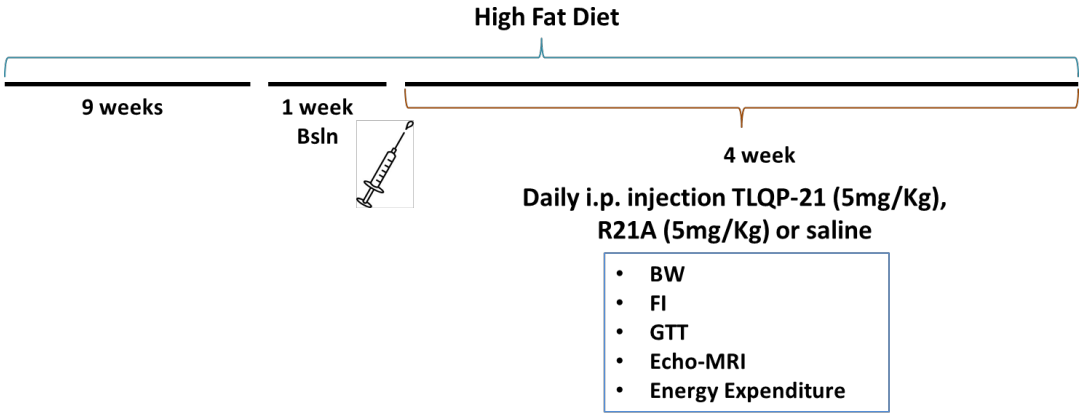


**Figure 4.1. Cartoon of experimental protocol for chronic *in vivo* peripheral treatment studies.**

### Indirect calorimetry and body composition

For the chronic studies, oxygen consumption (VO2) and carbon dioxide production (VCO2) were measured for each mouse after 24h acclimatization to the metabolic chamber using the Oxymax Comprehensive Lab Animal Monitoring System (Columbus Instruments, Ohio); respiratory exchange ratio (RER) calculated as VCO2/VO2. Data were expressed as ml/h/mouse and analyzed with fat-free and fat mass as continuous predictors in an ANCOVA model [Tschop et al., 2011]. Body composition was measured with Echo MRI 3-in-1 (Echo Medical System).

### Tissue and plasma collection

Following decapitation plasma was promplty collected from trunk blood in heparinized tubes (Sarstedt, s.r.l., IT). Epididymal (eWAT) and subcutaneous inguinal (scWAT) were manually collected, immediatly frozen in dry ice and stored at

−80°C. Liver and muscle biopsies were dissected and chemical composition analyzed with the Echo MRI 3-in-1.

**Lipid Extraction**

Lipids were extracted using a chloroform:methanol:water extraction with the final solution containing chloroform:methanol (1:2, v/v) and containing 3,4,5-trichloropyridine internal standard. NMR spectra were acquired using a gradient-enhanced 1D NOESY-presaturation pulse sequence for water suppression on a Bruker Avance III 700-MHz spectrometer with a TCI 1.7-mm cryoprobe at the Minnesota NMR Center. Acquisition parameters were as follows: 2s relaxation delay, 4.1ms mixing time, 4s acquisition time, 20 ppm sweep width, 8 dummy scans and 128 transients. 1H 90° pulse width and transmitter offset were optimized for each sample. All spectra were zero-filled to 128k data points, Fourier transformed with 1 Hz line broadening applied, manually phased, baseline corrected and integrated using Topspin software [Sparling ML et al., 1989; Pollesello P et al., 1997].

**Metabolomic Samples**

Plasma samples were diluted in a pH 7.4 phosphate buffer solution containing DSS internal standard and 20% D2O. To selectively detect small molecule metabolites, T2-edited spectra were acquired using a gradient-enhanced 1D CPMG pulse sequence with excitation sculpting for water suppression on a Bruker Avance III 700-MHz spectrometer with a TCI 1.7-mm cryoprobe at the Minnesota NMR Center. Acquisition parameters were as follows: 2s presaturation relaxation delay, 4.6s acquisition time, 20 ppm sweep width, 16 dummy scans and 1024 transients. 1H 90° pulse width and transmitter offset were optimized for each sample. All spectra were zero-filled to 256k data points, Fourier transformed with 0.3 Hz line broadening applied, and manually phased using Topspin software. Baseline correction and chemical shift referencing to the DSS peak at 0 ppm were performed using the Processor module in Chenomx NMR Suite 7.1. Metabolites were identified and quantified relative to DSS using the Profiler module in Chenomx NMR Suite 7.1 with the Chenomx 700-MHz Compound Library [Beckonert et al., 2007; Papathanasiou et al., 2008].

**mRNA extration, reverse transcription and quantitative Real-Time PCR**

RNA was obtained by homogenizing around 50 to 100mg of frozen tissue in 500μl of TRI REAGENT (Molecular Research Center, Inc., Cincinnati, Ohio) on ice following manufacturer's instructions. Total RNA was digested with Dnase I using DNA-free (Ambion, Austin, TX) and tested for the presence of DNA contamination using PCR. Total RNA concentration and purity was then determined using NanoDrop at the UV absorbency of 260 nm (NanoDrop 2000 UV-Vis Spectrophotometer, Thermo Scientific). 1μg of RNA was converted into cDNA using iScript cDNA Synthesis Kit (Bio-Rad Laboratories, Hercules, CA) and relative quantification of mRNAs was performed with 3.5μl of cDNA used in each 11.5μl real-time-RT-PCR reaction using C1000 thermal cycler ™ (Bio-Rad Laboratories, Hercules, CA). The PCR reactions were carried out using IQ™ Syber Green Supermix (BIO-RAD). Primers for the target genes are on Table 1. Thermal cycling parameters were as follows: an initial denaturing step (95°C for 10 min), followed by 40 cycles of denaturing- annealing and extending (95 °C for 45 s, 58 °C for 45 s and then 60°C for 1min) in a 96-well BioRad plate. The results were calculated by the comparative $C_t$ method using β-actin as an endogenous reference gene, according to the Applied Biosystems ABI PRISM 7700 User Bulletin #2. The expression relative to β-actin was determined by calculating $2^{-\Delta Ct}$. See Table 1 for list and sequence of primers.

| Gene name: | | Primer sequence (5'-3') |
|---|---|---|
| β-actin | FP: | GGC ACC ACA CCT TCT ACA ATG |
| | RP: | GGG GTG TTG AAG GTC TCA AAC |
| C3aR1 | FP: | TCGATGCTGACACCAATTCAA |
| | RP: | TCCCAATAGACAAGTGAGACCAA |
| UCP1 | FP: | GTCCCCTGCCATTTACTGTCAG |
| | RP: | ATTCGTGGTCTCCCAGCATAG |
| NRF-1 | FP: | ACATTGGCTGATGCTTCAGAA |
| | RP: | TGCGTCGTCTGGATGGTCAT |
| ATP5b | FP: | TGCCACTTCCAAGGTAGCGT |
| | RP: | TCTTGGCCCTCCTGGTCTCT |
| Ndufs1 | FP: | TTGCCGTGGCCGCCATATTG |
| | RP: | GCTGTGCCAGTTGTGCGAACA |
| COX-1 | FP: | GGATTTGTTCACTGATTCCCATTA |
| | RP: | GCATCTGGGTAGTCTGAGTAGCG |
| PGC-1a | FP: | TCACACCAAACCCACAGAAA |
| | RP: | TCTGGGGTCAGAGGAAGAGA |
| Tfam | FP: | GATGATTCGGCTCAGGGAAAA |
| | RP: | CAGCCATCTGCTCTTCCCAAG |

**Table 4.1**. **List of primers used in this study.** Primers sequences. FP and RP, are referred to as forward and reverse primers, respectively. UCP1 uncoupling protein 1; NRF1 nuclear respiratory factor 1; COX1 mitochondrially encoded cytochrome c oxidase I; ATP5B ATP synthase, H+ transporting, mitochondrial F1 complex; Ndufs1 NADH dehydrogenase (ubiquinone) Fe-S protein 1; PGC1a peroxisome proliferator-activated receptor gamma, coactivator 1 alpha; Tfam transcription factor A, mitochondrial

**Acute in vivo lypolisis protocol**

After approval of the protocol by the Mayo Animal Care and Use Committee, two series of experiments were performed, as described below, in Sprague Dawley rats fed a regular rodent chow diet (4.5% dietary fat). The experiments were conducted in the morning under natural living conditions (i.e., non-fasting). Tail arterial and i.v. infusion catheters were placed acutely as described above. The stable isotope [U-$^{13}$C] palmitate was infused constantly for 90 min via the infusion catheter at 0.5μmol•kg$^{-1}$•min$^{-1}$. After 20 minutes of infusion for tracer equilibration, blood samples were taken at 5 min intervals for the measurement of basal lipolysis. Isoproterenol infusion (30ng/min) was then started and continued for 60 minutes. After 15 min of equilibration, TLQP-21 (40μg) (n=8) or saline (n=8) were injected i.v. as a bolus. Blood was sampled periodically thereafter to determine the rate of appearance ($R_a$) of plasma palmitate. Palmitate Ra was calculated using non-steady steady state assumptions.

**Measure of C3aR1 in humans**

Percutaneous abdominal adipose tissue biopsies were obtained from 208 non-diabetic Pima Indians. Subjects had undergone a 12-hour overnight fast prior to the biopsy, and the specimens were immediately frozen in liquid nitrogen. Total RNA was extracted using TRIzol reagent (Invitrogen, Carlsbad, CA, USA) and was further purified using a RNeasy Micro Kit (Qiagen, Valencia, CA, USA). The rRNA was prepared and the cDNA synthesized for analysis on Human Exon 1.0 ST Array microarrays (Affymetrix, Santa Clara, CA, USA) using the GeneChip Whole Transcript Sense Target Labeling Assay kits (Affymetrix). Processing and analyses of the Human Exon 1.0 ST arrays was done as previously described [Mason et al., 2011]. All data were standardized for sex and exon array batch as described [Mason et al. 2011].

**Statistical Analysis**

Data are reported as mean ± SEM. Statistical Analysis was evaluated using t-test for comparison of two groups and analysis of variance (ANOVA), with repeated measures followed by Tukey post hoc multiple comparison analyses which can be used also in case of non significant F value [Wilcox, 1987]. Statistical analyses were performed with Statistics software version 12 and significance was set at $p<0.05$.

# 4.4 RESULTS

## Increased adipose tissue C3ar1 expression in obese mice and humans

The identification of C3aR1 as the TLQP-21 receptor [Hannedouche et al., 2013: Cero et al., 2014; See **Chapter 2**] prompted us to determine the receptor expression in the adipose tissue of mice and humans. C3aR1 mRNA level was increased in the eWAT of diet-induced obese wild type [$t_{14}$=4.005, p=0.0013] and β-less [$t_{11}$=4.327, p=0.0012] mice (**Figure 4.2A**), thus supporting previous observations [Mamane et al., 2009; Possenti et al., 2012]. Importantly, we also established that the same association is also present in humans. We studied the tissue expression of C3aR1 in non-diabetic Pima Indians of Arizona, a population having the highest prevalence of type 2 diabetes of any population worldwide, and a very obese population [Urquidez-Romero et al., 2014; Hanson et al., 2015]. A positive correlation was observed between C3aR1 expression in adipose tissue and the BMI (r=0.27, p= 7 x $10^{-5}$). No difference in correlation was observed in males vs. females (P value for sex interaction =0.42) (**Figure 4.2B**).[1]

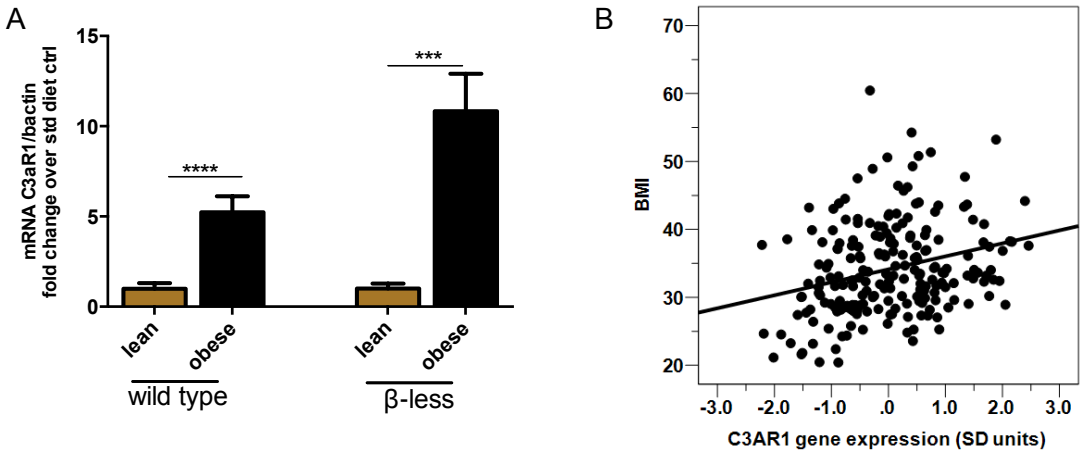


**Figure 4.2. Positive association between C3aR1 expression and obesity in mice and humans.** (**A**) High fat diet increases C3aR1 in eWAT of wt and β-less mice. n=6-7 per group. Data represent the mean +/- SEM. ***p<0.0005, **** p<0.00001 vs respective lean group. (**B**) A positive correlation between C3aR1 expression in adipose tissue and BMI in 208 Pima Indians (r=0.27, p= 7 x $10^{-5}$).

[1]Preliminary analysis using a commercially available kit for TLQP-21 showed an association between plasma TLQP-21 and obesity. However, recent results obtained in our lab with a new genetic model of loss of TLQP-21 function casted some doubt on the specificity of the immunoassay, thus data are not included here.

## Chronic TLQP-21 treatment exerts an anti-obesity effect in mice

Having previously established that TLQP-21 enhance β-adrenergic receptors (β-ARs)–mediated lipolysis in mature and 3T3L1 adipocytes [Possenti et al., 2012; Cero et al., 2014; **Chapter 3**], prompted us to test whether TLQP-21 required functional β-ARs to promote lipolysis and weight loss *in vivo*. To address this question we used a triple knockout of the $\beta_1$, $\beta_2$, $\beta_3$-ARs [β-less; Bachman et al. 2002]. β-less and wt mice were fed a 60% high fat diet (HFD) for 9 weeks to induce obesity. As expected diet induced higher body weight and fat mass gain and glucose intolerance in β-less compared to the wt mice (**Figure S4.1)**. Once the obese phenotype was established, both experimental groups received a daily intra-peritoneal (i.p.) injection for 28 consecutive days of 5mg/kg/d TLQP-21 or saline (**Table 4.2**). The dose was chosen based on previous data [Possenti et al., 2012; Stephens et al., 2012] and a preliminary dose-response study conducted in a small sample of wt mice (not shown). After only seven days of consecutive peripheral TLQP-21 treatment, wt obese mice displayed a significant decrease in body weight compared to saline injected controls, difference that was maintained over the course of the 28 days of treatment [$F(2,23)=5.13$, $p=.001879$] (**Figure 4.3A**). Consistent with the decreased body weight observed in wt TLQP-21-treated mice, body composition analysis revealed a significant decrease in fat mass [$F(3,69)=3.616$, $p=.0431$] (**Figure 4.3B**) but no change in lean mass compared to saline-treated control (**Figure 4.3C**). Conversely β-less mice receiving the same chronic TLQP-21 treatment displayed no reduction in body weight (**Figure 4.3A**) fat [$F(1,21)=.59363$, NS] (**Figure 4.3B**) or in lean mass (**Figure 4.3C**) [$F(1,21)=1.9166$, NS] compared to saline-treated controls.

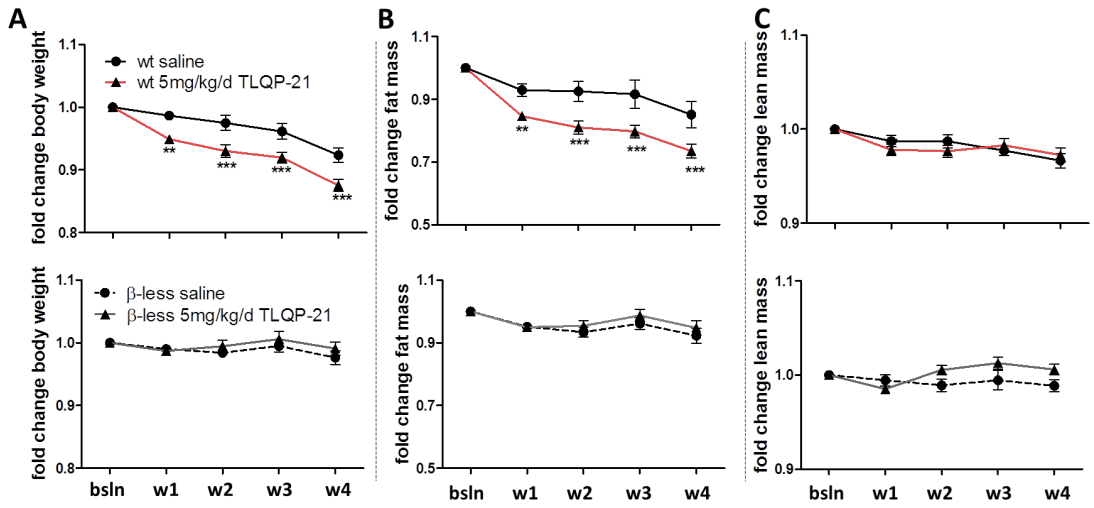


**Figure 4.3**. **TLQP-21 opposes obesity in wt but not β-ARs knockout mice.** Fold changes in (**A**) body weight (**B**) fat mass (**C**) and lean mass of mice treated with TLQP-21 and saline, (wt saline: n=11; 5mg/kg/d T-21: n= 9); (β-less saline: n=12; 5mg/kg/d T-21: n= 11). Data represent the mean +/- SEM. * represents p<0.05, **p<0.005, *** p<0.0005 vs respective saline group.

We next aimed to identify the physiological mechanism of TLQP-21 anti-obesity effect. Chronic peripheral TLQP-21 treatment did not affect food intake (**Figure 4.4A**), indicating that the anti-obesity effect is not mediated by lower energy intake. Based on the evidence that TLQP-21 enhances Iso-induced lipolysis *in vitro* and decreases adipocyte diameter *in vivo* [Possenti et al., 2012; Cero C et al., 2014; **Chapter 3**], we hypothesized that the decreased fat mass could be associated with a low grade pro-lipolytic profile. We first tested the acute effect of TLQP-21 on ISO-induced lipolysis in rats. During ISO infusion (30ng/min), FFA (measured with the Palmitate method) more than doubled in both groups. However, in the saline group FFA progressively waned, so that by the end of the experiment it was ~75% of the initial Iso-stimulated rate. In contrast, there was no waning of FFA in the TLQP-21 treatment group (TLQP-21 at 40μg) (**Figure 4.4B**), indicating a potentiation of ISO-induced lipolysis [$F(2,18)=2.7$, $p=0.09$]. Based on this evidence we performed an MRI-based lipidomic profiling of the plasma of wt mice chronically treated with TLQP-21 *in vivo* under both fed and fasting conditions. Consistent with the mild acute pro-lipolytic effect, TLQP-21 showed a trend for enhanced plasma FFA (**Figure 4.4C**). Conversely TLQP-21 did not affect the concentration of other lipid species nor average chain length and unsaturation ratio (**Table 4.2**). Overall we conclude that

TLQP-21 exerts a mild but consistent pro-lipolytic effect *in vivo*. This result prompted us to determine associated change in energy expenditure. Somewhat surprisingly, chronic TLQP-21 treatment was not associated with increased energy expenditure measured with indirect calorimetry after 24 days of treatment in either wt or β-less mice (**Figure 4.4D and Figure S4.2)**, a finding that was confirmed in acute (**Figure S4.3)** and sub-chronic injected lean wt mice (**Figure S4.4**).

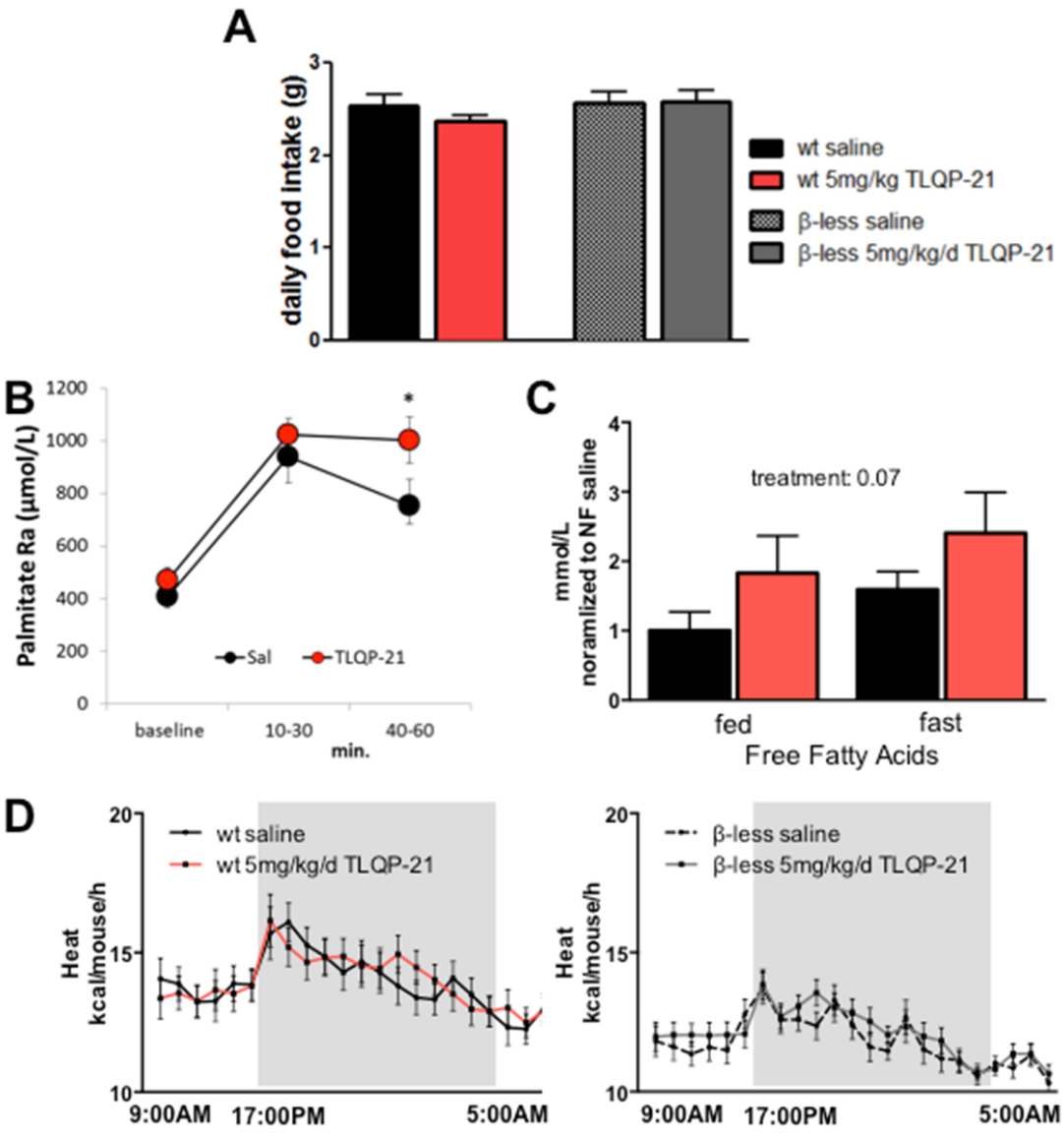


**Figure 4.4. Physiological effects of acute and chronic *in vivo* TLQP-21 treatment.** (**A)** Food intake. (**B)** TLQP-21 (40µg) acutely prolongs isoproterenol (30ng/min) (ISO)-induced lipolysis determined with plasma palmitate rate of appearance (Ra). (n=8). (**C**) Plasma free fatty acids (FFA) following 28 days treatment in a fed and fasted state. (**D**) Energy expenditure (wt saline: n=7; 5mg/kg/d TLQP-21: n= 7 and β-less saline: n=8; 5mg/kg TLQP-21: n= 9 mice per group) Data represent the mean +/- SEM. * represents $p<0.05$

Overall our data demonstrate that TLQP-21-anti-obesity effect requires functional β-ARs and suggest that the physiological mechanism is a chronic low-grade amplification of adrenergic-induced lipolysis likely resulting in local, rather than systemic, increase in energy expenditure [Bal et al., 2012]. In partial support of local activation, we detected increased expression of Tfam and a modest increase of other mitochondrial markers in the scWAT of TLQP-21 treated mice (**Figure S4.5**).

## The anti-obesity effects of TLQP-21 are mediated by C3aR1 activation.

We next aimed to test the hypothesis that TLQP-21 induced-C3aR1 activation is necessary and sufficient to explain its anti-obesity effect. We recently characterized a functionally inactive R21A mutant of TLQP-21 [Cero et al., 2014; **Chapter 2**]. Therefore we injected wt obese mice with the R21A (5mg/kg/d) following the same protocol used for the endogenous peptide. Chronic R21A i.p. treatment had no effects on body weight (**Figure 4.5A**), fat mass (**Figure 4.5B**), food intake (**Figure 4.5D**), or energy expenditure (**Figure 4.5E**). Surprisingly, a significant increase in lean mass was observed by the end of the experimental treatment [$F(2,23)=4.81$, $p=.0179$] (**Figure 4.5C)** for which we currently lack a functional explanation.

We next asked the question if TLQP-21 anti-obesity effect requires functional C3aR1 expression. We treated HFD-fed C3aR1 KO mice with saline or TLQP-21 (5mg/kg/d) in our standard protocol. TLQP-21 treated C3aR1 KO mice did not differ from saline-injected controls in body weight (**Figure 4.6A**), fat mass (**Figure 4.6B**), lean mass (**Figure 4.6**), food intake and energy expenditure (**Figure 4.6 and Figure S4.6)**. The drastic weight lowering effect of chronic injections (both saline and peptide injection) can probably be explained with the altered metabolic profile of this strain [Mamane et al., 2009]. Overall, our results demonstrate that TLQP-21 activation of C3aR1 is necessary and sufficient to explain its anti-obesity effect.

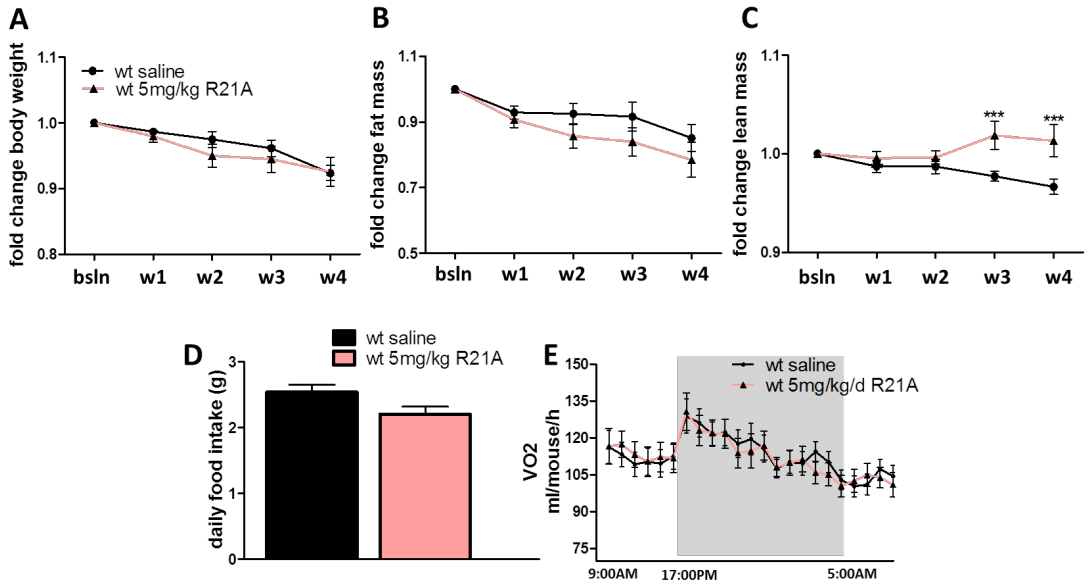


**Figure 4.5**. **The C-terminal Arg (R) is essential for TLQP-21 weight-lowering effects in high fat diet fed mice.** Fold changes in (**A**) body weight (**B**) fat mass (**C**) and lean mass of mice treated with (**D**) food intake and (**E**) energy expenditure wt mice treated with R21A and saline over 4 weeks (wt saline: n=11; 5mg/kg/d R21A: n= 6). *** p<0.0005 vs respective saline group.

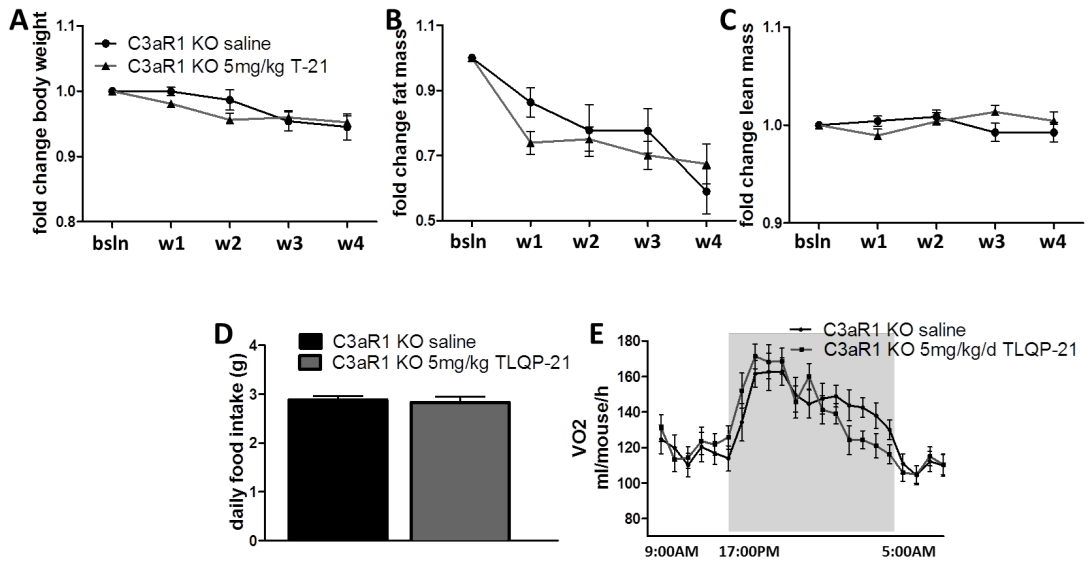


**Figure 4.6**. **TLQP-21 requires C3aR1 receptor to exert its anti-obesity effect.** (**A**) Longitudinal body weight, (**B**) fat mass, (**C**) lean mass, (**D**) food intake and (**E**) energy expenditure wt mice treated with R21A and saline over 4 weeks of treatment (C3aR1 KO saline: n=6; 5mg/kg/d TLQP-21: n= 7).

## TLQP-21 anti-obesity effect is associated with a healthier metabolic phenotype

Elevated level of branch chain amino acids (BCAA; valine, leucine, isoleucine) has consistently been associated with obesity and type 2 diabetes in humans and murine models [Newgard et al., 2009; Huffman et al., 2009]. We investigated the consequences of TLQP-21 treatment on circulating BCAA in fed or fasting condition using an MRI-based metabolomics profiling. As expected [She et al., 2007], fasting lowered circulating BCAAs in saline treated mice (**Figure 4.7A**). Remarkably, TLQP-21 treated wt mice showed significantly lower isoleucine, leucine and valine already in the fed state with values indistinguishable from overnight fasted saline-treated mice (**Figure 4.7A**) (**Table 4.3**). Furthermore TLQP-21 also lowered fed but not fasting plasma glucose concentration (**Figure 4.7A**) (**Table 4.3**). Contrasting evidences have previously been published on the role of TLQP-21 on glucose tolerance and insulin secretion [Stephens et al., 2012; Christiansen et al., 2015; Petrocchi et al. 2015]. In our study, despite improved BCCAs and lower fat mass and body weight, fasting glycemia and glucose tolerance were not improved by chronic TLQP-21 treatment (**Figure 4.7B**). In further support, acute injection of TLQP-21 in both lean and leptin receptor deficient db/db mice did not improve glucose tolerance as well (**Figure S4.7**).

Finally, we asked the question whether the mild increase in circulating FFA in absence of detectable increase in whole body energy expenditure was associated with ectopic fat accumulation. We measured liver and quadriceps skeletal muscle concentration of fat and fat-free mass at sacrifice in chronically treated saline and TLQP-21 wt mice. No difference emerged between groups in either organ (**Figure 4.7 C, D**), thus excluding that increase FFA would cause fat accumulation and associated lypopoxicity [Schaffer, 2003].

Overall, TLQP-21 opposes obesity and promotes a healthier metabolic phenotype in mice.

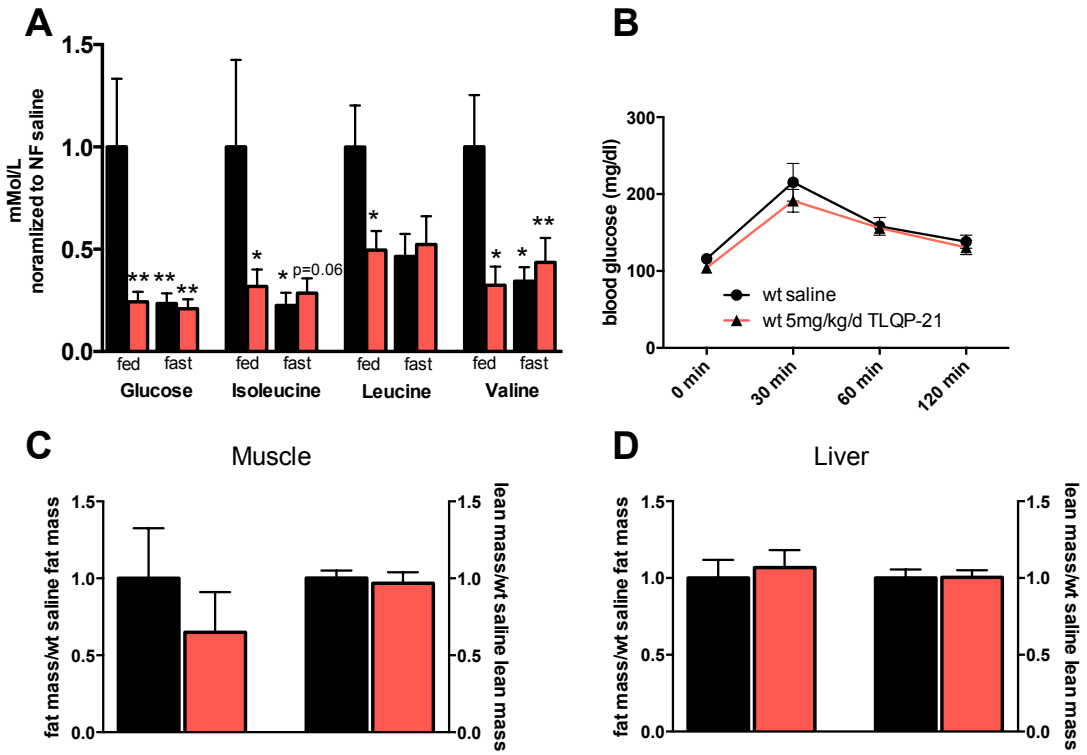


**Figure 4.7**. **TLQP-21 opposes obesity and promotes a healthier metabolic phenotype in high fat diet fed mice.** (**A**) Metabolomic analysis of glucose and branch chain amino acids (**B**) glucose tolerance test. (**C-D**) Fat and fat-free mass in muscle and liver following chronic TLQP-21 treatment (wt saline: n=7; 5mg/kg/d TLQP-21: n= 7). Data represent the mean +/- SEM. * represents $p<0.05$ **$p<0.005$

## 4.6 DISCUSSION

These data demonstrate an anti-obesity effect of chronic peripheral TLQP-21 treatment. In this study we show that *in vivo* TLQP-21 requires β-ARs and C3aR1 receptors to limit body weight and fat mass accumulation, a finding that is consistent with our *in vitro* results discussed in the **Chapter 3**.

Our gene expression analysis confirms and extends previous findings demonstrating a positive association between C3aR1 expression in both adipocyte and stromal vascular fraction and obesity [Mamane et al., 2009; Possenti et al., 2012]. In addition, we detected a positive correlation between the C3aR1 expression and BMI independent from gender in non-diabetic obese Pima Indians of Arizona. These murine and human data clearly suggest that obesity increases the expression of C3aR1 on adipocytes. In contrast to our human data, Gupta et al., [2014] have reported no change in C3aR1 in female obese omental adipose tissue but significant downregulation in the subcutaneous adipose tissue of obese vs control subjects. The discrepancy could arise from the samples used, women undergoing weight loss surgery was used in the latter study compared to non-obese and non-diabetic subjects. Furthermore ethnicity can also explain the discrepant findings.

In adipocytes TLQP-21 enhances β-ARs and cAMP-activated lipolysis (see **Chapter 3**). We have previously reported that two weeks of peripheral TLQP-21 treatment increases lipolysis decreasing adipocyte diameter and augmenting sympathetic innervation [Possenti et al., 2012]. Therefore, we explored the effects of chronic peripheral TLQP-21 treatment in wt and β-less obese mice. Obese wt mice undergoing four weeks TLQP-21 treatment decreased body weight and fat mass, despite normal food consumption. Conversely, obese β-less resulted fully resistant to the TLQP-21 anti-obesity effect. These data are in line with our *in vitro* data on β-less pre-adipocytes that do not increase lipolysis in response to ISO treatment (**Chapter 3**). However, we observed that forskolin could rescue the defective response of β-less pre-adipocytes to TLQP-21. Therefore, we believe that since lipolysis *in vivo* is mainly driven by the sympathetic nervous system through the activation of the β-ARs, TLQP-21 treatment in β-less mice cannot overcome the defective lipolysis. Interestingly, chronic TLQP-21 treatment did not affect energy expenditure. Chronic central TQLP-21 administration upturns energy expenditure limiting body weight [Bartolomucci et al., 2006], therefore we speculate that the mechanisms used by central and peripheral TLQP-21 in lowering body weight are

distinct. Nonetheless, the question on where the fat hydrolyzed by TLQP-21 is dissipated still remains. Because TLQP-21 induces a concentration dependent contractile activity on rat longitudinal forestomach [Severini et al., 2009], we could speculate that TLQP-21 could be increasing peristalsis, however we have not observed abnormal frequency in excretion or dysentery in mice treated with TLQP-21, confirming previously published results showing no effects on gastric emptying when TLQP-21 is administered peripherally [Severini et al., 2009]. Another possibility is that TLQP-21 might cause malabsorption of lipids and these are therefore excreted. A bomb calorimetry on feces, bile acids and pancreatic lipase analysis could help answering our question.

By mutating the C-terminal amino acid of TLQP-21 sequence we generated a null peptide that still binds to the C3aR1 receptor forming an alpha helix conformation, but is completely ineffective in all our functional assays, such as contraction of stomach fundus and lipolysis [Cero et al., 2014; **Chapter 2, Chapter 3**]. In order to ascertain whether the TLQP-21's anti-obesity effects are dependent on the presence of the arginine 21, we chronically treated obese wild type mice with the mutant peptide R21A. Opposite to TLQP-21, 28 days of R21A treatment had no effects on body weight or fat mass. We also tested the specificity of the C3aR1 receptor, identified as the target receptor for TLQP-21 [Hannedouche et al., 2013], for it's the anti-obesity effects. Our results show that the anti-obesity effect of TLQP-21 is abolished in C3aR1 KO mice.

The complement-binding protein, gC1qR that binds to the globular heads of C1q, has been suggested as an alternative receptor for TLQP-21 important in modulating neuropathic pain [Chen et al., 2013]. There is controversy regarding the expression of gC1qR on adipocytes [Kim et al., 2009; Dembitzer et al. 2012]. In addition as discussed in the **Chapter 2**, there is no structural similarity between TLQP-21 and the specific gC1qR ligands; moreover TLQP-21 does not undergo the transition to alpha helix in C3aR1 KO cells [Cero et al., 2014]. Since we unambiguously demonstrate that lack of C3aR1 prevents the anti-obesity effects of TLQP-21, we thus suggest that TLQP-21's metabolic effect is entirely C3aR1 mediated.

Since TLQP-21 promotes *in vitro* lipolysis (see **Chapter 3**), we tested its pro-lipoltyic effect *in vivo* and observed that TLQP-21 prolonged and increased ISO-induced lipolysis. Moreover, TLQP-21 in wt obese mice promoted a low grade but consistent pro-lipolytic effect. Increased lipolysis is associated with excess fat

accumulation in non-adipose depots and increased circulating free fatty acids (FFA) causing lipotoxixity insulin resistance, inflammation and cardiovascular disease [Arner and Rydén, 2015]. However, TLQP-21 induced weight loss and a mild increase in lipolysis but had no effect on ectopic fat deposition in metabolically active tissue such as muscle and liver and did not cause adverse metabolic effects, but rather led to a healthier metabolic phenotype.

Chronic TLQP-21 treatment increased mRNA expression of the mitochondrial gene Tfam, the single mitochondrial transcription factor that controls the transcription of the mitochondrial genome [Gaspari et al., 2004], in scWAT but not eWAT. Mitochondrial dysfunction, activity and decreased MtDNA are present in white adipose tissue of obese and diabetic patients [Kaaman et al., 2007; Choo et al., 2006] therefore the increased Tfam expression suggests an increase in mitochondrial number and biogenesis.

It has been reported that TLQP-21 prevents the onset of diabetes by enhancing glucose-stimulated insulin secretion (GSIS) and protecting β-cells degeneration [Stephens et al., 2012]. In our model, chronic TLQP-21 does not ameliorate glucose tolerance. We also detected no improvement in glucose tolerance with a single TLQP-21 injection in lean and diabetic mice suggesting that TLQP-21 has little or no insulinotropic effects on β-islets, a finding in line with recent work by Christiansen et al., [2015] and Petrocchi et al. [2015]. However, TLQP-21 treated mice displayed a significant lower plasma glucose levels in the fed state associated with lower levels of all five metabolites being Leu, Ile, Val, Phe, and Tyr that are highly association with metabolic disease [Newgard et al., 2009; Wang et al., 2011; Huffman et al., 2009]. These data suggest that TLQP-21 treatment promotes an overall improvement in the metabolic phenotype. Adipose tissue has been hypothesized to be the major site where excess BCAAs are stored in the form of lipid [Felig et al., 1969] and adipose tissue has been shown to catabolize circulating BCAAs *in vivo* [Herman et al., 2010] in line with our increased mitochondria hypothesis since the first enzyme in the catabolism of BCAAs, branched chain aminotransferase BCAT2 or BCATm are expressed on mitochondria.

Overall our data show that TLQP-21 *in vivo* requires β-AR's and C3aR1 receptors to exert its anti-obesity effects. TLQP-21 anti-obesity effect and mechanism are consistent with a potentiation of β-AR-induced lipolysis In a translational prospective, the possibility to have a drug target that promotes lipolysis without causing adverse

cardiovascular side-effects [Faragli et al., 2014; Possenti et al., 2012], and inducing a healthy metabolic phenotype would be of great interest for the pharmacotherapy of obesity. Therefore, increasing our knowledge about the *in vivo* anti-obesity mechanism of action of TLQP-21 may add to the development of peptides that can be used as against obesity and type 2 diabetes.

## ACKNOWLEDGMENTS

Supported by Minnesota Partnership for Biotechnology and Medical Genomic, Decade of Discovery in Diabetes Grant and NIH/DK102496 (to A.B.). β-less mice were a gift from Dr. Bradford Lowell. We would like to thanks Dr. Veglia and Todd Rappe for the lipidomics and metabolimics analysis. We would also like to thank Dr. Mashek for proving the primer sequences for the PCR analysis.

## 4.6 SUPPLEMENTARY FIGURES

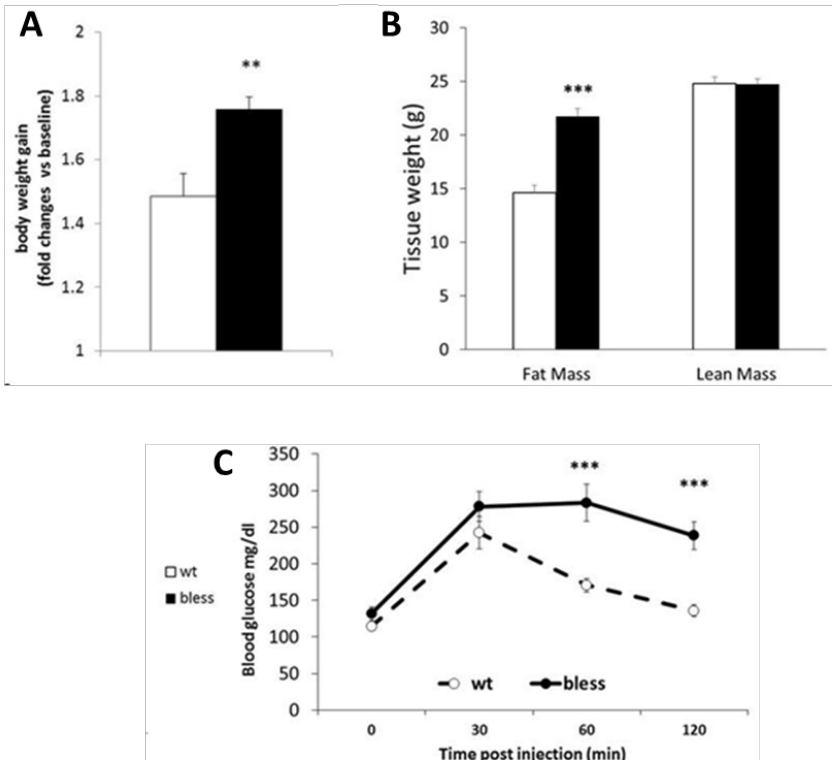


**Figure S4.1**. **Phenotype of β-less and wt mice under 9 weeks of 60% HFD.** (**A**) Body weight change, (**B**) fat and fat free mass and (**C**) glucose tolerance in obese β-less mice. **p<0.005, *** p<0.0005 vs respective wt.

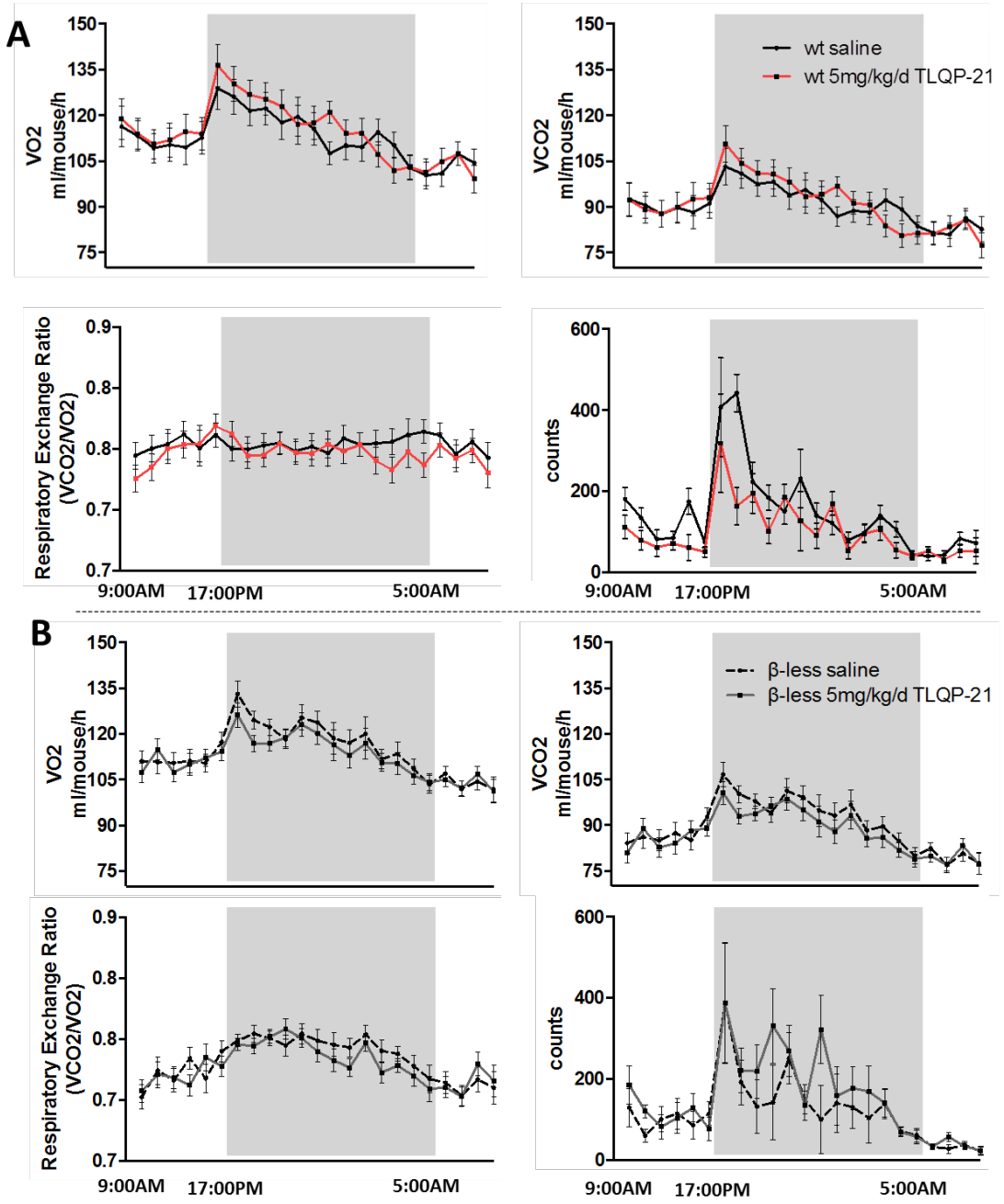


**Figure S4.2. Chronic TLQP-21 treatment does not alter energy expenditure.** Metabolic cages analysis reveled that chronic TLQP-21 treatment has no effect on VO2, VCO2, RER or locomotor activity in (**A**) wt nor (**B**) β-less mice (wt saline: n=7; 5mg/kg/d T-21: n= 7 and bless saline: n=8; 5mg/kg/d T-21: n= 9 mice per group). Data represent the mean +/- SD.

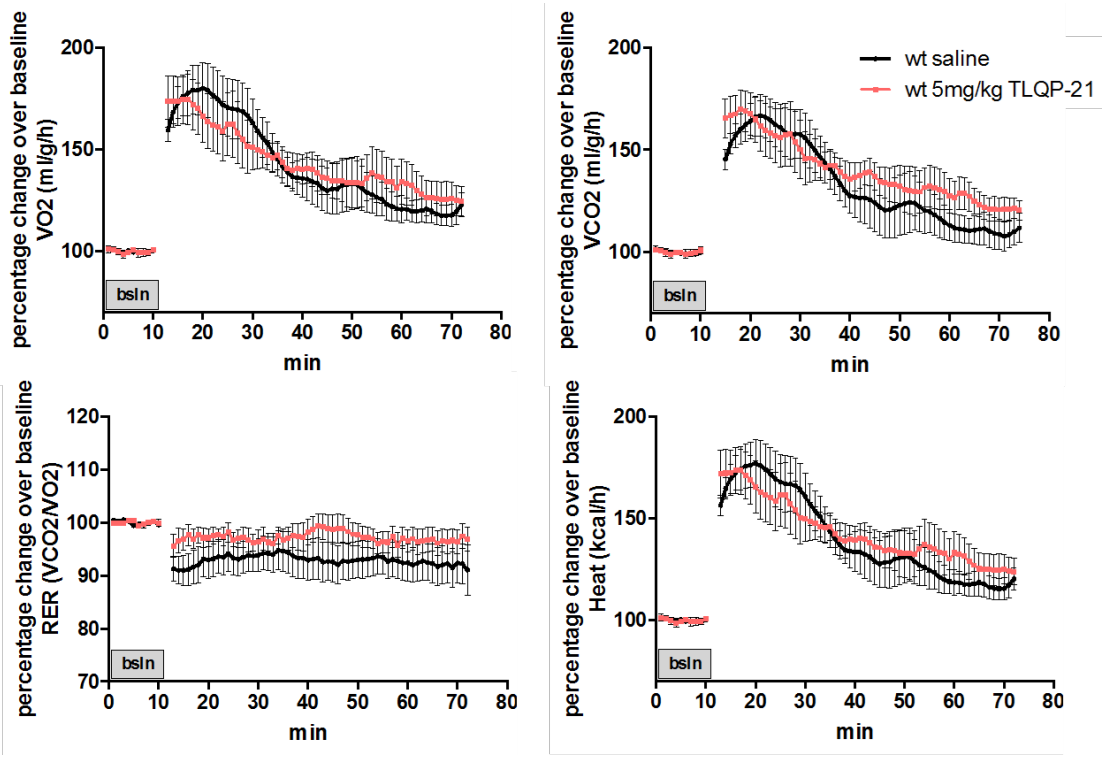


**Figure S4.3**. **Acute TLQP-21 treatment does not affect energy expenditure.** A single injection of 5mg/kg/d TLQP-21 treatment had no effects on energy expenditure. (n=4 mice of each group, saline and TLQP-21). Data represent the mean +/- SD.

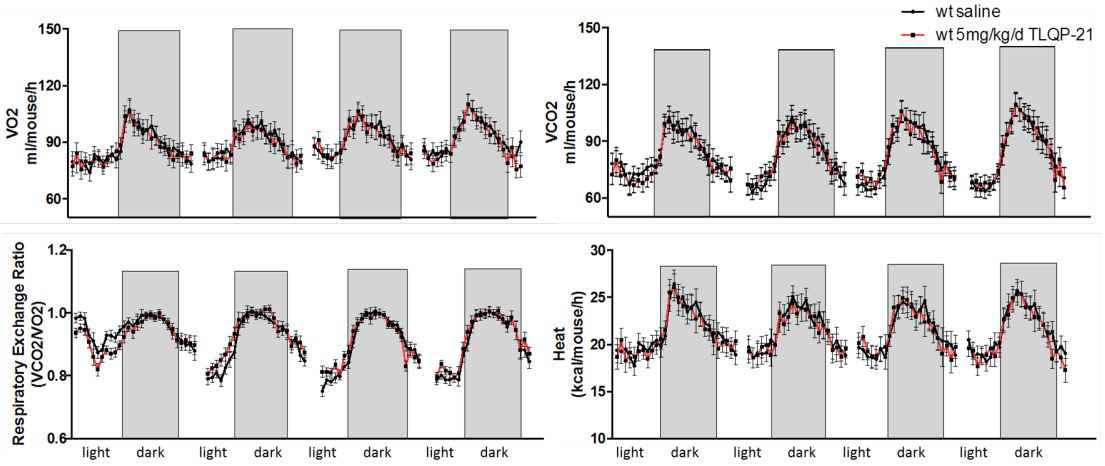


**Figure S4.4**. **Sub-chronic TLQP-21 treatment does not affect energy expenditure.** 4 days of 5mg/kg/d TLQP-21 treatment had no effects on energy expenditure. (n=6 mice of each group, saline and TLQP-21). Data represent the mean +/- SD.

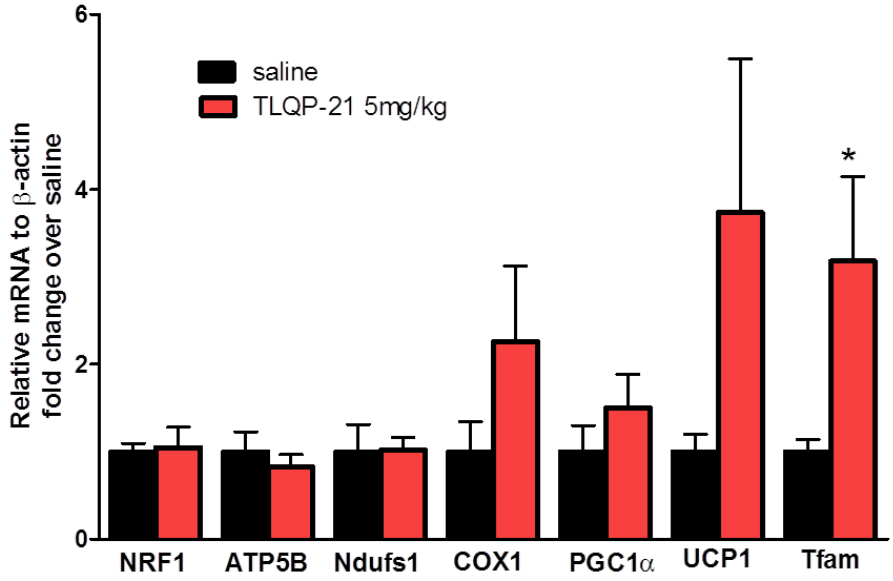


**Figure S4.5**. **Effects of TLQP-21 on mitochondrial genes.** Relative gene expression of mitochondrial genes in scWAT of saline and TLQP-21 wt mice. (n=6-7 per group). Data represent the mean +/- SEM.

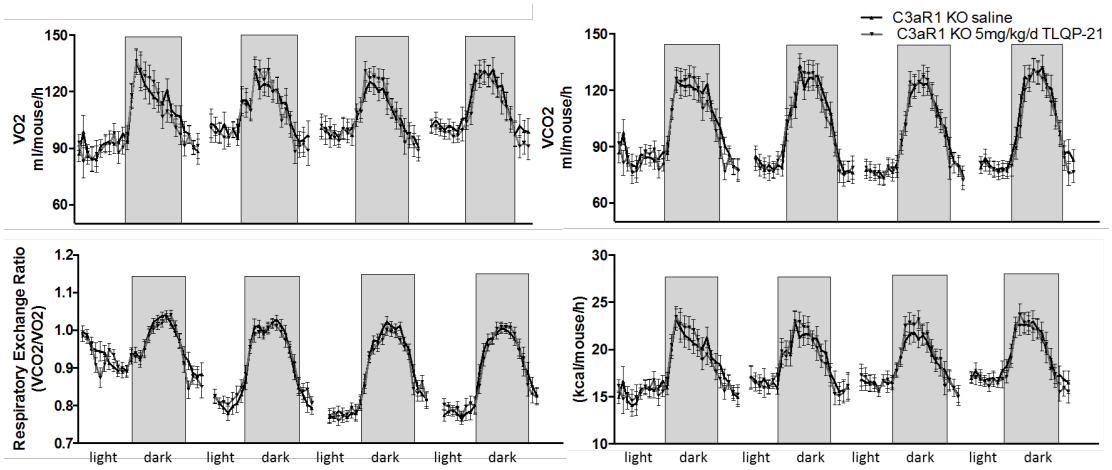


**Figure S4.6**. **Sub-chronic TLQP-21 treatment in C3aR1 KO does not affect energy expenditure.** 4days of 5mg/kg/d TLQP-21 treatment had no effects on energy expenditure. (n=6 mice of each group, saline and TLQP-21). Data represent the mean +/- SD.

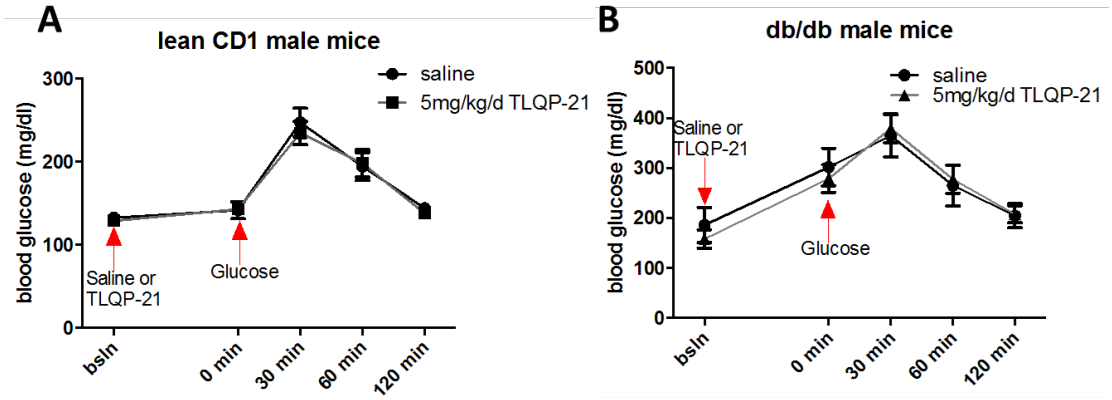


**Figure S4.7**. **Acute TLQP-21 treatment does not affect glucose clearance in mice.** Glucose tolerance phenotype 30 min after i.p. injection of glucose (2 g $kg^{-1}$) (A) in lean CD1 and (B) db/db male mice. (db/db: saline: n=9; 5mg T-21: n= 9); (CD1: saline: n=6; 5mg T-21: n= 6). Data represent the mean +/- SEM.

| ***Condition*** | **fed** | | **fasting** | | **statistical analysis** |
|---|---|---|---|---|---|
| ***Treatment*** | **saline** | **TLQP-21** | **saline** | **TLQP-21** | |
| **Total cholestrol mmol/L** | 0.53 ± 0.13 | 0.63 ± 0.2 | 1.05 ± 0.31 | 1.4 ± 0.34 | |
| **Tryglycerides mmol/L** | 0.32 ± 0.07 | 0.54 ± 0.14 | 0.9 ± 0.24 | 1.26 ± 0.17 | condition p<0.05 |
| **Phospholipids mmol/L** | 0.48 ± 0.07 | 0.65 ± 0.27 | 1.1 ± 0.33 | 1.64 ± 0.28 | condition p<0.005 |
| **Free FA mmol/L** | 1.66 ± 0.45 | 3.03 ± 0.89 | 2.63 ± 0.43 | 3.98 ± 0.97 | treat p=0.07 |
| **Polyunsaturated mmol/L** | 0.75 ± 0.21 | 1.01 ± 0.36 | 1.74 ± 0.53 | 2.47 ± 0.4 | condition p<0.05 |
| **Linoleic acid mmol/L** | 0.37 ± 0.1 | 0.43 ± 0.13 | 1.04 ± 0.32 | 1.4 ± 0.24 | condition p<0.005 |
| **DHA mmol/L** | 0.05 ± 0.01 | 0.03 ± 0.005 | 0.1 ± 0.03 | 0.07 ± 0.003 | |
| **ARA+EPA mmol/L** | 1.31 ± 0.3 | 2.71 ± 0.72 | 2.37 ± 0.41 | 3.73 ± 1.07 | |
| **Unsaturation ratio** | 0.56 ± 0.05 | 0.44 ± 0.06 | 0.61 ± 0.11 | 0.63 ± 0.1 | |
| **Average chain length** | 10.91 ± 0.5 | 10.6 ± 0.32 | 10.71 ± 0.13 | 11.1 ± 0.39 | |

**Table 4.2. TLQP-21 treatment does not affect lipodomics.** Lipodomics on plasma samples from fed and fasted saline and 5mg/kg/d T-21 subjected mice. (n=5-6 mice of each group). All lipids are expressed as mMol/L. Data represent the mean +/- SEM. DHA: docosahexaenoic acid; ARA: arachidonic acid; EPA: eicosapentaenoic acid.

| *Condition* | fed | | fasting | | statistical analysis |
|---|---|---|---|---|---|
| *Treatment* | saline | TLQP-21 | saline | TLQP-21 | |
| **3-Hydroxybutyrate** | 0.04 ± 0.06 | 0.03 ± 0.06 | 1.17 ± 0.08 | 0.27 ± 0.07 | condition p<0.0000001; treat p<0.000002; condition*treat p<0.000002 |
| **Acetate** | 0.1 ± 0.07 | 0.1 ± 0.07 | 0.59 ± 0.1 | 0.13 ± 0.08 | condition p<0.003; treat p<0.007; condition*treat p<0.007 |
| **Acetone** | 0.02 ± 0.01 | 0.01 ± 0.01 | 0.07 ± 0.02 | 0.02 ± 0.02 | |
| **Alanine** | 0.17 ± 0.07 | 0.23 ± 0.08 | 0.58 ± 0.1 | 0.19 ± 0.09 | condition*treat p<0.01 |
| **Creatine** | 0.09 ± 0.034 | 0.1 ± 0.037 | 0.59 ± 0.05 | 0.14 ± 0.04 | condition p<0.000002; treat p<0.00002; condition*treat p<0.00002 |
| **Creatine phosphate** | 0.11 ± 0.02 | 0.1 ± 0.02 | 0.32 ± 0.03 | 0.11 ± 0.03 | condition p<0.0004; treat p<0.0008; condition*treat p<0.001 |
| **Formate** | 0.17 ± 0.07 | 0.18 ± 0.08 | 0.91 ± 0.1 | 0.26 ± 0.1 | condition p<0.0001; treat p<0.001; condition*treat p<0.001 |
| **Glucose** | 2.39 ± 1.02 | 2.13 ± 1.09 | 10.19 ± 1.44 | 2.48 ± 1.29 | condition p<0.003; treat p<0.004; condition*treat p<0.006 |
| **Glycerol** | 0.14 ± 0.07 | 0.11 ± 0.07 | 0.63 ± 0.08 | 0.25 ± 0.07 | condition p<0.001; treat p<0.005; condition*treat p<0.01 |
| **Isoleucine** | 0.05 ± 0.03 | 0.06 ± 0.03 | 0.22 ± 0.04 | 0.07 ± 0.04 | condition p<0.01; condition*treat p<0.02 |
| **Lactate** | 0.86 ± 0.45 | 0.1 ± 0.48 | 3.88 ± 0.63 | 0.1 ± 0.57 | condition p<0.01; treat p<0.01; condition*treat p<0.01 |
| **Leucine** | 0.18 ± 0.04 | 0.2 ± 0.05 | 0.38 ± 0.06 | 0.19 ± 0.06 | condition*treat p<0.05 |
| **Lysine** | 0.13 ± 0.04 | 0.18 ± 0.04 | 0.35 ± 0.06 | 0.16 ± 0.05 | condition*treat p<0.02 |
| **Phenylalanine** | 0.03 ± 0.01 | 0.04 ± 0.01 | 0.11 ± 0.01 | 0.03 ± 0.01 | condition p<0.003; treat p<0.006; condition*treat p<0.002 |
| **Pyruvate** | 0.005 ± 0.002 | 0.004 ± 0.002 | 0.03 ± 0.002 | 0.004 ± 0.002 | condition p<0.00007; treat p<0.00005; condition*treat p<0.0002 |
| **Succinate** | 0.03 ± 0.01 | 0.03 ± 0.01 | 0.15 ± 0.01 | 0.03 ± 0.01 | condition p<0.00006; treat p<0.00003; condition*treat p<0.0002 |
| **Taurine** | 0.21 ± 0.12 | 0.2 ± 0.13 | 1.42 ± 0.17 | 0.26 ± 0.15 | condition p<0.0002; treat p<0.0005; condition*treat p<0.0006 |
| **Tyrosine** | 0.05 ± 0.02 | 0.06 ± 0.02 | 0.15 ± 0.03 | 0.06 ± 0.03 | condition p<0.04; condition*treat p<0.02 |
| **Valine** | 0.12 ± 0.04 | 0.15 ± 0.04 | 0.34 ± 0.05 | 0.11 ± 0.05 | condition p<0.04; treat p<0.03; condition*treat p<0.007 |

**Table 4.3. Effects of TLQP-21 treatment on metabolomics.** Summary of metabolites investigated in plasma samples from fed and fasted saline and 5mg/kg/d T-21 subjected mice. (n=5-6 mice of each group). All metabolities are expressed as mMol/L. Data represent the mean +/- SEM.

# Chapter Five

# CONCLUSION and PRESPECTIVE

Since the discovery of the biologically-active VGF derived peptide TLQP-21 and the identification of its role in energy homeostasis [Bartolomucci et al., 2006], there has been a growing interest in the biology of this neuropeptide. TLQP-21 was shown to regulate energy expenditure, food intake, body mass, glucose metabolism, gastric functions, stress, nociception, hypertension and reproduction demonstrating [Bartolomucci et al., 2006; Jethwa et al., 2007, Severini et al., 2009; Razzoli et al., 2012; Rizzi et al. 2008; Fairbanks et a., 2014; Fargali et al., 2014; Aguilar et al., 2013; Pinilla et al., 2011]. Compared to the extensive pharmacological and gain of functions studies very little was known, until recently, about its molecular mechanism of action. Thus, the focus of my work has been to elucidate the structural and chemical properties of TLQP-21 and to characterize its pro-lipolytic and anti-obesity mechanism of the action. The goal of this chapter is to summarize concepts and outcomes discussed in the preceding chapters putting these findings into prospective.

## C3aR1 is the target receptor for mouse TLQP-21

Among the several biologically active VGF derived peptides described [**Table 5.1**], TLQP-21 is the only peptide for which two putative receptors have recently been identified, namely the complement 3a Receptor 1 (C3aR1) [Hanneduche et al., 2013] and globular head domains of complement component C1q, designated gC1qR [Chen et al., 2013].

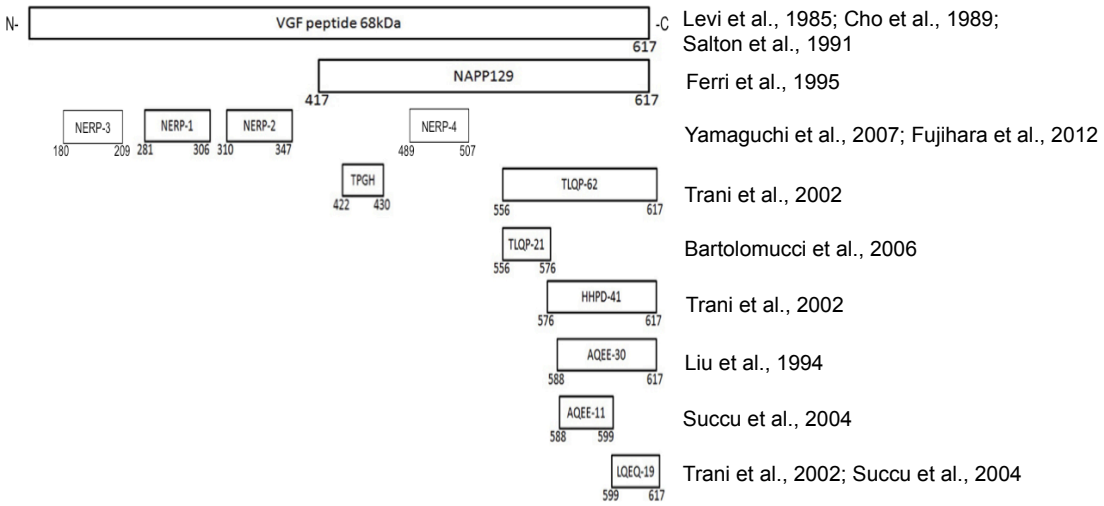


**Table 5.1. VGF derived peptides in rat** [modified from Lewis et al., 2015]. The proVGF polypeptide and derived peptides along with the first study where the specific peptide was first described.

In 2012 we were the first to demonstrate that TLQP-21 binds with high affinity to adipocyte membranes and that the binding was increases in obesity [Possenti et al., 2012]. Based on the phosphorylation pattern and the increase in $[Ca^{2+}]_i$ in several cell lines, we had hypothesized that TLQP-21 would bind to a G coupled protein receptor (GPCR) [Possenti et al., 2012]. Additionally, atomic force microscopy of living cells revealed significant amounts of TLQP-21 binding sites, all part of a single class of binding sites for TLQP-21 in CHO cells [Cassina et al., 2012]. Hanneduche et al., [2013] identified the C3aR1 as the target receptor for TLQP-21 in CHO and O-342 cells. C3aR1 is a GPCR part of the immune innate complement pathway with C3a protein being its primary ligand [Klos et al., 2013]. We confirmed and extended this result by using crosslinking experiments using pholabeled TLQP-21 peptide, murine C3aR1 antagonists, C3aR1 antagonists as well as structural analysis using NMR [Cero et al., 2014]

Despite the name, the role of C3aR1 is not restricted to the innate and complement response, but it plays functional roles in neurogenesis [Klos et al., 2013], cancer [Opstal-van Winden et al., 2012] and hormone release from pituitary gland [Francis et al., 2013]. C3aR1 KO mice are transiently resistant to diet induced obesity emphasizing the importance of this receptor in metabolism as well [Mamane et al., 2009]. Germaline knockout of C3aR1 could be activating alternative pathways that could explain the resistance to obesity not allowing to fully evaluating the role of C3aR1.

C3a, a derived C3 complement peptide, is the first identified and thus far the most potent agonist at C3aR1 [Markiewski et al., 2007]. C3a is 77-aa peptide consisting of three to four helical regions and a series of nonregular residues at the C-terminal responsible for binding at C3aR1 [Chazin et al., 1988; Markiewski et al., 2007; Coulthard and Woodruff, 2015]. C3a is a potent anaphylatoxin molecule that directly triggers degranulation of mast cells initiating the anti-inflammatory response [Markiewski et al., 2007]. Serum carboxypeptidase regulates the activity of this powerful biological active peptide by rapidly cleaving off C-terminal arginine residue (R77) generating a peptide devoid of its pro-inflmmatory activity biological activities [Bokisch et al., 1970] that loses its ability to bind to C3aR1 but instead binds to C5L2 [Johswich et al., 2006]. Compared to C3a that adopts an ordered helical conformation in solution [Nettesheim et al., 1988], TLQP-21 acquires an $\alpha$-helix conformation only upon receptor binding while being unstructured in solution [Cero et al., 2014]. Similar to TLQP-21 the hot-spots for C3a are located at the C-terminus. $R_{77}$ in C3a plays a critical role for C3a function since deletion at this site does also generate a null peptide still able to form an ordered helix [Ames et al., 2001; Hugli and Erickson 1977; Nettesheim et al., 1988]. In 2005 Garcia et al., using secondary structure predictions predicted within the VGF polypeptide the presence of three $\alpha$-helix structures, one at the N-terminal VGF domain while the other two at the C-terminal VGF domain, one of which embedded within the TLQP-21 sequence [Garcia et al., 2005]. Similarly, by mutating R21A in the TLQP-21 sequence we generate a null TLQP-21 peptide that preserves its ability to bind to C3aR1 forming a $\alpha$-helix [Cero et al., 2014]. C3a is produced by adipocytes; it is the product of adipsin, the first adipokine ever described [White et al., 1992; Choy and Spiegelman, 1996; Lo et al., 2014]. However the role of C3a in adipocyte function remains poorly characterized. C3a acting on its C3aR1 receptor has been shown to limit lipolysis [Lim et al., 2013]. It is important to note that Lim J et al. used human C3a on murine

C3aR1 receptors. We demonstrate here that mouse C3aR1 agonist $C3a_{70-77}$ [Hugli and Erickson 1977] produces similar contractile activity on fundus strips to rodent TLQP-21 and potentiates ISO-lipolysis in 3T3L1 cells. It remains to be established if TLQP-21 does also exert an anaphylatoxic effect.

Chen et al., [2013] identified the complement-binding protein that binds to the globular heads of C1q, gC1qR, as an alternative receptor for TLQP-21 that activates rat macrophages casing mechanical hypersensitivity in rats modulating neuropathic pain [Chen et al., 2013]. The gC1qR is a ubiquitously expressed multi-binding hydrophilic protein lacking transmembrane-spanning regions that interacts with components of the complement, kinin, coagulation cascades and select microbial and viral pathogens [Ghebrehiwet et al., 1994; Dembitzer et al., 2012; Peerschke and Ghebrehiwet, 2007]. gC1qR has been found in the cellular compartments including mitochondria, nucleus and cytoplasm and is also thought to be located at the plasma membrane [Dedio et al., 1998; Petersen-Mahrt et al., 1999; Ghebrehiwet et al., 1995; van Leeuwen et al., 2011]. There have been contrasting data regarding the expression of gC1qR in adipose tissue. Kim KB et al. [2009] report gC1qR as a lipid draft protein expressed in adipocytes. Conversely Dembitzer et al. [2012] report the complete lack of this protein in adipose tissue.

Overall our *in vitro* and *in vivo* finding strongly indicates that C3aR1 is the mouse TLQP-21 receptor and it entirely mediates TLQP-21's metabolic effect. Moreover, there is no structural similarity between TLQP-21 and the specific gC1qR ligands [Gaboriaud et al., 2003].

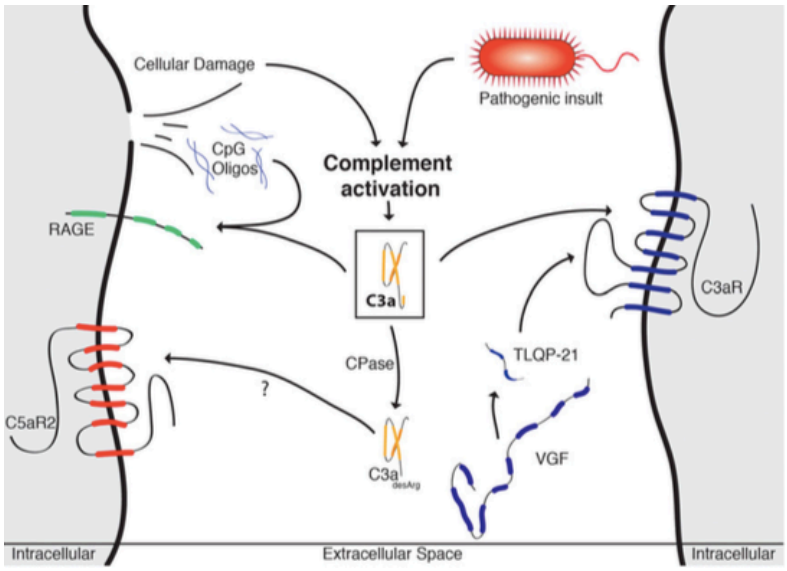


**Figure 5.1. Schematic diagram of C3aR1 receptor–ligand interactions of complement proteins C3a and the VGF cleaved product TLQP-21** [adapted from Coulthard LG and Woodruff TM, 2015]. C3a and TLQP-21 are both C3aR1 ligands.

## TLQP-21 reverses obesity by potentiating adrenergic-induced lipolysis

Having established the TLQP-21's structure and chemical properties we then focused on its function. We had previously shown that TLQP-21 decreases adipocyte diameter by increasing β-agonist induced phosphorylation of HSL and ERK [Possenti et al., 2012] and therefore hypothesized that TLQP-21 enhances β-agonist induced lipolysis. To test this hypothesis we established an *in vitro* protocol in 3T3L1 adipocytes. First, we confirmed that TLQP-21 *per se* does not affect lipolysis in adipocytes, [Possenti et al., 2012]; however TLQP-21 peptide potentiates isoproterenol (ISO) and forskolin (Forsk) induced lipolysis. The potentiation of Forsk induced lipolysis demonstrates that TLQP-21 mediated lipolysis is cAMP dependent rather β-AR-dependent. These results are validated by the enhancement of TLQP-21 Forsk induced lipolysis in β-less pre-adipocytes. Based on the increase of $[Ca^{2+}]_i$ induced by TLQP-21 in several cell lines we hypothesized that TLQP-21 requires $[Ca^{2+}]_i$ to potentiate lipolysis and therefore blocked intracellular and extracellular $Ca^{2+}$ using specific $Ca^{2+}$ chelants and found that TLQP-21 loses its ability to enhance lipolysis. Moreover, by specifically blocking the MAPK/ERK pathway we observed that TLQP-21 mediated lipolysis is completely abolished. Overall we demonstrate

that TLQP-21 pro-lipolytic effect is mediated by increase $[cAMP]_i$ and $[Ca^{2+}]_i$ via the MAPK/ERK pathway.

After pinpointing the pro-lipolytic *in vitro* effects of TLQP-21 we addressed the whole body physiological effects of chronic peripheral TLQP-21 treatment. Having previously demonstrated that TLQP-21 is selectively expressed in sympathetic nerve terminals innervating WAT and that TLQP-21 treatment increases ISO-induced lipolysis and sympathetic nerve sprouting within the adipose tissue, we hypothesized that TLQP-21 requires β-ARs to enhance lipolysis and limit body weight. Chronic TLQP-21 treatment decreased body weight and fat mass in diet-induced obese wild type mice. Conversely, obese β-less and C3aR1 KO mice resulted fully resistant to the TLQP-21 anti-obesity effect, thus demonstrating that TLQP-21 *in vivo* requires β-AR and C3aR1 to exert its anti-obesity effect. However, the decreased fat mass was not associated with increased energy expenditure indicating that peripheral TLQP-21 acts on different pathways compared to central administration of TLQP-21 where increased energy expenditure was observed [Bartolomucci et al., 2006]. Our results suggest that weight loss is mediated by TLQP-21 activation of moderate but significant lipolysis without causing ectopic fat deposition in other metabolically active tissue. Since peripheral TLQP-21 *in vivo* promotes fat loss without increasing energy expenditure, we remain with the question where is the fat is winding up. Despite being unlikely to justify a ~25% decrease in fat mass, it is possible that TLQP-21 is affecting fat absorption leading to the excretion of lipids in the feces. A bomb calorimetry on feces would answer this question. Nevertheless it is interesting to note that TLQP-21 induced a generalized healthier phenotype consisting in normalized branch chain amino acids and glycaemia.

## Human versus rodent TLQP-21 peptide

Primate`s, including human, TLQP-21 sequence differs from rodent TLQP-21 sequence by only three amino acids, S6A, L8A and S20A (**Figure 5.3**) [Bartolomucci et al., 2011]. Since the C-terminal portion is essential for the biological activity of TLQP-21, we believe that the serine present at position 21 in the human peptide is mostly responsible for its lower potency at C3aR1. Compared to rodent TLQP-21, human TLQP-21 induces a fifth of gastric contraction on rat stomach which could suggest specie-specific interaction [Cero et al., 2014]. However, our binding assay

studies using human C3aR1 also showed that human TLQP-21 has 8 time lower potency compared to the rodent TLQP-21 on the human receptor [Cero et al., 2014]. Hannedouche et al., [2013] have also reported that the human TLQP-21 sequence is 5-fold less potent toward the rodent C3aR1 than the corresponding rodent sequence. Overall these data suggest that the human TLQP-21 peptide is poorly active at C3aR1. In support of this hypothesis, we have recently published a study showing that humanized VGF KO mouse expressing full-length hVGF instead of the mouse VGF are obese prone with heavier weight and fat pads compared to the wild type mice [Sadahiro et al., 2015].

Given the size of their side chain, serine and alanine are classified as small/tiny aminoacids. Alanine is an aliphatic amino acid not particularly hydrophobic that can be substituted by any other small amino acids [Betts and Russell, 2003], while serine is a non-aromatic small amino acid with a hydroxyl group, polar but neural amino acid. It is possible that during evolution either S20 in the mouse TLQP-21 was substituted by A20 or A20 in human TLQP-21 substituted by S20. It has been show that Ser substations with Ala results in higher biological activity [Stockhaus et al., 1992]. Preliminary analysis on VGF evolutionary biology suggest that S20 is the ancestral form of TLQP-21 peptide, while the mutation occurred in the murine lineage thus causing a gain of function in the mouse TLQP-21 increasing the binding potency to C3aR1 and its metabolic/lipolytic efficiency (unpublished).

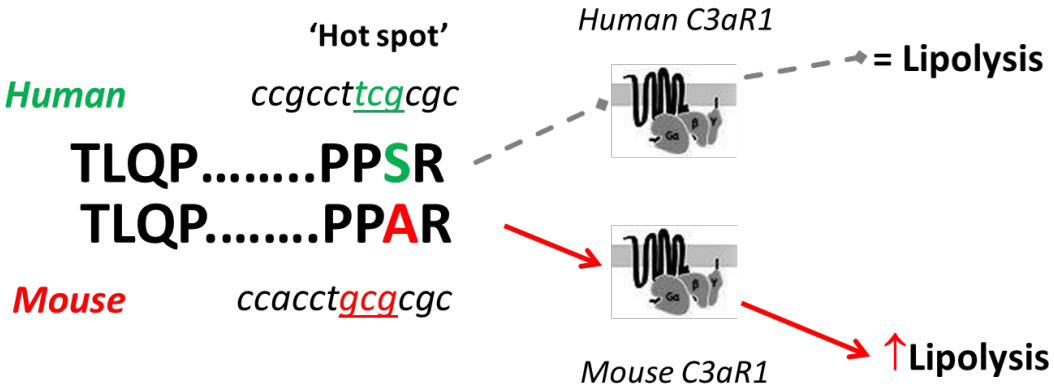


**Figure 5.3. Human and mouse gene and TLQP-21 sequence.** Due to a single base modification in the three base codon for serine within the mouse TLQP-21 peptide, serine was substituted by alanine generating a gain in function in mouse TLQP-21 peptide.

Since rodent TLQP-21 promotes lipolysis and opposes obesity, it would be worth investigating whether rodent TLQP-21 produces the same effects in humans.

Considering that rodent TLQP-21 binds more potently to the human C3aR1 in comparison to the human TLQP-21, we could speculate that rodent TLQP-21 could also potentiate lipolysis in human adipocytes limiting obesity. This hypothesis is strengthened by preliminary lipolytic data where murine but not human TLQP-21 increased lipolysis on human adipocytes (unpublished). Because pharmacological TLQP-21 treatment specifically targets lipolysis without causing adverse cardiovascular side effects, instead it lowers blood pressure and normalizes obesity-induced hypertension [Possenti et al., 2012; Fargali et al., 2014] and circulating free fatty acids and glucose and downturns the obesity–induced branch chain amino acid promoting a healthier phenotype, we believe that TLQP-21 would be an interesting target for anti-obesity drug discovery projects.

## Conclusion and future prospective

Even though we provided compelling evidences that the pro-lipolytic mechanism of action for TLQP-21 requires the activation of the MAP/ERK pathway, we have not yet elucidated all the molecular steps in this activation. Future works should aim to have a better understanding of the downstream signaling pathways activated by TLQP-21. Moreover, keeping in mind that the MAP/ERK pathway is a key signaling pathway in cell differentiation, survival and proliferation, it is natural to ask whether TLQP-21 promotes any of these effects on adipocytes.

Based on the functional role of TLQP-21 and the identification of $R_{21}$ being essential its biological activity, we have engineered a mouse that carries a germline point mutation in the sequence encoding for TLQP-21, generating a selective loss of function for TLQP-21 while peptide preserving other VGF peptides (Δ-TLQP-21). We have been breeding and started the phenotyping characterization of this model of TLQP-21 loss of functions and predict that homozygous Δ-TLQP-21 mice will present impaired lipolysis and increased vulnerability to obesity.

In conclusion, the work presented here identifies the molecular mechanism whereby TLQP-21 enhances adrenergic-induced lipolysis and exerts an anti-obesity effect in rodents via activation of C3aR1. Its mechanism of action could be a key component in safely limiting obesity by reducing fat mass, therefore having positive effects in obesity. Together, these data enriches the obesity field in understanding alternative lipolytic pathways that could be used to mildly increasing lipolysis without the side effects associated with β-AR agonists.

# REFERENCES


**Adessi C, Soto C.** Converting a peptide into a drug: strategies to improve stability and bioavailability. Curr Med Chem. 2002 May;9(9):963-78. Review.

**Agell N, Bachs O, Rocamora N, Villalonga P.** Modulation of the Ras/Raf/MEK/ERK pathway by Ca(2+), and calmodulin. Cell Signal. 2002 Aug;14(8):649-54.

**Aguilar E, Pineda R, Gaytán F, Sánchez-Garrido MA, Romero M, Romero-Ruiz A, Ruiz-Pino F, Tena-Sempere M, Pinilla L.** Characterization of the reproductive effects of the Vgf-derived peptide TLQP-21 in female rats: in vivo and in vitro studies. Neuroendocrinology. 2013;98(1):38-50.

**Ames RS, Lee D, Foley JJ, Jurewicz AJ, Tornetta MA, Bautsch W, Settmacher B, Klos A, Erhard KF, Cousins RD, Sulpizio AC, Hieble JP, McCafferty G, Ward KW, Adams JL, Ammoun S, Holmqvist T, Shariatmadari R, Oonk HB, Detheux M, Parmentier M, Akerman KE, Kukkonen JP.** Distinct recognition of OX1 and OX2 receptors by orexin peptides. J Pharmacol Exp Ther. 2003 May;305(2):507-14.

**Arner P, Rydén M.** Fatty Acids, Obesity and Insulin Resistance. Obes Facts. 2015;8(2):147-55.

**Arner P.** Catecholamine-induced lipolysis in obesity. Int J Obes Relat Metab Disord. 1999 Feb;23 Suppl 1:10-3. Review.

**Arner P.** Human fat cell lipolysis: biochemistry, regulation and clinical role. Best Pract Res Clin Endocrinol Metab. 2005 Dec;19(4):471-82. Review.

**Asensio CS, Arsenijevic D, Lehr L, Giacobino JP, Muzzin P, Rohner-Jeanrenaud F.** Effects of leptin on energy metabolism in beta-less mice. Int J Obes (Lond).2008 Jun;32(6):936-42.

**Bachman ES, Dhillon H, Zhang CY, Cinti S, Bianco AC, Kobilka BK, Lowell BB.** betaAR signaling required for diet-induced thermogenesis and obesity resistance. Science. 2002 Aug 2;297(5582):843-5.

**Bachman ES, Dhillon H, Zhang CY, Cinti S, Bianco AC, Kobilka BK, Lowell BB.** betaAR signaling required for diet-induced thermogenesis and obesity resistance. Science. 2002 Aug 2;297(5582):843-5.

**Baker NA, Sept D, Joseph S, Holst MJ, McCammon JA.** Electrostatics of nanosystems: application to microtubules and the ribosome. Proc Natl Acad Sci U S A. 2001 Aug 28;98(18):10037-41. Epub 2001 Aug 21.

**Bal NC, Maurya SK, Sopariwala DH, Sahoo SK, Gupta SC, Shaikh SA, Pant M,Rowland LA, Bombardier E, Goonasekera SA, Tupling AR, Molkentin JD, Periasamy M.** Sarcolipin is a newly identified regulator of muscle-based thermogenesis in mammals. Nat Med. 2012 Oct;18(10):1575-9.

**Baldo A, Sniderman AD, St-Luce S, Avramoglu RK, Maslowska M, Hoang B, Monge JC, Bell A, Mulay S, Cianflone K.** The adipsin-acylation stimulating protein system and regulation of intracellular triglyceride synthesis. J Clin Invest. 1993 Sep;92(3):1543-7.

**Bamshad M, Aoki VT, Adkison MG, Warren WS, Bartness TJ.** Central nervous system origins of the sympathetic nervous system outflow to white adipose tissue. Am J Physiol. 1998 Jul;275(1 Pt 2):R291-9.

**Barrett P, Ross AW, Balik A, Littlewood PA, Mercer JG, Moar KM, Sallmen T, Kaslin J, Panula P, Schuhler S, Ebling FJ, Ubeaud C, Morgan PJ.** Photoperiodic regulation of histamine H3 receptor and VGF messenger ribonucleic acid in the arcuate nucleus of the Siberian hamster. Endocrinology. 2005 Apr;146(4):1930-9. Epub 2004 Dec 23.

**Barsh GS, Ollmann MM, Wilson BD, Miller KA, Gunn TM.** Molecular pharmacology of Agouti protein in vitro and in vivo. Ann N Y Acad Sci. 1999 Oct 20;885:143-52. Review.

**Bartness TJ, Bamshad M.** Innervation of mammalian white adipose tissue: implications for the regulation of total body fat. Am J Physiol. 1998 Nov;275(5 Pt 2):R1399-411. Review.

**Bartness TJ, Demas GE, Song CK.** Seasonal changes in adiposity: the roles of the photoperiod, melatonin and other hormones, and sympathetic nervous system. Exp Biol Med (Maywood). 2002 Jun;227(6):363-76. Review.

**Bartness TJ, Hamilton JM, Wade GN, Goldman BD.** Regional differences in fat pad responses to short days in Siberian hamsters. Am J Physiol. 1989 Dec;257(6 Pt 2):R1533-40.

**Bartness TJ, Shrestha YB, Vaughan CH, Schwartz GJ, Song CK.** Sensory and sympathetic nervous system control of white adipose tissue lipolysis. Mol Cell Endocrinol. 2010 Apr 29;318(1-2):34-43. Review.

**Bartness TJ.** Short day-induced depletion of lipid stores is fat pad- and gender-specific in Siberian hamsters. Physiol Behav. 1995 Sep;58(3):539-50.

**Bartolomucci A, Bresciani E, Bulgarelli I, Rigamonti AE, Pascucci T, Levi A, Possenti R, Torsello A, Locatelli V, Muller EE, Moles A.** Chronic intracerebroventricular injection of TLQP-21 prevents high fat diet induced weight gain in fast weight-gaining mice. Genes Nutr. 2009 Mar;4(1):49-57.

**Bartolomucci A, La Corte G, Possenti R, Locatelli V, Rigamonti AE, Torsello A, Bresciani E, Bulgarelli I, Rizzi R, Pavone F, D'Amato FR, Severini C, Mignogna G, Giorgi A, Schininà ME, Elia G, Brancia C, Ferri GL, Conti R, Ciani B, Pascucci T,Dell'Omo G, Muller EE, Levi A, Moles A.** TLQP-21, a VGF-derived peptide, increases energy expenditure and prevents the early phase of diet-induced obesity. Proc Natl Acad Sci U S A. 2006 Sep 26;103(39):14584-9.

**Bartolomucci A, Possenti R, Mahata SK, Fischer-Colbrie R, Loh YP, Salton SR.** The extended granin family: structure, function, and biomedical implications. Endocr Rev. 2011 Dec;32(6):755-97. doi: 10.1210/er.2010-0027. Epub 2011 Aug 23. Review.

**Bartolomucci A, Possenti R, Mahata SK, Fischer-Colbrie R, Loh YP, Salton SR.** The extended granin family: structure, function, and biomedical implications. Endocr Rev. 2011 Dec;32(6):755-97.

**Beck-Sickinger AG, Wieland HA, Wittneben H, Willim KD, Rudolf K, Jung G.** Complete L-alanine scan of neuropeptide Y reveals ligands binding to Y1 and Y2 receptors with distinguished conformations. Eur J Biochem. 1994 Nov 1;225(3):947-58.

**Beckonert O, Keun HC, Ebbels TM, Bundy J, Holmes E, Lindon JC, Nicholson JK.** Metabolic profiling, metabolomic and metabonomic procedures for NMR spectroscopy of urine, plasma, serum and tissue extracts. Nat Protoc. 2007;2(11):2692-703.

**Bergman RN, Kim SP, Catalano KJ, Hsu IR, Chiu JD, Kabir M, Hucking K, Ader M.** Why visceral fat is bad: mechanisms of the metabolic syndrome. Obesity (Silver Spring). 2006 Feb;14 Suppl 1:16S-19S. Review.

**Betts MJ and Russel RB.** Amino Acid Properties and Consequences of Substitutions. *Bioinformatics for Geneticists.* Edited by Michael R. Barnes and Ian C. Gray Copyright 2003 John Wiley & Sons, Ltd.

**Bishnoi M, Kondepudi KK, Gupta A, Karmase A, Boparai RK.** Expression of multiple Transient Receptor Potential channel genes in murine 3T3-L1 cell lines and adipose tissue. Pharmacol Rep. 2013;65(3):751-5.

**Bondinell WE, Underwood DC, Osborn RR, Badger AM, Sarau HM.** Identification of a selective nonpeptide antagonist of the anaphylatoxin C3a receptor that demonstrates antiinflammatory activity in animal models. J Immunol. 2001 May 15;166(10):6341-8.

**Bonni A, Ginty DD, Dudek H, Greenberg ME.** Serine 133-phosphorylated CREB induces transcription via a cooperative mechanism that may confer specificity to neurotrophin signals. Mol Cell Neurosci. 1995 Apr;6(2):168-83.

**Brancia C, Cocco C, D'Amato F, Noli B, Sanna F, Possenti R, Argiolas A, Ferri GL.** Selective expression of TLQP-21 and other VGF peptides in gastric neuroendocrine cells and modulation by feeding. J Endocrinol. 2010 Dec;207(3):329-41.

**Bulló M, Peeraully MR, Trayhurn P.** Stimulation of NGF expression and secretion in 3T3-L1 adipocytes by prostaglandins PGD2, PGJ2, and Delta12-PGJ2. Am J Physiol Endocrinol Metab. 2005 Jul;289(1):E62-7.

**Canu N, Possenti R, Ricco AS, Rocchi M, Levi A.** Cloning, structural organization analysis, and chromosomal assignment of the human gene for the neurosecretory protein VGF. Genomics. 1997 Oct 15;45(2):443-6.

**Cassina V, Torsello A, Tempestini A, Salerno D, Brogioli D, Tamiazzo L, Bresciani E, Martinez J, Fehrentz JA, Verdié P, Omeljaniuk RJ, Possenti R, Rizzi L, Locatelli V, Mantegazza F.** Biophysical characterization of a binding site for TLQP-21, a naturally occurring peptide which induces resistance to obesity. Biochim Biophys Acta. 2013 Feb;1828(2):455-60.

**Cassina V, Torsello A, Tempestini A, Salerno D, Brogioli D, Tamiazzo L, Bresciani E, Martinez J, Fehrentz JA, Verdié P, Omeljaniuk RJ, Possenti R, Rizzi L, Locatelli V, Mantegazza F.** Biophysical characterization of a binding site for TLQP-21, a naturally occurring peptide which induces resistance to obesity. Biochim Biophys Acta. 2013 Feb;1828(2):455-60.

**Cero C C, Vostrikov VV, Verardi R, Severini C, Gopinath T, Braun PD, Sassano MF, Gurney A, Roth BL, Vulchanova L, Possenti R, Veglia G, Bartolomucci A.** The TLQP-21 peptide activates the G-protein-coupled receptor C3aR1 via a folding-upon-binding mechanism. Structure. 2014 Dec 2;22(12):1744-53.

**Chazin WJ, Hugli TE, Wright PE.** 1H NMR studies of human C3a anaphylatoxin in solution: sequential resonance assignments, secondary structure, and global fold. Biochemistry. 1988 Dec 27;27(26):9139-48.

**Chen YC, Pristerá A, Ayub M, Swanwick RS, Karu K, Hamada Y, Rice AS, Okuse K.** Identification of a receptor for neuropeptide VGF and its role in neuropathic pain. J Biol Chem. 2013 Nov 29;288(48):34638-46.

**Cho KO, Skarnes WC, Minsk B, Palmieri S, Jackson-Grusby L, Wagner JA.** Nerve growth factor regulates gene expression by several distinct mechanisms. Mol Cell Biol. 1989 Jan;9(1):135-43.

**Choy LN, Rosen BS, Spiegelman BM.** Adipsin and an endogenous pathway of complement from adipose cells. J Biol Chem. 1992 Jun 25;267(18):12736-41.

**Choy LN, Spiegelman BM.** Regulation of alternative pathway activation and C3a production by adipose cells. Obes Res. 1996 Nov;4(6):521-32.

**Christiansen CB, Svendsen B, Holst JJ.** The VGF-Derived Neuropeptide TLQP-21 Shows No Impact on Hormone Secretion in the Isolated Perfused Rat Pancreas. Horm Metab Res. 2015 Jan 20.Bachman ES, Dhillon H, Zhang CY, Cinti S, Bianco AC, Kobilka BK, Lowell BB. betaAR signaling required for diet-induced thermogenesis and obesity resistance. Science. 2002 Aug 2;297(5582):843-5.

**Chuderland D, Seger R.** Calcium regulates ERK signaling by modulating its protein-protein interactions. Commun Integr Biol. 2008;1(1):4-5.

**Cianflone K, Xia Z, Chen LY.** Critical review of acylation-stimulating protein physiology in humans and rodents. Biochim Biophys Acta. 2003 Jan 31;1609(2):127-43. Review.

**Cinti S, Frederich RC, Zingaretti MC, De Matteis R, Flier JS, Lowell BB.** Immunohistochemical localization of leptin and uncoupling protein in white and brown adipose tissue. Endocrinology. 1997 Feb;138(2):797-804.

**Cinti S.** Adipocyte differentiation and transdifferentiation: plasticity of the adipose organ. J Endocrinol Invest. 2002 Nov;25(10):823-35. Review.

**Cinti S.** The adipose organ at a glance. Dis Model Mech. 2012 Sep;5(5):588-94.

**Cinti S.** The adipose organ: morphological perspectives of adipose tissues. Proc Nutr Soc. 2001 Aug;60(3):319-28.

**Cinti S.** The Adipose Organ. Editrice Kurtis: Milano, 1999.

**Clifford GM, Londos C, Kraemer FB, Vernon RG, Yeaman SJ.** Translocation of hormone-sensitive lipase and perilipin upon lipolytic stimulation of rat adipocytes. J Biol Chem. 2000 Feb 18;275(7):5011-5.

**Cocco C, Brancia C, Pirisi I, D'Amato F, Noli B, Possenti R, Ferri GL.** VGF metabolic-related gene: distribution of its derived peptides in mammalian pancreatic islets. J Histochem Cytochem. 2007 Jun;55(6):619-28.

**Collins S, Surwit RS.** The beta-adrenergic receptors and the control of adipose tissue metabolism and thermogenesis. Recent Prog Horm Res. 2001;56:309-28. Review.

**Cone RD, Cowley MA, Butler AA, Fan W, Marks DL, Low MJ.** The arcuate nucleus as a conduit for diverse signals relevant to energy homeostasis. Int J Obes Relat Metab Disord. 2001 Dec;25 Suppl 5:S63-7. Review.

**Coulthard LG, Woodruff TM.** Is the complement activation product C3a a proinflammatory molecule? Re-evaluating the evidence and the myth. J Immunol. 2015 Apr 15;194(8):3542-8. doi: 10.4049/jimmunol.1403068. Review.

**Cousin B, Munoz O, Andre M, Fontanilles AM, Dani C, Cousin JL, Laharrague P, Casteilla L, Pénicaud L.** A role for preadipocytes as macrophage-like cells. FASEB J. 1999 Feb;13(2):305-12.

**Crandall DL, DiGirolamo M.** Hemodynamic and metabolic correlates in adipose tissue: pathophysiologic considerations. FASEB J. 1990 Feb 1;4(2):141-7. Review.

**Cullen PJ, Lockyer PJ.** Integration of calcium and Ras signalling. Nat Rev Mol Cell Biol. 2002 May;3(5):339-48. Review.

**D'Amato F, Noli B, Brancia C, Cocco C, Flore G, Collu M, Nicolussi P, Ferri GL.** Differential distribution of VGF-derived peptides in the adrenal medulla and evidence for their selective modulation. J Endocrinol. 2008 May;197(2):359-69.

**D'Arcangelo G, Habas R, Wang S, Halegoua S, Salton SR.** Activation of codependent transcription factors is required for transcriptional induction of the vgf gene by nerve growth factor and Ras. Mol Cell Biol. 1996 Sep;16(9):4621-31.

**Dedio J, Jahnen-Dechent W, Bachmann M, Müller-Esterl W.** The multiligand-binding protein gC1qR, putative C1q receptor, is a mitochondrial protein. J Immunol. 1998 Apr 1;160(7):3534-42.

**Dembitzer FR, Kinoshita Y, Burstein D, Phelps RG, Beasley MB, Garcia R, Harpaz N, Jaffer S, Thung SN, Unger PD, Ghebrehiwet B, Peerschke EI.** gC1qR expression in normal and pathologic human tissues: differential expression in tissues of epithelial and mesenchymal origin. J Histochem Cytochem. 2012 Jun;60(6):467-74.

**Després JP, Lemieux I, Bergeron J, Pibarot P, Mathieu P, Larose E, Rodés-Cabau J, Bertrand OF, Poirier P.** Abdominal obesity and the metabolic syndrome: contribution to global cardiometabolic risk. Arterioscler Thromb Vasc Biol. 2008 Jun;28(6):1039-49. Review.

**Després JP, Lemieux I.** Abdominal obesity and metabolic syndrome. Nature. 2006 Dec 14;444(7121):881-7. Review.

**Diniz YS, Cicogna AC, Padovani CR, Santana LS, Faine LA, Novelli EL.** Diets rich in saturated and polyunsaturated fatty acids: metabolic shifting and cardiac health. Nutrition. 2004.

**Dogiel AS.** Die sensiblen Nervenendigungen im Herzen und in den Blutgefassen der Saugethiere. *Arch Mikr Anat* 1898; **52**: 44–70.

**Drira R, Sakamoto K.** Hydroxytyrosol stimulates lipolysis via A-kinase and extracellular signal-regulated kinase activation in 3T3-L1 adipocytes. Eur J Nutr. 2014 Apr;53(3):743-50.

**Duncan RE, Ahmadian M, Jaworski K, Sarkadi-Nagy E, Sul HS.** Regulation of lipolysis in adipocytes. Annu Rev Nutr. 2007;27:79-101. Review.

**Engelke F., Steuernagel S.** (2007) Cross Polarization in Rotating Solids: Spin-1/2 Nuclei. Encyclopedia of Magnetic Resonance. (John Wiley & Sons, Ltd).

**Fairbanks CA, Peterson CD, Speltz RH, Riedl MS, Kitto KF, Dykstra JA, Braun PD, Sadahiro M, Salton SR, Vulchanova L.** The VGF-derived peptide TLQP-21 contributes to inflammatory and nerve injury-induced hypersensitivity. Pain. 2014 Jul;155(7):1229-37.

**Fargali S, Garcia AL, Sadahiro M, Jiang C, Janssen WG, Lin WJ, Cogliani V, Elste A, Mortillo S, Cero C C, Veitenheimer B, Graiani G, Pasinetti GM, Mahata SK, Osborn JW, Huntley GW, Phillips GR, Benson DL, Bartolomucci A, Salton SR.** The granin VGF promotes genesis of secretory vesicles, and regulates circulating catecholamine levels and blood pressure. FASEB J. 2014 May;28(5):2120-33.

**Fargali S, Scherer T, Shin AC, Sadahiro M, Buettner C, Salton SR.** Germline ablation of VGF increases lipolysis in white adipose tissue. J Endocrinol. 2012 Nov;215(2):313-22.

**Felig P, Marliss E, Cahill GF Jr.** Plasma amino acid levels and insulin secretion in obesity. N Engl J Med. 1969 Oct 9;281(15):811-6.

**Ferri GL, Gaudio RM, Cossu M, Rinaldi AM, Polak JM, Berger P, Possenti R.** The "VGF" protein in rat adenohypophysis: sex differences and changes during the estrous cycle and after gonadectomy. Endocrinology. 1995 May;136(5):2244-51.

**Ferri GL, Levi A, Possenti R.** A novel neuroendocrine gene product: selective VGF8a gene expression and immuno-localisation of the VGF protein in endocrine and neuronal populations. Brain Res Mol Brain Res. 1992 Mar;13(1-2):139-43.

**Ferri GL, Noli B, Brancia C, D'Amato F, Cocco C.** VGF: an inducible gene product, precursor of a diverse array of neuro-endocrine peptides and tissue-specific disease biomarkers. J Chem Neuroanat. 2011 Dec;42(4):249-61.

**Fishman RB, Dark J.** Sensory innervation of white adipose tissue. Am J Physiol. 1987 Dec;253(6 Pt 2):R942-4.

**Foster MT, Bartness TJ.** Sympathetic but not sensory denervation stimulates white adipocyte proliferation. Am J Physiol Regul Integr Comp Physiol. 2006 Dec;291(6):R1630-7.

**Francis K, Lewis BM, Akatsu H, Monk PN, Cain SA, Scanlon MF, Morgan BP, Ham J, Gasque P.** Complement C3a receptors in the pituitary gland: a novel pathway by which an innate immune molecule releases hormones involved in the control of inflammation. FASEB J. 2003 Dec;17(15):2266-8.

**Fujihara H, Sasaki K, Mishiro-Sato E, Ohbuchi T, Dayanithi G, Yamasaki M, Ueta Y, Minamino N.** Molecular characterization and biological function of neuroendocrine regulatory peptide-3 in the rat. Endocrinology. 2012 Mar;153(3):1377-86.

**Fujishiro M, Gotoh Y, Katagiri H, Sakoda H, Ogihara T, Anai M, Onishi Y, Ono H, Abe M, Shojima N, Fukushima Y, Kikuchi M, Oka Y, Asano T.** Three mitogen-activated protein kinases inhibit insulin signaling by different mechanisms in 3T3-L1 adipocytes. Mol Endocrinol. 2003 Mar;17(3):487-97.

**Fyfe CA, Wong-Moon KC, Huang Y, Grondey H.** (1995) INEPT Experiments in Solid-State NMR. *J Am Chem Soc* 117, 10397-10398.

**Gaboriaud C, Juanhuix J, Gruez A, Lacroix M, Darnault C, Pignol D, Verger D, Fontecilla-Camps JC, Arlaud GJ.** The crystal structure of the globular head of complement protein C1q provides a basis for its versatile recognition properties. J Biol Chem. 2003 Nov 21;278(47):46974-82.

**Garcia AL, Han SK, Janssen WG, Khaing ZZ, Ito T, Glucksman MJ, Benson DL, Salton SR.** A prohormone convertase cleavage site within a predicted alpha-helix mediates sorting of the neuronal and endocrine polypeptide VGF into the regulated secretory pathway. J Biol Chem. 2005 Dec 16;280(50):41595-608.

**Garton AJ, Campbell DG, Carling D, Hardie DG, Colbran RJ, Yeaman SJ.** Phosphorylation of bovine hormone-sensitive lipase by the AMP-activated protein kinase. A possible antilipolytic mechanism. Eur J Biochem. 1989 Jan 15;179(1):249-54.

**Gaspari M, Larsson NG, Gustafsson CM.** The transcription machinery in mammalian mitochondria. Biochim Biophys Acta. 2004 Dec 6;1659(2-3):148-52. Review.

**Gericke MT, Kosacka J, Koch D, Nowicki M, Schröder T, Ricken AM, Nieber K, Spanel-Borowski K.** Receptors for NPY and PACAP differ in expression and activity during adipogenesis in the murine 3T3-L1 fibroblast cell line. Br J Pharmacol.2009 Jun;157(4):620-32.

**Ghebrehiwet B, Kew RR, Gruber BL, Marchese MJ, Peerschke EI, Reid KB.** Murine mast cells express two types of C1q receptors that are involved in the induction of chemotaxis and chemokinesis. J Immunol. 1995 Sep 1;155(5):2614-9.

**Ghebrehiwet B, Lim BL, Peerschke EI, Willis AC, Reid KB.** Isolation, cDNA cloning, and overexpression of a 33-kD cell surface glycoprotein that binds to the globular "heads" of C1q. J Exp Med. 1994 Jun 1;179(6):1809-21.

**Giordano A, Frontini A, Cinti S.** Adipose organ nerves revealed by immunohistochemistry. Methods Mol Biol. 2008;456:83-95.

**Giordano A, Morroni M, Santone G, Marchesi GF, Cinti S.** Tyrosine hydroxylase, neuropeptide Y, substance P, calcitonin gene-related peptide and vasoactive intestinal peptide in nerves of rat periovarian adipose tissue: an immunohistochemical and ultrastructural investigation. J Neurocytol. 1996 Feb;25(2):125-36.

**Giordano A, Song CK, Bowers RR, Ehlen JC, Frontini A, Cinti S, Bartness TJ.** White adipose tissue lacks significant vagal innervation and immunohistochemical evidence of parasympathetic innervation. Am J Physiol Regul Integr Comp Physiol. 2006 Nov;291(5):R1243-55.

**Giralt M, Villarroya F.** White, brown, beige/brite: different adipose cells for different functions? Endocrinology. 2013 Sep;154(9):2992-3000.

**Grace CR, Perrin MH, Cantle JP, Vale WW, Rivier JE, Riek R.** Common and divergent structural features of a series of corticotropin releasing factor-related peptides. J Am Chem Soc. 2007 Dec 26;129(51):16102-14.

**Green H, Kehinde O.** An established preadipose cell line and its differentiation in culture. II. Factors affecting the adipose conversion. Cell. 1975 May;5(1):19-27.

**Greenberg AS, Shen WJ, Muliro K, Patel S, Souza SC, Roth RA, Kraemer FB.** Stimulation of lipolysis and hormone-sensitive lipase via the extracellular signal-regulated kinase pathway. J Biol Chem. 2001 Nov 30;276(48):45456-61.

**Guh DP, Zhang W, Bansback N, Amarsi Z, Birmingham CL, Anis AH.** The incidence of co-morbidities related to obesity and overweight: a systematic review and meta-analysis. BMC Public Health. 2009 Mar 25;9:88.

**Gupta A, Rezvani R, Lapointe M, Poursharifi P, Marceau P, Tiwari S, Tchernof A, Cianflone K.** Downregulation of complement C3 and C3aR expression in subcutaneous adipose tissue in obese women. PLoS One. 2014 Apr 17;9(4):e95478.

**Haemmerle G, Lass A, Zimmermann R, Gorkiewicz G, Meyer C, Rozman J, Heldmaier G, Maier R, Theussl C, Eder S, Kratky D, Wagner EF, Klingenspor M, Hoefler G, Zechner R.** Defective lipolysis and altered energy metabolism in mice lacking adipose triglyceride lipase. Science. 2006 May 5;312(5774):734-7.

**Haemmerle G, Zimmermann R, Hayn M, Theussl C, Waeg G, Wagner E, Sattler W, Magin TM, Wagner EF, Zechner R.** Hormone-sensitive lipase deficiency in mice causes diglyceride accumulation in adipose tissue, muscle, and testis. J Biol Chem. 2002 Feb 15;277(7):4806-15.

**Hahm S, Fekete C, Mizuno TM, Windsor J, Yan H, Boozer CN, Lee C, Elmquist JK, Lechan RM, Mobbs CV, Salton SR.** VGF is required for obesity induced by diet, gold thioglucose treatment, and agouti and is differentially regulated in pro-opiomelanocortin- and neuropeptide Y-containing arcuate neurons in response to fasting. J Neurosci. 2002 Aug 15;22(16):6929-38.

**Hahm S, Mizuno TM, Wu TJ, Wisor JP, Priest CA, Kozak CA, Boozer CN, Peng B, McEvoy RC, Good P, Kelley KA, Takahashi JS, Pintar JE, Roberts JL, Mobbs CV, Salton SR.** Targeted deletion of the Vgf gene indicates that the encoded secretory peptide precursor plays a novel role in the regulation of energy balance. Neuron. 1999 Jul;23(3):537-48.

**Hannedouche S, Beck V, Leighton-Davies J, Beibel M, Roma G, Oakeley EJ, Lannoy V, Bernard J, Hamon J, Barbieri S, Preuss I, Lasbennes MC, Sailer AW, Suply T, Seuwen K, Parker CN, Bassilana F.** Identification of the C3a receptor (C3AR1) as the target of the VGF-derived peptide TLQP-21 in rodent cells. J Biol Chem. 2013 Sep 20;288(38):27434-43.

**Hanson RL, Rong R, Kobes S, Muller YL, Weil EJ, Curtis JM, Nelson RG, Baier LJ.** Role of Established Type 2 Diabetes-Susceptibility Genetic Variants in a High Prevalence American Indian Population. Diabetes. 2015 Jul;64(7):2646-57.

**Hausman DB, DiGirolamo M, Bartness TJ, Hausman GJ, Martin RJ.** The biology of white adipocyte proliferation. Obes Rev. 2001 Nov;2(4):239-54. Review.

**Herman MA, She P, Peroni OD, Lynch CJ, Kahn BB.** Adipose tissue branched chain amino acid (BCAA) metabolism modulates circulating BCAA levels. J Biol Chem. 2010 Apr 9;285(15):11348-56.

**Himms-Hagen J, Melnyk A, Zingaretti MC, Ceresi E, Barbatelli G, Cinti S,** 2000. Multilocular fat cells in WAT of CL-316243-treated rats derive directly from white adipocytes. Am J Physiol Cell Physiol 279(3):C670-81.

**Hollenstein K, de Graaf C, Bortolato A, Wang MW, Marshall FH, Stevens RC.** Insights into the structure of class B GPCRs. Trends Pharmacol Sci. 2014 Jan;35(1):12-22. doi: 10.1016/j.tips.2013.11.001. Epub 2013 Dec 18. Review.

**Holm C.** Molecular mechanisms regulating hormone-sensitive lipase and lipolysis. Biochem Soc Trans. 2003 Dec;31(Pt 6):1120-4. Review.

**Horvath TL.** The hardship of obesity: a soft-wired hypothalamus. Nat Neurosci. 2005 May;8(5):561-5. Review.

**Huffman KM, Shah SH, Stevens RD, Bain JR, Muehlbauer M, Slentz CA, Tanner CJ, Kuchibhatla M, Houmard JA, Newgard CB, Kraus WE.** Relationships between circulating metabolic intermediates and insulin action in overweight to obese, inactive men and women. Diabetes Care. 2009 Sep;32(9):1678-83.

**Hugli TE, Erickson BW.** Synthetic peptides with the biological activities and specificity of human C3a anaphylatoxin. Proc Natl Acad Sci U S A. 1977 May;74(5):1826-30.

**Jaworski K, Sarkadi-Nagy E, Duncan RE, Ahmadian M, Sul HS.** Regulation of triglyceride metabolism. IV. Hormonal regulation of lipolysis in adipose tissue. Am J Physiol Gastrointest Liver Physiol. 2007 Jul;293(1):G1-4. Epub 2007 Jan 11. Review.

**Jethwa PH, Ebling FJ.** Role of VGF-derived peptides in the control of food intake, body weight and reproduction. Neuroendocrinology. 2008;88(2):80-7. doi: 10.1159/000127319.

**Jethwa PH, Warner A, Nilaweera KN, Brameld JM, Keyte JW, Carter WG, Bolton N, Bruggraber M, Morgan PJ, Barrett P, Ebling FJ.** VGF-derived peptide, TLQP-21, regulates food intake and body weight in Siberian hamsters. Endocrinology. 2007 Aug;148(8):4044-55.

**Kahn SE, Hull RL, Utzschneider KM.** Mechanisms linking obesity to insulin resistance and type 2 diabetes. Nature. 2006 Dec 14;444(7121):840-6. Review.

**Karnik SS, Gogonea C, Patil S, Saad Y, Takezako T.** Activation of G-protein-coupled receptors: a common molecular mechanism. Trends Endocrinol Metab. 2003 Nov;14(9):431-7. Review.

**Kershaw EE, Flier JS.** Adipose tissue as an endocrine organ. J Clin Endocrinol Metab. 2004 Jun;89(6):2548-56. Review.

**Kim KB, Kim BW, Choo HJ, Kwon YC, Ahn BY, Choi JS, Lee JS, Ko YG.** Proteome analysis of adipocyte lipid rafts reveals that gC1qR plays essential roles in adipogenesis and insulin signal transduction. Proteomics. 2009 May;9(9):2373-82.

**Kissebah AH, Krakower GR.** Regional adiposity and morbidity. Physiol Rev. 1994 Oct;74(4):761-811. Review.

**Klingenspor M, Dickopp A, Heldmaier G, Klaus S.** Short photoperiod reduces leptin gene expression in white and brown adipose tissue of Djungarian hamsters. FEBS Lett. 1996 Dec 16;399(3):290-4.

**Klos A, Tenner AJ, Johswich KO, Ager RR, Reis ES, Köhl J.** The role of the anaphylatoxins in health and disease. Mol Immunol. 2009 Sep;46(14):2753-66.

**Klos A, Wende E, Wareham KJ, Monk PN.** International Union of Basic and Clinical Pharmacology. [corrected]. LXXXVII. Complement peptide C5a, C4a, and C3a receptors. Pharmacol Rev. 2013 Jan;65(1):500-43. Review.

**Kolditz CI, Langin D.** Adipose tissue lipolysis. Curr Opin Clin Nutr Metab Care. 2010 Jul;13(4):377-81. Review.

**Kreier F, Buijs RM.** Evidence for parasympathetic innervation of white adipose tissue, clearing up some vagaries. Am J Physiol Regul Integr Comp Physiol. 2007 Jul;293(1):R548-9.

**Kuo LE, Kitlinska JB, Tilan JU, Li L, Baker SB, Johnson MD, Lee EW, Burnett MS, Fricke ST, Kvetnansky R, Herzog H, Zukowska Z.** Neuropeptide Y acts directly in the periphery on fat tissue and mediates stress-induced obesity and metabolic syndrome. Nat Med. 2007 Jul;13(7):803-11.

**Kwan WH, van der Touw W, Paz-Artal E, Li MO, Heeger PS.** Signaling through C5a receptor and C3a receptor diminishes function of murine natural regulatory T cells. J Exp Med. 2013 Feb 11;210(2):257-68.

**Lafontan M, Barbe P, Galitzky J, Tavernier G, Langin D, Carpéné C, Bousquet-Melou A, Berlan M.** Adrenergic regulation of adipocyte metabolism. Hum Reprod. 1997 Oct;12 Suppl 1:6-20. Review.

**Langin D.** Adipose tissue lipolysis as a metabolic pathway to define pharmacological strategies against obesity and the metabolic syndrome. Pharmacol Res. 2006 Jun;53(6):482-91. Epub 2006 Mar 27. Review.

**Langin D.** Control of fatty acid and glycerol release in adipose tissue lipolysis. C R Biol. 2006 Aug;329(8):598-607; discussion 653-5.

**Large V, Reynisdottir S, Langin D, Fredby K, Klannemark M, Holm C, Arner P.** Decreased expression and function of adipocyte hormone-sensitive lipase in subcutaneous fat cells of obese subjects. J Lipid Res. 1999 Nov;40(11):2059-66.

**Lass A, Zimmermann R, Haemmerle G, Riederer M, Schoiswohl G, Schweiger M, Kienesberger P, Strauss JG, Gorkiewicz G, Zechner R.** Adipose triglyceride lipase-mediated lipolysis of cellular fat stores is activated by CGI-58 and defective in Chanarin-Dorfman Syndrome. Cell Metab. 2006 May;3(5):309-19.

**Lass A, Zimmermann R, Oberer M, Zechner R.** Lipolysis - a highly regulated multi-enzyme complex mediates the catabolism of cellular fat stores. Prog Lipid Res. 2011 Jan;50(1):14-27. Review.

**Levi A, Eldridge JD, Paterson BM.** Molecular cloning of a gene sequence regulated by nerve growth factor. Science. 1985 Jul 26;229(4711):393-5.

**Levi A, Ferri GL, Watson E, Possenti R, Salton SR.** Processing, distribution, and function of VGF, a neuronal and endocrine peptide precursor. Cell Mol Neurobiol. 2004 Aug;24(4):517-33. Review.

**Lewis JE, Brameld JM, Jethwa PH.** Neuroendocrine Role for VGF. Front Endocrinol (Lausanne). 2015 Feb 2;6:3.

**Lim J, Iyer A, Suen JY, Seow V, Reid RC, Brown L, Fairlie DP.** C5aR and C3aR antagonists each inhibit diet-induced obesity, metabolic dysfunction, and adipocyte and macrophage signaling. FASEB J. 2013 Feb;27(2):822-31.

**Lin H, Sassano MF, Roth BL, Shoichet BK.** A pharmacological organization of G protein-coupled receptors. Nat Methods. 2013 Feb;10(2):140-6.

**Lin WJ, Jiang C, Sadahiro M, Bozdagi O, Vulchanova L, Alberini CM, Salton SR.** VGF and Its C-Terminal Peptide TLQP-62 Regulate Memory Formation in Hippocampus via a BDNF-TrkB-Dependent Mechanism. J Neurosci. 2015 Jul 15;35(28):10343-56.

**Litosch I, Hudson TH, Mills I, Li SY, Fain JN.** Forskolin as an activator of cyclic AMP accumulation and lipolysis in rat adipocytes. Mol Pharmacol. 1982 Jul;22(1):109-15.

**Liu JW, Andrews PC, Mershon JL, Yan C, Allen DL, Ben-Jonathan N.** Peptide V: a VGF-derived neuropeptide purified from bovine posterior pituitary. Endocrinology. 1994 Dec;135(6):2742-8.

**Lo JC, Ljubicic S, Leibiger B, Kern M, Leibiger IB, Moede T, Kelly ME, Chatterjee Bhowmick D, Murano I, Cohen P, Banks AS, Khandekar MJ, Dietrich A, Flier JS, Cinti S, Blüher M, Danial NN, Berggren PO, Spiegelman BM.** Adipsin is an adipokine that improves β cell function in diabetes. Cell. 2014 Jul 3;158(1):41-53.

**Lönngvist F, Nyberg B, Wahrenberg and Arner P.** Catecholamine-induced lipolysis in adipose tissue of the elderly. J Clin Invest. 1990 May; 85(5): 1614–1621.

**Mamane Y, Chung Chan C, Lavallee G, Morin N, Xu LJ, Huang J, Gordon R, Thomas W, Lamb J, Schadt EE, Kennedy BP, Mancini JA.** The C3a anaphylatoxin receptor is a key mediator of insulin resistance and functions by modulating adipose tissue macrophage infiltration and activation. Diabetes. 2009 Sep;58(9):2006-17.

**Markiewski MM, Lambris JD.** The role of complement in inflammatory diseases from behind the scenes into the spotlight. Am J Pathol. 2007 Sep;171(3):715-27.

**Mason CC, Hanson RL, Ossowski V, Bian L, Baier LJ, Krakoff J, Bogardus C.** Bimodal distribution of RNA expression levels in human skeletal muscle tissue. BMC Genomics. 2011 Feb 7;12:98.

**Melis MR, Sanna F, Succu S, Ferri GL, Argiolas A.** Neuroendocrine regulatory peptide-1 and neuroendocrine regulatory peptide-2 influence differentially feeding and penile erection in male rats: sites of action in the brain. Regul Pept. 2012 Aug 20;177(1-3):46-52.

**Mishiro-Sato E, Sasaki K, Matsuo T, Kageyama H, Yamaguchi H, Date Y, Matsubara M, Ishizu T, Yoshizawa-Kumagaye K, Satomi Y, Takao T, Shioda S, Nakazato M, Minamino N.** Distribution of neuroendocrine regulatory peptide-1 and -2, and proteolytic processing of their precursor VGF protein in the rat. J Neurochem. 2010 Aug;114(4):1097-106.

**Mizuno TM, Kleopoulos SP, Bergen HT, Roberts JL, Priest CA, Mobbs CV.** Hypothalamic pro-opiomelanocortin mRNA is reduced by fasting and [corrected] in ob/ob and db/db mice, but is stimulated by leptin. Diabetes. 1998 Feb;47(2):294-7.

**Moin AS, Yamaguchi H, Rhee M, Kim JW, Toshinai K, Waise TM, Naznin F, Matsuo T, Sasaki K, Minamino N, Yoon KH, Nakazato M.** Neuroendocrine regulatory peptide-2 stimulates glucose-induced insulin secretion in vivo and in vitro. Biochem Biophys Res Commun. 2012 Nov 30;428(4):512-7.

**Monk PN, Scola AM, Madala P, Fairlie DP.** Function, structure and therapeutic potential of complement C5a receptors. Br J Pharmacol. 2007 Oct;152(4):429-48. Epub 2007 Jul 2. Review.

**Morrison KL, Weiss GA.** Combinatorial alanine-scanning. Curr Opin Chem Biol. 2001 Jun;5(3):302-7. Review.

**Moss A, Ingram R, Koch S, Theodorou A, Low L, Baccei M, Hathway GJ, Costigan M, Salton SR, Fitzgerald M.** Origins, actions and dynamic expression patterns of the neuropeptide VGF in rat peripheral and central sensory neurones following peripheral nerve injury. Mol Pain. 2008 Dec 10;4:62.

**Mowers J, Uhm M, Reilly SM, Simon J, Leto D, Chiang SH, Chang L, Saltiel AR.** Inflammation produces catecholamine resistance in obesity via activation of PDE3B by the protein kinases IKKε and TBK1. Elife. 2013 Dec 24;2:e01119.

**Murage EN, Schroeder JC, Beinborn M, Ahn JM.** Search for alpha-helical propensity in the receptor-bound conformation of glucagon-like peptide-1. Bioorg Med Chem. 2008 Dec 1;16(23):10106-12.

**Murano I, Barbatelli G, Giordano A, Cinti S.** Noradrenergic parenchymal nerve fiber branching after cold acclimatisation correlates with brown adipocyte density in mouse adipose organ. J Anat. 2009 Jan;214(1):171-8.

**Neelamkavil S, Arison B, Birzin E, Feng JJ, Chen KH, Lin A, Cheng FC, Taylor L, Thornton ER, Smith AB 3rd, Hirschmann R.** Replacement of Phe6, Phe7, and Phe11 of D-Trp8-somatostatin-14 with L-pyrazinylalanine. Predicted and observed effects on binding affinities at hSST2 and hSST4. An unexpected effect of the chirality of Trp8 on NMR spectra in methanol. J Med Chem. 2005 Jun 16;48(12):4025-30.

**Nettesheim DG, Edalji RP, Mollison KW, Greer J, Zuiderweg ER.** Secondary structure of complement component C3a anaphylatoxin in solution as determined by NMR spectroscopy: differences between crystal and solution conformations. Proc Natl Acad Sci U S A. 1988 Jul;85(14):5036-40.

**Newgard CB, An J, Bain JR, Muehlbauer MJ, Stevens RD, Lien LF, Haqq AM, Shah SH, Arlotto M, Slentz CA, Rochon J, Gallup D, Ilkayeva O, Wenner BR, Yancy WS Jr, Eisenson H, Musante G, Surwit RS, Millington DS, Butler MD, Svetkey LP.** A branched-chain amino acid-related metabolic signature that differentiates obese and lean humans and contributes to insulin resistance. Cell Metab. 2009.

**Niijima A.** Nervous regulation of metabolism. Prog Neurobiol. 1989;33(2):135-47. Review.

**Nisoli E, Tonello C, Benarese M, Liberini P, Carruba MO.** Expression of nerve growth factor in brown adipose tissue: implications for thermogenesis and obesity. Endocrinology. 1996 Feb;137(2):495-503.

**Ogden CL, Carroll MD, Kit BK, Flegal KM.** Prevalence of childhood and adult obesity in the United States, 2011-2012. JAMA. 2014 Feb 26;311(8):806-14.

**Olsson H, Strålfors P, Belfrage P.** Phosphorylation of the basal site of hormone-sensitive lipase by glycogen synthase kinase-4. FEBS Lett. 1986 Dec 15;209(2):175-80.

**Opstal-van Winden AW, Vermeulen RC, Peeters PH, Beijnen JH, van Gils CH.** Early diagnostic protein biomarkers for breast cancer: how far have we come? Breast Cancer Res Treat. 2012 Jul;134(1):1-12.

**Pal K, Melcher K, Xu HE.** Structure and mechanism for recognition of peptide hormones by Class B G-protein-coupled receptors. Acta Pharmacol Sin. 2012 Mar;33(3):300-11. Review.

**Papathanasiou A, Kostara C, Cung MT, Seferiadis K, Elisaf M, Bairaktari E, Goudevenos IA.** Analysis of the composition of plasma lipoproteins in patients with extensive coronary heart disease using 1H NMR spectroscopy. Hellenic J Cardiol. 2008 Mar-Apr;49(2):72-8.

**Parthier C, Reedtz-Runge S, Rudolph R, Stubbs MT.** Passing the baton in class B GPCRs: peptide hormone activation via helix induction? Trends Biochem Sci. 2009 Jun;34(6):303-10. Review.

**Patti ME, Corvera S.** The role of mitochondria in the pathogenesis of type 2 diabetes. Endocr Rev. 2010 Jun;31(3):364-95.

**Pedersen S, Hoffmann EK, Hougaard C, Jorgensen NK, Wybrandt GB, Lambert IH.** Leukotriene D4-induced Ca2+ mobilization in Ehrlich ascites tumor cells. J Membr Biol. 1997 Jan 1;155(1):61-73.

**Peeraully MR, Jenkins JR, Trayhurn P.** NGF gene expression and secretion in white adipose tissue: regulation in 3T3-L1 adipocytes by hormones and inflammatory cytokines. Am J Physiol Endocrinol Metab. 2004 Aug;287(2):E331-9.

**Peerschke EI, Ghebrehiwet B.** The contribution of gC1qR/p33 in infection and inflammation. Immunobiology. 2007;212(4-5):333-42.

**Pellecchia M, Bertini I, Cowburn D, Dalvit C, Giralt E, Jahnke W, James TL, Homans SW, Kessler H, Luchinat C, Meyer B, Oschkinat H, Peng J, Schwalbe H, Siegal G.** Perspectives on NMR in drug discovery: a technique comes of age. Nat Rev Drug Discov. 2008 Sep;7(9):738-45. Review.

**Pénicaud L, Cousin B, Leloup C, Lorsignol A, Casteilla L.** The autonomic nervous system, adipose tissue plasticity, and energy balance. Nutrition. 2000 Oct;16(10):903-8. Review.

**Petersen-Mahrt SK, Estmer C, Ohrmalm C, Matthews DA, Russell WC, Akusjärvi G.** The splicing factor-associated protein, p32, regulates RNA splicing by inhibiting ASF/SF2 RNA binding and phosphorylation. EMBO J. 1999 Feb 15;18(4):1014-24.

**Petrella C, Broccardo M, Possenti R, Severini C, Improta G.** TLQP-21, a VGF-derived peptide, stimulates exocrine pancreatic secretion in the rat. Peptides. 2012 Jul;36(1):133-6.

**Petrocchi Passeri P, Biondini L, Mongiardi MP, Mordini N, Quaresima S, Frank C, Baratta M, Bartolomucci A, Levi A, Severini C, Possenti R.** Neuropeptide TLQP-21, a VGF internal fragment, modulates hormonal gene expression and secretion in GH3 cell line. Neuroendocrinology. 2013;97(3):212-24.

**Petrocchi-Passeri P, Cero C, Cutarelli A, Frank C, Severini C, Bartolomucci A, Possenti R.** The VGF-derived peptide TLQP-62 modulates insulin secretion and glucose homeostasis. J Mol Endocrinol. 2015 Jun;54(3):227-39.

**Pollesello P, Masutti F, Crocè LS, Toffanin R, Eriksson O, Paoletti S, Höckerstedt K, Tiribelli C.** 1H NMR spectroscopic studies of lipid extracts from human fatty liver. Biochem Biophys Res Commun. 1993 May 14;192(3):1217-22.

**Possenti R, Eldridge JD, Paterson BM, Grasso A, Levi A.** A protein induced by NGF in PC12 cells is stored in secretory vesicles and released through the regulated pathway. EMBO J. 1989 Aug;8(8):2217-23.

**Possenti R, Muccioli G, Petrocchi P, Cero C, Cabassi A, Vulchanova L, Riedl MS, Manieri M, Frontini A, Giordano A, Cinti S, Govoni P, Graiani G, Quaini F, Ghè C, Bresciani E, Bulgarelli I, Torsello A, Locatelli V, Sanghez V, Larsen BD, Petersen JS, Palanza P, Parmigiani S, Moles A, Levi A, Bartolomucci A.** Characterization of a novel peripheral pro-lipolytic mechanism in mice: role of VGF-derived peptide TLQP-21. Biochem J. 2012 Jan 1;441(1):511-22.

**Possenti R, Rinaldi AM, Ferri GL, Borboni P, Trani E, Levi A.** Expression, processing, and secretion of the neuroendocrine VGF peptides by INS-1 cells.Endocrinology. 1999 Aug;140(8):3727-35.

**Rapold RA, Wueest S, Knoepfel A, Schoenle EJ, Konrad D.** Fas activates lipolysis in a Ca2+-CaMKII-dependent manner in 3T3-L1 adipocytes. J Lipid Res.2013 Jan;54(1):63-70.

**Ravussin E, Knowler WC, Hanson RL, Bennett PH, Schulz LO, Valencia ME.** Study design of the Maycoba Project: obesity and diabetes in Mexican Pimas. Am J Health Behav. 2014 May;38(3):370-8.

**Razavi S, Razavi MR, Kheirollahi-Kouhestani M, Mardani M, Mostafavi FS.** Co-culture with neurotrophic factor secreting cells induced from adipose-derived stem cells: promotes neurogenic differentiation. Biochem Biophys Res Commun. 2013 Oct 25;440(3):381-7.

**Razzoli M, Bo E, Pascucci T, Pavone F, D'Amato FR, Cero C, Sanghez V, Dadomo H, Palanza P, Parmigiani S, Ceresini G, Puglisi-Allegra S, Porta M, Panzica GC, Moles A, Possenti R, Bartolomucci A.** Implication of the VGF-derived peptide TLQP-21 in mouse acute and chronic stress responses. Behav Brain Res. 2012 Apr 15;229(2):333-9.

**Reid RC, Yau MK, Singh R, Hamidon JK, Reed AN, Chu P, Suen JY, Stoermer MJ, Blakeney JS, Lim J, Faber JM, Fairlie DP.** Downsizing a human inflammatory protein to a small molecule with equal potency and functionality. Nat Commun. 2013;4:2802.

**Reynisdottir S, Wahrenberg H, Carlström K, Rössner S, Arner P.** Catecholamine resistance in fat cells of women with upper-body obesity due to decreased expression of beta 2-adrenoceptors. Diabetologia. 1994 Apr;37(4):428-35.

**Riedl MS, Braun PD, Kitto KF, Roiko SA, Anderson LB, Honda CN, Fairbanks CA, Vulchanova L.** Proteomic analysis uncovers novel actions of the neurosecretory protein VGF in nociceptive processing. J Neurosci. 2009 Oct 21;29(42):13377-88.

**Rizzi R, Bartolomucci A, Moles A, D'Amato F, Sacerdote P, Levi A, La Corte G, Ciotti MT, Possenti R, Pavone F.** The VGF-derived peptide TLQP-21: a new modulatory peptide for inflammatory pain. Neurosci Lett. 2008 Aug 15;441(1):129-33.

**Robinson MJ, Cobb MH.** Mitogen-activated protein kinase pathways. Curr Opin Cell Biol. 1997 Apr;9(2):180-6. Review.Rosell S, Belfrage E. Blood circulation in adipose tissue. Physiol Rev. 1979 Oct;59(4):1078-1104. Review.

**Roglic A, Prossnitz ER, Cavanagh SL, Pan Z, Zou A, Ye RD.** cDNA cloning of a novel G protein-coupled receptor with a large extracellular loop structure. Biochim Biophys Acta. 1996 Feb 7;1305(1-2):39-43.

**Rothwell NJ, Stock MJ.** A role for brown adipose tissue in diet-induced thermogenesis. Obes Res. 1997 Nov;5(6):650-6. Review.

**Roy C, Paglialunga S, Fisette A, Schrauwen P, Moonen-Kornips E, St-Onge J, Hesselink MK, Richard D, Joanisse DR, Cianflone K.** Shift in metabolic fuel in acylation-stimulating protein-deficient mice following a high-fat diet. Am J Physiol Endocrinol Metab. 2008 Jun;294(6):E1051-9.

**Ruan BH, Li X, Winkler AR, Cunningham KM, Kuai J, Greco RM, Nocka KH, Fitz LJ, Wright JF, Pittman DD, Tan XY, Paulsen JE, Lin LL, Winkler DG.** Complement C3a, CpG oligos, and DNA/C3a complex stimulate IFN-α production in a receptor for advanced glycation end product-dependent manner. J Immunol. 2010 Oct 1;185(7):4213-22.

**Sadahiro M, Erickson C, Lin WJ, Shin AC, Razzoli M, Jiang C, Fargali S, Gurney A, Kelley KA, Buettner C, Bartolomucci A, Salton SR.** Role of VGF-derived carboxy-terminal peptides in energy balance and reproduction: analysis of "humanized" knockin mice expressing full-length or truncated VGF. Endocrinology. 2015 May;156(5):1724-38.

**Salton SR, Ferri GL, Hahm S, Snyder SE, Wilson AJ, Possenti R, Levi A.** VGF: a novel role for this neuronal and neuroendocrine polypeptide in the regulation of energy balance. Front Neuroendocrinol. 2000 Jul;21(3):199-219. Review.

**Salton SR, Fischberg DJ, Dong KW.** Structure of the gene encoding VGF, a nervous system-specific mRNA that is rapidly and selectively induced by nerve growth factor in PC12 cells. Mol Cell Biol. 1991 May;11(5):2335-49.

**Salton SR.** Nucleotide sequence and regulatory studies of VGF, a nervous system-specific mRNA that is rapidly and relatively selectively induced by nerve growth factor. J Neurochem. 1991 Sep;57(3):991-6.

**Schaffer JE.** Lipotoxicity: when tissues overeat. Curr Opin Lipidol. 2003 Jun;14(3):281-7. Review.

**Schimmel RJ.** Stimulation of cAMP accumulation and lipolysis in hamster adipocytes with forskolin. Am J Physiol. 1984 Jan;246(1 Pt 1):C63-8.

**Schwartz MW, Woods SC, Porte D Jr, Seeley RJ, Baskin DG.** Central nervous system control of food intake. Nature. 2000 Apr 6;404(6778):661-71. Review.

**Schwarzinger S, Kroon GJ, Foss TR, Wright PE, Dyson HJ.** Random coil chemical shifts in acidic 8 M urea: implementation of random coil shift data in NMRView. J Biomol NMR. 2000 Sep;18(1):43-8.

**Schweiger M, Schreiber R, Haemmerle G, Lass A, Fledelius C, Jacobsen P, Tornqvist H, Zechner R, Zimmermann R.** Adipose triglyceride lipase and hormone-sensitive lipase are the major enzymes in adipose tissue triacylglycerol catabolism. J Biol Chem. 2006 Dec 29;281(52):40236-41.

**Schwieters CD, Kuszewski JJ, Tjandra N, Clore GM.** The Xplor-NIH NMR molecular structure determination package. J Magn Reson. 2003 Jan;160(1):65-73.

**Seidah NG, Chrétien M.** Proprotein and prohormone convertases: a family of subtilases generating diverse bioactive polypeptides. Brain Res. 1999 Nov 27;848(1-2):45-62. Review.

**Sengenès C, Berlan M, De Glisezinski I, Lafontan M, Galitzky J.** Natriuretic peptides: a new lipolytic pathway in human adipocytes. FASEB J. 2000 Jul;14(10):1345-51.

**Severini C, Ciotti MT, Biondini L, Quaresima S, Rinaldi AM, Levi A, Frank C, Possenti R.** TLQP-21, a neuroendocrine VGF-derived peptide, prevents cerebellar granule cells death induced by serum and potassium deprivation. J Neurochem. 2008 Jan;104(2):534-44.

**Severini C, La Corte G, Improta G, Broccardo M, Agostini S, Petrella C, Sibilia V, Pagani F, Guidobono F, Bulgarelli I, Ferri GL, Brancia C, Rinaldi AM, Levi A, Possenti R.** In vitro and in vivo pharmacological role of TLQP-21, a VGF-derived peptide, in the regulation of rat gastric motor functions. Br J Pharmacol. 2009 Jul;157(6):984-93.

**She P, Van Horn C, Reid T, Hutson SM, Cooney RN, Lynch CJ.** Obesity-related elevations in plasma leucine are associated with alterations in enzymes involved in branched-chain amino acid metabolism. Am J Physiol Endocrinol Metab. 2007 Dec;293(6):E1552-63.

**Shoichet BK, Kobilka BK.** Structure-based drug screening for G-protein-coupled receptors. Trends Pharmacol Sci. 2012 May;33(5):268-72.

**Sibilia V, Pagani F, Bulgarelli I, Mrak E, Broccardo M, Improta G, Severini C,Possenti R, Guidobono F.** TLQP-21, a VGF-derived peptide, prevents ethanol-induced gastric lesions: insights into its mode of action. Neuroendocrinology. 2010;92(3):189-97.

**Sibilia V, Pagani F, Bulgarelli I, Tulipano G, Possenti R, Guidobono F.** Characterization of the mechanisms involved in the gastric antisecretory effect of TLQP-21, a vgf-derived peptide, in rats. Amino Acids. 2012 Apr;42(4):1261-8.

**Sibilia V, Pagani F, Guidobono F, Bulgarelli I, Ferri GL, Brancia C, Rinaldi AM, Levi A, Possenti R.** In vitro and in vivo pharmacological role of TLQP-21, a VGF-derived peptide, in the regulation of rat gastric motor functions. Br J Pharmacol. 2009 Jul;157(6):984-93.

**Slavin BG, Ballard KW.** Morphological studies on the adrenergic innervation of white adipose tissue. Anat Rec. 1978 Jul;191(3):377-89.

**Slavin BG, Ong JM, Kern PA.** Hormonal regulation of hormone-sensitive lipase activity and mRNA levels in isolated rat adipocytes. J Lipid Res. 1994 Sep;35(9):1535-41.

**Snyder SE, Pintar JE, Salton SR.** Developmental expression of VGF mRNA in the prenatal and postnatal rat. J Comp Neurol. 1998 Apr 27;394(1):64-90.

**Snyder SE, Salton SR.** Expression of VGF mRNA in the adult rat central nervous system. J Comp Neurol. 1998 Apr 27;394(1):91-105.

**Song CK, Bartness TJ.** CNS sympathetic outflow neurons to white fat that express MEL receptors may mediate seasonal adiposity. Am J Physiol Regul Integr Comp Physiol. 2001 Aug;281(2):R666-72.

**Song CK, Schwartz GJ, Bartness TJ.** Anterograde transneuronal viral tract tracing reveals central sensory circuits from white adipose tissue. Am J Physiol Regul Integr Comp Physiol. 2009 Mar;296(3):R501-11.

**Sparling ML, Zidovetzki R, Muller L, Chan SI.** Analysis of membrane lipids by 500 MHz 1H NMR. Anal Biochem. 1989 Apr;178(1):67-76.

**Stallknecht B, Bülow J, Frandsen E, Galbo H.** Desensitization of human adipose tissue to adrenaline stimulation studied by microdialysis. J Physiol. 1997 Apr 1;500 ( Pt 1):271-82.

**Stark M, Danielsson O, Griffiths WJ, Jörnvall H, Johansson J.** Peptide repertoire of human cerebrospinal fluid: novel proteolytic fragments of neuroendocrine proteins. J Chromatogr B Biomed Sci Appl. 2001 Apr 25;754(2):357-67.

**Steiner DF.** The proprotein convertases. Curr Opin Chem Biol. 1998 Feb;2(1):31-9. Review.

**Stephens SB, Schisler JC, Hohmeier HE, An J, Sun AY, Pitt GS, Newgard CB.** A VGF-derived peptide attenuates development of type 2 diabetes via enhancement of islet β-cell survival and function. Cell Metab. 2012 Jul 3;16(1):33-43.

**Steppan CM, Bailey ST, Bhat S, Brown EJ, Banerjee RR, Wright CM, Patel HR, Ahima RS, Lazar MA.** The hormone resistin links obesity to diabetes. Nature. 2001 Jan 18;409(6818):307-12.

**Stockhaus J, Nagatani A, Halfter U, Kay S, Furuya M, Chua NH.** Serine-to-alanine substitutions at the amino-terminal region of phytochrome A result in an increase in biological activity. Genes Dev. 1992 Dec;6(12A):2364-72.

**Succu S, Cocco C, Mascia MS, Melis T, Melis MR, Possenti R, Levi A, Ferri GL, Argiolas A.** Pro-VGF-derived peptides induce penile erection in male rats: possible involvement of oxytocin. Eur J Neurosci. 2004 Dec;20(11):3035-40.

**Succu S, Mascia MS, Melis T, Sanna F, Melis MR, Possenti R, Argiolas A.** Pro-VGF-derived peptides induce penile erection in male rats: Involvement of paraventricular nitric oxide. Neuropharmacology. 2005 Dec;49(7):1017-25.

**Sukumar P, Sedo A, Li J, Wilson LA, O'Regan D, Lippiat JD, Porter KE, Kearney MT, Ainscough JF, Beech DJ.** Constitutively active TRPC channels of adipocytes confer a mechanism for sensing dietary fatty acids and regulating adiponectin. Circ Res. 2012 Jul 6;111(2):191-200.

**Takahashi M, Moriguchi S, Ikeno M, Kono S, Ohata K, Usui H, Kurahashi K, Sasaki R, Yoshikawa M.** Studies on the ileum-contracting mechanisms and identification as a complement C3a receptor agonist of oryzatensin, a bioactive peptide derived from rice albumin. Peptides. 1996;17(1):5-12.

**Takahashi M, Moriguchi S, Suganuma H, Shiota A, Tani F, Usui H, Kurahashi K, Sasaki R, Yoshikawa M.** Identification of casoxin C, an ileum-contracting peptide derived from bovine kappa-casein, as an agonist for C3a receptors. Peptides. 1997;18(3):329-36.

**Tavernier G, Jimenez M, Giacobino JP, Hulo N, Lafontan M, Muzzin P, Langin D.** Norepinephrine induces lipolysis in beta1/beta2/beta3-adrenoceptor knockout mice. Mol Pharmacol. 2005 Sep;68(3):793-9.

**Thakker-Varia S, Krol JJ, Nettleton J, Bilimoria PM, Bangasser DA, Shors TJ, Black IB, Alder J.** The neuropeptide VGF produces antidepressant-like behavioral effects and enhances proliferation in the hippocampus. J Neurosci. 2007 Nov 7;27(45):12156-67.

**Toshinai K, Nakazato M.** Neuroendocrine regulatory peptide-1 and -2: novel bioactive peptides processed from VGF. Cell Mol Life Sci. 2009 Jun;66(11-12):1939-45. doi: 10.1007/s00018-009-8796-0. Review.

**Toshinai K, Yamaguchi H, Kageyama H, Matsuo T, Koshinaka K, Sasaki K, Shioda S, Minamino N, Nakazato M.** Neuroendocrine regulatory peptide-2 regulates feeding behavior via the orexin system in the hypothalamus. Am J Physiol Endocrinol Metab. 2010 Sep;299(3):E394-401.

**Trani E, Ciotti T, Rinaldi AM, Canu N, Ferri GL, Levi A, Possenti R.** Tissue-specific processing of the neuroendocrine protein VGF. J Neurochem. 1995 Dec;65(6):2441-9.

**Trani E, Giorgi A, Canu N, Amadoro G, Rinaldi AM, Halban PA, Ferri GL, Possenti R, Schininà ME, Levi A.** Isolation and characterization of VGF peptides in rat brain. Role of PC1/3 and PC2 in the maturation of VGF precursor. J Neurochem. 2002 May;81(3):565-74.

**Trayhurn P, Duncan JS, Rayner DV.** Acute cold-induced suppression of ob (obese) gene expression in white adipose tissue of mice: mediation by the sympathetic system. Biochem J. 1995 Nov 1;311 ( Pt 3):729-33.

**Turtzo LC, Marx R, Lane MD.** Cross-talk between sympathetic neurons and adipocytes in coculture. Proc Natl Acad Sci U S A. 2001 Oct 23;98(22):12385-90. Epub 2001 Oct 16.

**Urquidez-Romero R, Esparza-Romero J, Chaudhari LS, Begay RC, Giraldo M, Valet P, Berlan M, Beauville M, Crampes F, Montastruc JL, Lafontan M.** Neuropeptide Y and peptide YY inhibit lipolysis in human and dog fat cells through a pertussis toxin-sensitive G protein. J Clin Invest. 1990 Jan;85(1):291-5.

**Vale W, Spiess J, Rivier C, Rivier J.** Characterization of a 41-residue ovine hypothalamic peptide that stimulates secretion of corticotropin and beta-endorphin. Science. 1981 Sep 18;213(4514):1394-7.

**van den Pol AN, Decavel C, Levi A, Paterson B.** Hypothalamic expression of a novel gene product, VGF: immunocytochemical analysis. J Neurosci. 1989 Dec;9(12):4122-37.

**van Leeuwen HC, O'Hare P.** Retargeting of the mitochondrial protein p32/gC1Qr to a cytoplasmic compartment and the cell surface. J Cell Sci. 2001 Jun;114(Pt 11):2115-23.

**Veglia, G. et al.** Comprehensive Biophysics. Vol. 1: Biophysical Techniques for Structural Characterization of Macromolecules Ch 1.11 (Elsevier, 2012).

**Vernochet C, Mourier A, Bezy O, Macotela Y, Boucher J, Rardin MJ, An D, Lee KY, Ilkayeva OR, Zingaretti CM, Emanuelli B, Smyth G, Cinti S, Newgard CB, Gibson BW, Larsson NG, Kahn CR.** Adipose-specific deletion of TFAM increases mitochondrial oxidation and protects mice against obesity and insulin resistance. Cell Metab. 2012 Dec 5;16(6):765-76.

**Villena JA, Roy S, Sarkadi-Nagy E, Kim KH, Sul HS.** Desnutrin, an adipocyte gene encoding a novel patatin domain-containing protein, is induced by fasting and glucocorticoids: ectopic expression of desnutrin increases triglyceride hydrolysis. J Biol Chem. 2004 Nov 5;279(45):47066-75.

**Waldén TB, Hansen IR, Timmons JA, Cannon B, Nedergaard J.** Recruited vs. nonrecruited molecular signatures of brown, "brite," and white adipose tissues. Am J Physiol Endocrinol Metab. 2012 Jan 1;302(1):E19-31.

**Wang B, Trayhurn P.** Acute and prolonged effects of TNF-alpha on the expression and secretion of inflammation-related adipokines by human adipocytes differentiated in culture. Pflugers Arch. 2006 Jul;452(4):418-27.

**Wang TJ, Larson MG, Vasan RS, Cheng S, Rhee EP, McCabe E, Lewis GD, Fox CS,Jacques PF, Fernandez C, O'Donnell CJ, Carr SA, Mootha VK, Florez JC, Souza A, Melander O, Clish CB, Gerszten RE.** Metabolite profiles and the risk of developing diabetes. Nat Med. 2011 Apr;17(4):448-53.

**Watson E, Fargali S, Okamoto H, Sadahiro M, Gordon RE, Chakraborty T, Sleeman MW, Salton SR.** Analysis of knockout mice suggests a role for VGF in the control of fat storage and energy expenditure. BMC Physiol. 2009 Oct 28;9:19.

**Watson E, Hahm S, Mizuno TM, Windsor J, Montgomery C, Scherer PE, Mobbs CV, Salton SR.** VGF ablation blocks the development of hyperinsulinemia and hyperglycemia in several mouse models of obesity. Endocrinology. 2005 Dec;146(12):5151-63.

**Weissman JT, Ma JN, Essex A, Gao Y, Burstein ES.** G-protein-coupled receptor-mediated activation of rap GTPases: characterization of a novel Galphai regulated pathway. Oncogene. 2004 Jan 8;23(1):241-9.

**White RT, Damm D, Hancock N, Rosen BS, Lowell BB, Usher P, FlierJS, Spiegelman BM.** Human adipsin is identical to complement factor D and is expressed at high levels in adipose tissue. J Biol Chem. 1992 May 5;267(13):9210-3.

**Wilcox RR.** New Statistical Procedures for the Social Sciences: Modern Solutions to the Basic Problems. Hillsdale, NJ: Erlbaum (1987)

**Williams G, Harrold JA, Cutler DJ.** The hypothalamus and the regulation of energy homeostasis: lifting the lid on a black box. Proc Nutr Soc. 2000 Aug;59(3):385-96. Review.

**Wisor JP, Takahashi JS.** Regulation of the vgf gene in the golden hamster suprachiasmatic nucleus by light and by the circadian clock. J Comp Neurol. 1997 Feb 10;378(2):229-38.

**Wu J, Boström P, Sparks LM, Ye L, Choi JH, Giang AH, Khandekar M, Virtanen KA, Nuutila P, Schaart G, Huang K, Tu H, van Marken Lichtenbelt WD, Hoeks J, Enerbäck S, Schrauwen P, Spiegelman BM.** Beige adipocytes are a distinct type of thermogenic fat cell in mouse and human. Cell. 2012 Jul 20;150(2):366-76.

**Wu J, Cohen P, Spiegelman BM.** Adaptive thermogenesis in adipocytes: is beige the new brown? Genes Dev. 2013 Feb 1;27(3):234-50.

**Yamaguchi H, Sasaki K, Satomi Y, Shimbara T, Kageyama H, Mondal MS, Toshinai K, Date Y, González LJ, Shioda S, Takao T, Nakazato M, Minamino N.** Peptidomic identification and biological validation of neuroendocrine regulatory peptide-1 and -2. J Biol Chem. 2007 Sep 7;282(36):26354-60.

**Yang X, Lu X, Lombès M, Rha GB, Chi YI, Guerin TM, Smart EJ, Liu J.** The G(0)/G(1) switch gene 2 regulates adipose lipolysis through association with adipose triglyceride lipase. Cell Metab. 2010 Mar 3;11(3):194-205.

**Yildiz BO, Suchard MA, Wong ML, McCann SM, Licinio J.** Alterations in the dynamics of circulating ghrelin, adiponectin, and leptin in human obesity. Proc Natl Acad Sci U S A. 2004 Jul 13;101(28):10434-9.

**Youngstrom TG, Bartness TJ.** Catecholaminergic innervation of white adipose tissue in Siberian hamsters. Am J Physiol. 1995 Mar;268(3 Pt 2):R744-51.

**Zaia CT, Gaziri LC, Zaia DA, Delattre E, Dolnikoff MS, Timo-Iaria C.** Effect of chemical stimulation of the dorsomedial hypothalamic nucleus on blood plasma glucose, triglycerides and free fatty acids in rats. Brain Res Bull. 1997;42(3):195-8.

**Zeng W, Pirzgalska RM, Pereira MM, Kubasova N, Barateiro A, Seixas E, Lu YH, Kozlova A, Voss H, Martins GG, Friedman JM, Domingos AI.** Sympathetic Neuro-adipose Connections Mediate Leptin-Driven Lipolysis. Cell. 2015 Sep 24;163(1):84-94.

**Zhang HH, Halbleib M, Ahmad F, Manganiello VC, Greenberg AS.** Tumor necrosis factor-alpha stimulates lipolysis in differentiated human adipocytes through activation of extracellular signal-related kinase and elevation of intracellular cAMP. Diabetes. 2002 Oct; 51(10):2929-35.

**Zhang W, Ni C, Sheng J, Hua Y, Ma J, Wang L, Zhao Y, Xing Y.** TLQP-21 protects human umbilical vein endothelial cells against high-glucose-induced apoptosis by increasing G6PD expression. PLoS One. 2013 Nov 21;8(11):e79760.

**Zimmermann R, Strauss JG, Haemmerle G, Schoiswohl G, Birner-Gruenberger R, Riederer M, Lass A, Neuberger G, Eisenhaber F, Hermetter A, Zechner R.** Fat mobilization in adipose tissue is promoted by adipose triglyceride lipase. Science. 2004 Nov 19;306(5700):1383-6.